COPPER(I), PALLADIUM(II) AND PLATINUM(II) COMPLEXES OF THE

2-DIPHENYLPHOSPHINO-1,10-PHENANTHROLINE LIGAND

by

NIYUM SATHYA RAMESAR B.Sc, (NATAL)

A thesis submitted in partial fulfilment of the requirements for the degree of Master of Science in the Faculty of Science, University of Natal, Pietermaritzburg

Department of Chemistry

University of Natal
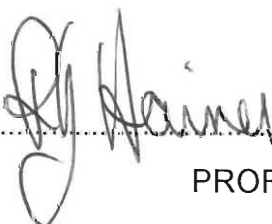
Pietermaritzburg

December 1998

DECLARATION

I hereby certify that this research is the result of my own investigation which has not already been accepted for any other degree and is not being submitted in candidature for any other degree.

Signed..

N. S. RAMESAR

I hereby certify that this statement is correct.

Signed..

PROFESSOR R. J. HAINES

(SUPERVISOR)

Signed..

PROFESSOR J. S. FIELD

(CO-SUPERVISOR)

Department of Chemistry

University of Natal

Pietermaritzburg

December 1998

to my mum and in memory of my dad............

CONTENTS

CHAPTER 3

DINUCLEAR 2-DIPHENYLPHOSPHINO-1,10-PHENANTHROLINE

CHAPTER 4

DIPALLADIUM(I) AND DIPLATINUM(I) COMPLEXES OF THE

ACKNOWLEDGEMENTS

ABBREVIATIONS

Å	Angstrom
$\{^1H\}$	proton noise decoupled
2-NHPh-phen	2-phenylamino-1,10-phenanthroline
4-Etpy	4-ethylpyridine
4-vinylpy	4-vinylpyridine
abipy	anion of 6-anilino-2,2'-bipyridine
bipy	2,2'-bipyridine
bptz	3,6-bis(4-pyridyl)-1,2,4,5-tetrazine
°C	degree Celsius
cm	centimetre
DMSO	dimethyl sulfoxide
Et(Ph)Pbipy	6-[ethyl(phenyl)phosphino]-2,2'-bipyridine
g	gram
Habipy	6-anilino-2,2'-bipyridine
HObipy	2,2'-bipyridyl-6-one
IR	infrared
L	ligand
M	molar
mabipy	6-N-methylanilino-2,2'-bipyridine
MeCN	acetonitrile
mg	milligram
mm	millimetre
mmol	millimole
mol	mole
Mpt	melting point
mV	millivolt
nmr	nuclear magnetic resonance
Obipy	anion of 2,2'-bipyridyl-6-one
pbpz	pyrido-[2,3-b]pyrazine

Ph$_2$Pbipy	6-diphenylphosphino-2,2'-bipyridine
Ph$_2$Pphen	2-diphenylphosphino-1,10-phenanthroline
Ph$_2$Ppy	2-diphenylphosphinopyridine
Ph$_2$Ppypz	2-diphenylphosphino-6-(pyrazol-1-yl)pyridine
Ph$_2$Ppyquin	6-(diphenylphosphino)-2-(2-quinolyl)pyridine
PhCN	benzonitrile
phen	1,10-phenanthroline
pipbipy	6-piperidino-2,2'-bipyridine
ppm	parts per million
py	pyridine
TBAP	tetrabutylammonium perchlorate
thf	tetrahydrofuran
V	volts

SUMMARY

Chapter 1 reviews the coordination behaviour of the 6-diphenylphosphino-2,2'-bipyridine, 6-anilino-2,2'-bipyridine, 2,2'-bipyridyl-6-one, 6-N-methylanilino-2,2'-bipyridine, 6-piperidyl-2,2'-bipyridine and 2-(phenylamino)-1,10-phenanthroline ligands. These ligands are all tridentate and contain well established chelating fragments viz., 2,2'-bipyridine and 1,10-phenanthroline. Thus the review of their coordination provides insight into the expected coordination of the 2-diphenylphosphino-1,10-phenanthroline (Ph$_2$Pphen) ligand. The synthesis and characterisation of this ligand is described in Chapter 2.

Chapter 3 describes the synthesis and characterisation of a range of Ph$_2$Pphen ligand-bridged dicopper(I) complexes. It has been shown that Ph$_2$Pphen reacts with a suitable copper(I) precursor, [Cu(MeCN)$_4$]$^+$, to form the versatile dinuclear [Cu$_2$(μ-Ph$_2$Pphen)$_2$(MeCN)$_2$]$^{2+}$ complex cation containing two bridging Ph$_2$Pphen ligands; the structure of the SbF$_6^-$ salt of this complex has been determined X-ray crystallographically. This complex possesses labile acetonitrile ligands which have been substituted by a variety of neutral and anionic ligands. Complexes prepared this way include [Cu$_2$(μ-Ph$_2$Pphen)$_2$(μ-Cl)]$^+$, [Cu$_2$(μ-Ph$_2$Pphen)$_2$(μ-I)]$^+$, [Cu$_2$(μ-Ph$_2$Pphen)$_2$(py)$_2$]$^{2+}$, [Cu$_2$(μ-Ph$_2$Pphen)$_2$\{μ-S$_2$CN(Et)$_2$\}]$^+$, [Cu$_2$(μ-Ph$_2$Pphen)$_2$(η-bipy)]$^{2+}$ and [Cu$_2$(μ-Ph$_2$Pphen)$_2$(η-phen)]$^{2+}$. X-ray structure determinations have been completed for [Cu$_2$(μ-Ph$_2$Pphen)$_2$\{μ-S$_2$CN(Et)$_2$\}]$^+$ and [Cu$_2$(μ-Ph$_2$Pphen)$_2$(η-bipy)]$^{2+}$. The X-ray crystal structures of these ligand-bridged complexes confirm that the phosphorus atom coordinates to one copper atom while the phenanthroline fragment chelates to the other copper atom with the result that each metal atom has a tetrahedral geometry.

Chapter 4 reviews the synthesis and characterisation of palladium and platinum complexes of the 2-diphenylphosphino-1,10-phenanthroline (Ph$_2$Pphen) ligand. The comproportionation reaction with Pd(II) and Pd(0) afforded the dinuclear complex [Pd$_2$(μ-Ph$_2$Pphen)$_2$](BF$_4$)$_2$. The reaction of Ph$_2$Pphen with platinum resulted in ill-defined products that could not be isolated and characterised.

CHAPTER 1

THE COORDINATION CHEMISTRY OF 6-SUBSTITUTED BIPYRIDYL LIGANDS AND OF THE 2-PHENYLAMINO-1,10-PHENANTHROLINE LIGAND

The work described in this thesis involves the synthesis and the study of the coordination behaviour of the ligand 2-diphenylphosphino-1,10-phenanthroline. This chapter reviews the coordination chemistry of closely related ligands, namely 6-substituted 2,2'-bipyridine and 2-substituted 1,10-phenanthroline where the substituent atom is a donor atom, with a particular focus on the coordination geometries of complexes whose structures have been determined X-ray crystallographically.

Polypyridyl ligands such as 1,10-phenanthroline (phen) [1] and 2,2'-bipyridine (bipy) [2] are well known chelating ligands [1,2a-c] which have the unique property of stabilizing metals over a wide range of oxidation states.

[1]   [2a]   [2b]
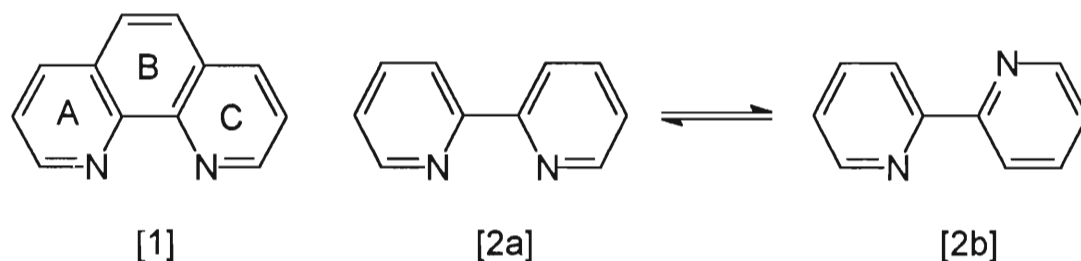
The rigid structure of phen imposed by the central ring B means that the two nitrogen atoms are always held in juxtaposition, whereas, in bipy, free rotation about the interannular bond allows the nitrogen atoms to separate (2a ⇌ 2b).

Bipy and phen also act as "electron reservoirs" by "storing" electrons in the π^* orbitals. The extra conjugation imposed by the central ring B of phen increases its ability to "store" electrons.

1.1 THE 6-DIPHENYLPHOSPHINO-2,2'-BIPYRIDINE (Ph₂Pbipy) LIGAND
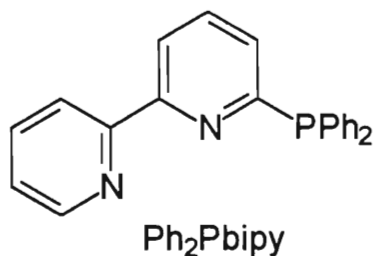
Ph₂Pbipy

The ligand 6-diphenylphosphino-2,2'-bipyridine (Ph₂Pbipy)[3] may be considered as being a combination of two extensively utilised ligands, *viz.* triphenylphosphine and bipy. It may also be regarded as an extension of the ligand 2-diphenylphosphinopyridine (Ph₂Ppy) with the monodentate pyridyl fragment having been replaced by the bidentate bipy fragment giving overall a tridentate ligand. The coordination chemistry of Ph₂Ppy [4] has been extensively studied which contrasts with that of Ph₂Pbipy.

Ph₂Ppy
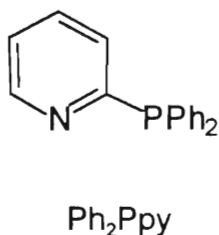
Four modes of coordination are feasible for Ph₂Pbipy (Scheme 1.1), a terminal mode (1), a bridging mode (2) and two chelating modes (3 and 4). Not illustrated is that whereby the bipy fragment bridges two metal atoms. Although this mode is possible in principle, it is very unlikely in practice as bipy is well established as a chelating ligand [1].

Scheme 1.1 : Possible modes of coordination of the Ph_2Pbipy ligand

1.1.1 TERMINAL Ph_2Pbipy

The only structurally characterised example of a complex which contains the Ph_2Pbipy ligand bonded pendantly through the phosphorus atom to a metal atom is that of $[Rh(\eta\text{-}Ph_2Pbipy)_2(CO)Cl]$ (Fig.1.1)[5]. The square planar geometry around the Rh atom is completed by the chloride ligand and the carbonyl group. The P1-Rh-P2 angle is 177.2° indicating that the two Ph_2Pbipy ligands are *trans* to each other.

Fig. 1.1: Structure of $[Rh(\eta\text{-}Ph_2Pbipy)_2(CO)Cl]$

Other examples of terminal coordination through the phosphorus atom to the metal atom include the neutral complexes $[Ru_2\{\mu\text{-}\eta^2\text{-}OC(H)O\}_2(CO)_4(\eta\text{-}Ph_2Pbipy)_2]$ [6] and $[Pt(\eta\text{-}Ph_2Pbipy)_2Cl_2]$[5]. However, these complexes have not been structurally characterised and their proposed formulations are based on spectroscopic data and elemental analysis.

1.1.2 BRIDGING Ph$_2$Pbipy

The majority of the complexes of Ph$_2$Pbipy that have been synthesised contain the ligand in a bridging mode with the phosphorus atom bonded to one metal atom and the nitrogen atoms of the bipy fragment bonded to the other metal atom. Furthermore virtually all of these bridged complexes are homodinuclear and contain two bridging Ph$_2$Pbipy ligands. Two orientations of the ligand with respect to each other are possible, the head-to-tail (HT) and the head-to-head (HH) species.

(HT)   (HH)
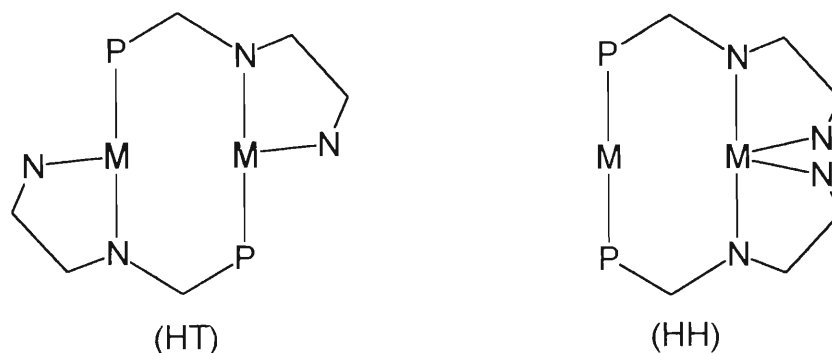
Table 1.1 lists these complexes that have been structurally characterised. A selection of these will now be discussed in detail, following which certain trends will be identified.

In most of the complexes listed in Table 1.1 the bridging ligands are orientated head-to-tail. The disilver complex, $[Ag_2(\mu\text{-}Ph_2Pbipy)_2(MeCN)_2](PF_6)_2$ [6] (Fig. 1.2), is a typical example of a compound with a structure that is common to many of these complexes which contain the ligand in a bridging coordination mode. The two silver atoms are non-bonded and are separated by a distance of 2.973 Å. The acetonitrile ligands complete the irregular tetrahedral geometry around the silver atoms. These acetonitrile ligands

Table 1.1 : Selected structural features of complexes containing the bridging Ph$_2$Pbipy ligand

COMPLEX[a]	M-M (Å)	P-M-M-N[b] TORSION ANGLE(S)(°)	DIHEDRAL ANGLE(S)(°)[c]	REF
[Cu$_2$(μ-Ph$_2$Pbipy)$_2$(MeCN)$_2$](PF$_6$)$_2$[d](HT)	3.940	27	20	7
[Cu$_2$(μ-Ph$_2$Pbipy)$_2$(py)$_2$](PF$_6$)$_2$[d](HT)	3.865	41	6	5
[Cu$_2$(μ-Ph$_2$Pbipy)$_2$(H$_2$O)$_2$](PF$_6$)$_2$[d](HT)	3.084	31	15	5
[Cu$_2$(μ-Ph$_2$Pbipy)$_2$(4-Etpy)$_2$](PF$_6$)$_2$[d](HT)	3.491	35	6	5
[Cu$_2$(μ-Ph$_2$Pbipy)$_2$(PhCN)$_2$](PF$_6$)$_2$[d](HT)	3.795	40	8	5
[Cu$_2$(μ-Ph$_2$Pbipy)$_2$(η-bipy)](PF$_6$)$_2$ (HH)	3.683	57, 46	12, 6	7
[Cu$_2$(μ-Ph$_2$Pbipy)$_2$(μ-Br)]PF$_6$[e](HT)	2.762	20	13	5
[Cu$_2$(μ-Ph$_2$Pbipy)$_2$(μ-I)]PF$_6$[e](HT)	2.770	20	12	5
[Cu$_2$(μ-Ph$_2$Pbipy)$_2$(μ-SEt)]PF$_6$(HT)	2.697	18, 23	13, 12	5
[Ni$_2$(μ-Ph$_2$Pbipy)$_2$(CO)$_2$](BF$_4$)$_2$ (HH)	4.259	51, 56	9, 6	8
[Ru$_2$(μ-Ph$_2$Pbipy)$_2$(CO)$_2$(NCEt)$_2$](PF$_6$)$_2$[f](HT)	2.765	17	8	6
[Ru$_2$(μ-Ph$_2$Pbipy)$_2${μ-OC(Me)O}(CO)$_2$]PF$_6$[f](HT)	2.688	22	11	9
[Ag$_2$(μ-Ph$_2$Pbipy)$_2$(NO$_3$)$_2$][d](HT)	2.935	46	14	6
{[Ag$_2$(μ-Ph$_2$Pbipy)$_2$(μ-bptz)](PF$_6$)$_2$}$_n$[d](HT)	3.012	40	8	6
{[Ag$_2$(μ-Ph$_2$Pbipy)$_2$(μ-4,4'-bipy)](PF$_6$)$_2$}$_n$[d](HT)	4.092	41	28	6
[Ag$_2$(μ-Ph$_2$Pbipy)$_2$(MeCN)$_2$](PF$_6$)$_2$[d](HT)	2.973	24	17	6
[Ag$_2$(μ-Ph$_2$Pbipy)$_2$(py)$_2$](PF$_6$)$_2$[d](HT)	4.092	41	7	6
[Ag$_2$(μ-Ph$_2$Pbipy)$_2$(EtOH)$_2$](BF$_4$)$_2$[d](HT)	2.984	20	9	6
[Ag$_2$(μ-Ph$_2$Pbipy)$_2$(4-vinylpy)$_2$](BF$_4$)$_2$[d](HT)	4.012	42	11	6
[Ag$_2$(μ-Ph$_2$Pbipy)$_2$(η-bipy)](BF$_4$)$_2$ (HH)	3.674	44, 48	7, 6	6
[Ag$_2$(μ-Ph$_2$Pbipy)$_2$(η-pbpz)$_2$](BF$_4$)$_2$[d](HT)	3.125	30	7	6
[Ag$_2$(μ-Ph$_2$Pbipy)$_2$(μ-I)]BF$_4$(HT)	2.920	13, 29	5, 14	6
[Ag$_2$(μ-Ph$_2$Pbipy)$_2${μ-OC(Me)O}]PF$_6$(HT)	2.988	30, 9	10, 30	6
[Ag$_2$(μ-Ph$_2$Pbipy)$_2${μ-OC(Ph)O}]PF$_6$(HT)	2.945	12, 27	27, 6	6
[Pd$_2$(μ-Ph$_2$Pbiby)$_2$](BF$_4$)$_2$[d] (HT)	2.568	3	8	19

[a] HH = ligand orientation head-to-head, HT = ligand orientation head-to-tail.

[b] This N belongs to the pyridine ring bonded directly to the phosphorus.

[c] Dihedral angle between the pyridine rings of the bipyridyl fragment.

[d] The complex cation has a centre of symmetry midway between the metal atoms.

[e] The complex cation has a two-fold axis passing through the bridging halide atom.

[f] The complex cation has a two-fold axis which bisects the Ru-Ru bond.

are *trans* disposed with respect to each other. Note that the complex has a centre of symmetry midway between the metal atoms. The P-Ag-Ag'-N torsion angle is 24° and the dihedral angle between the pyridyl rings of the bipy fragment is 17°.
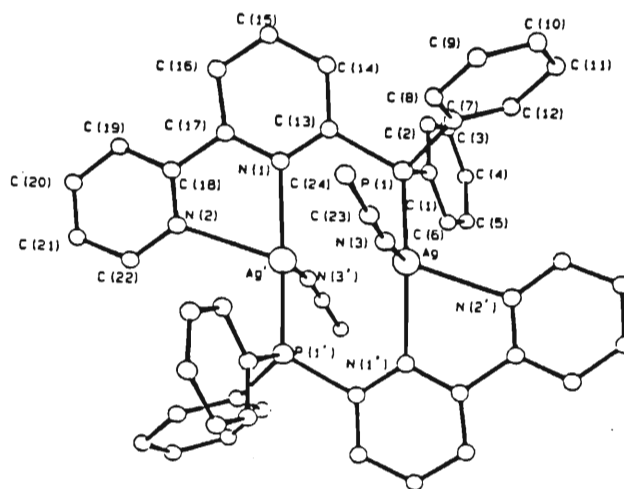
Fig. 1.2 : Structure of [Ag$_2$(μ-Ph$_2$Pbipy)$_2$(MeCN)$_2$]$^{2+}$

The acetonitrile ligands of the above-mentioned disilver complex are very labile and can be easily replaced by other ligands for example by 4-vinylpyridine (4-vinylpy) leading to the formation of [Ag$_2$(μ-Ph$_2$Pbipy)$_2$(4-vinylpy)$_2$]$^{2+}$ [6] (Fig. 1.3). The Ag⋯Ag separation is 4.012 Å which is much longer than the corresponding separation of 2.973 Å for [Ag$_2$(μ-Ph$_2$Pbipy)$_2$(MeCN)$_2$]$^{2+}$. The above-mentioned torsion and dihedral angles are 42 and 11° respectively which indicate that an increased torsional twist results when terminal substitution of the acetonitrile ligand occurs by a sterically more demanding ligand.
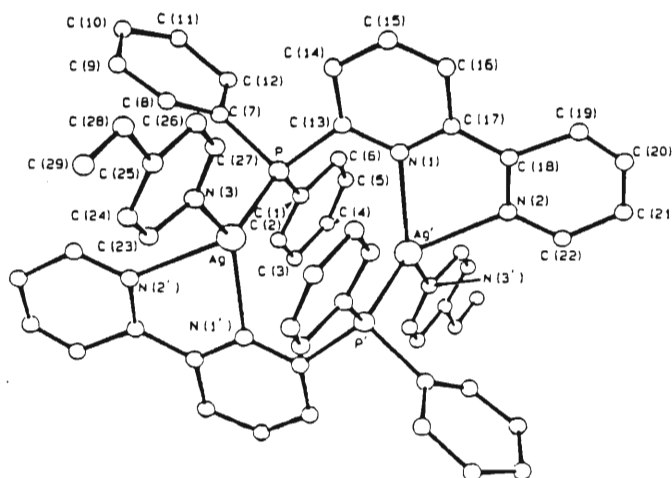
Fig. 1.3 : Structure of [Ag$_2$(μ-Ph$_2$Pbipy)$_2$(4-vinylpy)$_2$]$^{2+}$

The disilver complex [Ag$_2$(μ-Ph$_2$Pbipy)$_2${μ-OC(Me)O}]PF$_6$ [6] (Fig. 1.4) contains a bridging acetate ligand as well as two bridging Ph$_2$Pbipy ligands (head-to-tail). The bridging acetate group is compelled by virtue of its geometry to occupy *cis* sites on the metal atoms. Interestingly, it interacts sterically with the two bridging Ph$_2$Pbipy ligands to different extents. This is reflected by the very different P(2)-Ag(2)-Ag(1)-N(3) and P(1)-Ag(1)-Ag(2)-N(1) torsion angles of 10 and 30° respectively. The dihedral angles between the pyridyl rings of the bipy fragments of the corresponding Ph$_2$Pbipy ligands are 30 and 9° respectively. The inverse relationship between the torsion angle and the dihedral angle as well as the flexibility of the bridging Ph$_2$Pbipy ligand is well illustrated in this example.
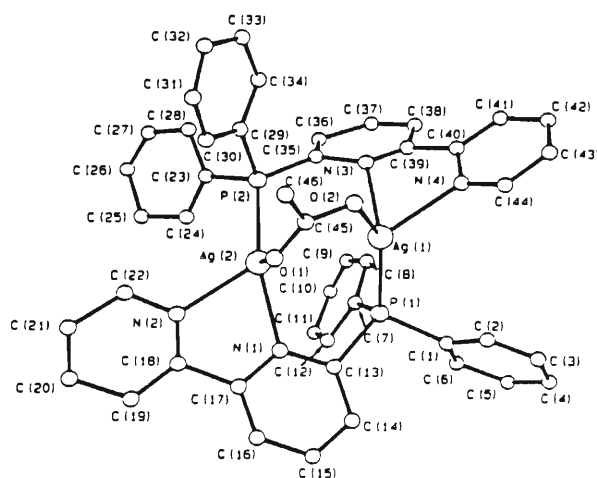
Fig. 1.4 : Structure of [Ag$_2$(μ-Ph$_2$Pbipy)$_2${μ-OC(Me)O}]$^+$

Another example of a complex containing a bridging acetate group is [Ru$_2$(μ-Ph$_2$Pbipy)$_2${μ-OC(Me)O}(CO)$_2$]PF$_6$ [9] (Fig. 1.5). The Ru-Ru distance is 2.688 Å, which corresponds to a formal Ru-Ru single bond. The octahedral geometry at each Ru atom is completed by a carbonyl group and the other Ru atom. These two carbonyl groups are situated at equatorial sites *trans* to the acetate group.

Fig. 1.5 : Structure of [Ru₂(μ-Ph₂Pbipy)₂{μ-OC(Me)O}(CO)₂]⁺
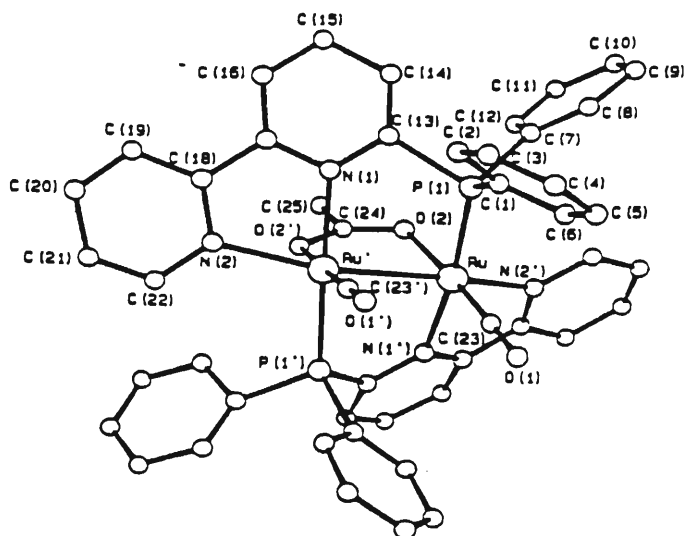
$$\text{Fig. 1.5 : Structure of } [Ru_2(\mu\text{-Ph}_2Pbipy)_2\{\mu\text{-OC(Me)O}\}(CO)_2]^+$$

The only structurally characterised neutral species containing the Ph₂Pbipy ligand in a bridging coordination mode is [Ag₂(μ-Ph₂Pbipy)₂(NO₃)₂] [6] (Fig. 1.6). The irregular tetrahedral geometry around each silver atom is completed by the nitrate anion which is bonded in a terminal fashion through one of the oxygen atoms to the silver metal atom. The Ag····Ag separation is 2.935 Å which is slightly shorter than the value of 2.973 Å found for [Ag₂(μ-Ph₂Pbipy)₂(MeCN)₂](PF₆)₂. A large P-Ag-Ag'-N torsion angle of 46° observed is consistent with the substitution of the acetonitrile ligand with the more bulky nitrate ligand.

Fig. 1.6 : Structure of [Ag₂(μ-Ph₂Pbipy)₂(NO₃)₂]
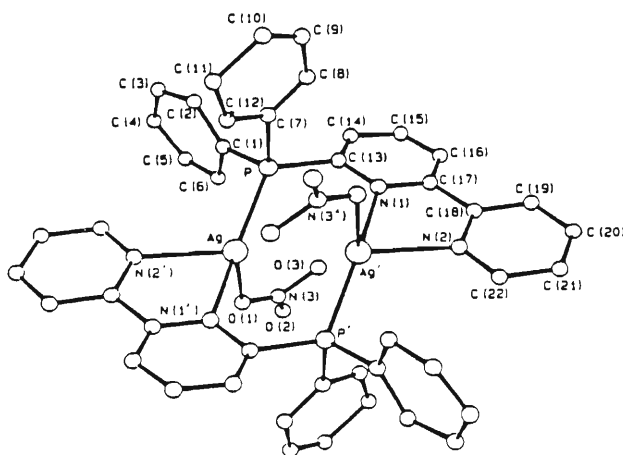
$$\text{Fig. 1.6 : Structure of } [Ag_2(\mu\text{-Ph}_2Pbipy)_2(NO_3)_2]$$

Very few complexes listed in Table 1.1 contain the bridging ligand coordinated in a head-to-head manner. The dicopper complex $[Cu_2(\mu\text{-}Ph_2Pbipy)_2(\eta\text{-}bipy)](PF_6)_2$ [7] (Fig. 1.7) is an example of a complex which exhibits this type of ligand coordination. The phosphorus atoms of the two bridging ligands and the chelating η-bipy ligand complete the tetrahedral geometry at Cu1. The bipy fragment of each of the Ph_2Pbipy ligands chelate at Cu2. The large P1-Cu1-Cu2-N1 and P2-Cu1-Cu2-N4 torsion angles of 46 and 57° respectively indicate that there is a great deal of steric crowding surrounding the metal atoms.
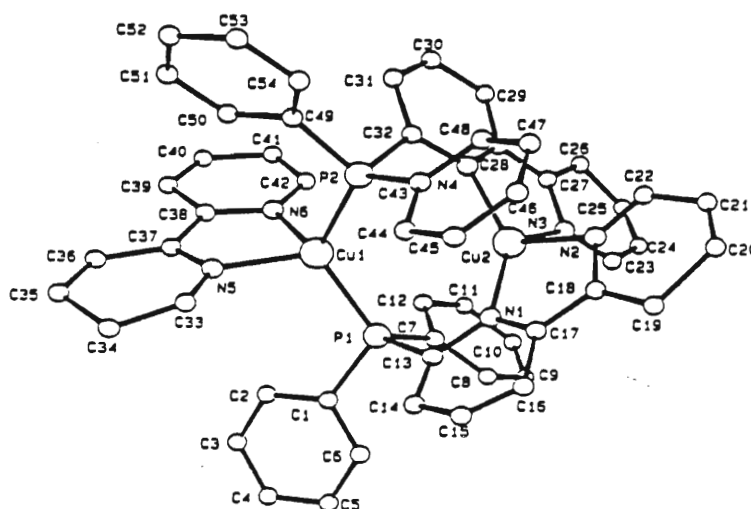
Fig. 1.7 : Structure of $[Cu_2(\mu\text{-}Ph_2Pbipy)_2(\eta\text{-}bipy)]^{2+}$

To date, only one nickel complex containing the Ph_2Pbipy ligand whose structure has been determined by X-ray crystallography is known. The complex is $[Ni_2(\mu\text{-}Ph_2Pbipy)_2(CO)_2](BF_4)_2$ [8] (Fig. 1.8). The nickel atoms are linked by two head-to-head Ph_2Pbipy ligands. Two cis-disposed carbonyl ligands and the phosphorus atoms of the Ph_2Pbipy ligands complete the coordination at the nickel atom. The Ni1····Ni2 separation of 4.259 Å is the longest metal-metal separation known to be spanned by the Ph_2Pbipy ligand (Table 1.1). An important feature of this complex is the existence of mixed valency. This complex can be formulated as a "d^8 - d^{10}" dimer with Ni1 being the d^{10} centre and Ni2 being the d^8 centre. This formulation is consistent with the softer carbonyl ligands and the phosphorus donor atoms being bonded to Ni1 and the harder

9

nitrogen donor atoms being bonded to Ni2. Had the Ph_2Pbipy ligand coordinated to the nickel atoms in a head-to-tail manner a "d^8-d^8" or Ni(II)-Ni(II) dimer would have ensued. This complex is one of the few mixed valence homodinuclear complexes known in which the metal atoms have the same coordination geometries [10].
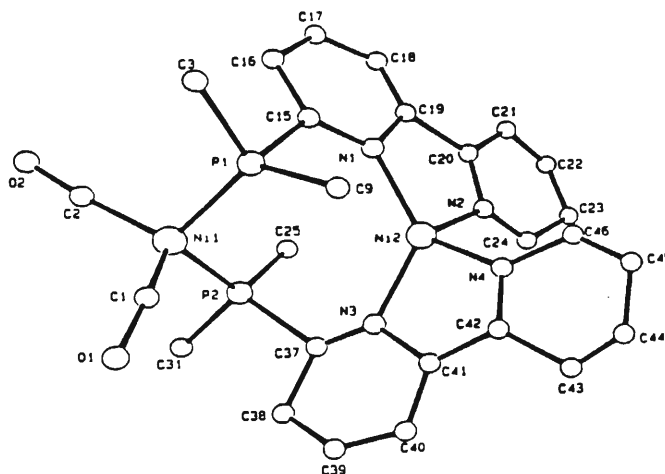
Fig. 1.8 : Structure of $[Ni_2(\mu-Ph_2Pbipy)_2(CO)_2]^{2+}$. Only the carbon atoms bound to P in the two Ph_2P entities are shown.

Table 1.1 summarises selected structural features for the bridging Ph_2Pbipy ligand in all complexes whose structures have been determined X-ray crystallographically. The M-M distances for the complexes vary between 2.688 - 4.259 Å which is much larger than the bite of 2.657 Å for the Ph_2Pbipy ligand[3]. This illustrates the flexibility of the ligand in terms of its ability to bridge a wide range of M-M distances.

The P-M-M-N torsion angles are related to the size of the terminal ligand bonded to each of the metal atoms, e.g. $[Cu_2(\mu-Ph_2Pbipy)_2(MeCN)_2](PF_6)_2$[7] has a torsion angle of 27° whereas $[Cu_2(\mu-Ph_2Pbipy)_2(PhCN)_2](PF_6)_2$[5] with the larger PhCN ligand has one of 40°. The presence of a third bridging ligand leads to a decrease in these torsion angles as found for $[Cu_2(\mu-Ph_2Pbipy)_2(\mu-Br)]PF_6$ [5] where the torsion angle is 20°. These results illustrate that the bridging Ph_2Pbipy ligand is able to twist about the M - M vector in order to accommodate the stereochemical demands of the other ligands. However, there is no direct correlation between the P-M-M-N torsion angle and the M-M distance.

The bipy fragment is not planar and can easily twist around the interannular bond which results in the dihedral angle between the pyridine rings of the bipy fragment varying between 5 and 30°. Interestingly, there appears to exist an inverse relationship between dihedral and torsion angles indicating that the ligand predominately twists either around the interannular bond in the bipy fragment or about the M-M vector. Furthermore, it seems that the larger the terminal ligand, the more is torsional twist favoured over dihedral rotation, while the reverse is true when a third bridging ligand is present in the complex.

1.1.3. CHELATING Ph$_2$Pbipy (mode 4)

There are no reported examples of the ligand itself bonding in the tridentate chelating mode to a single metal centre. However, the oxidized form of the ligand *viz* Ph$_2$P(O)bipy has been shown to adopt a chelating mode in which the two bipy nitrogen atoms and the oxygen atom bond to the same metal atom. The complex formed is [Ni{η^3-Ph$_2$P(O)bipy}$_2$](BF$_4$)$_2$ [8] (Fig. 1.9). The geometry around the nickel atom is octahedral. The two oxygen atoms are *cis* with respect to each other. Of significance here is that the oxidized ligand forms a 5-membered chelate ring with the metal and, as such, is more likely to chelate a single metal centre rather than bridge two metal centres. Thus is in contrast to the unoxidized form of the ligand which is unlikely to chelate because of the inherent stability in a 4-membered ring; as already discussed it prefers to bridge two metal atoms.
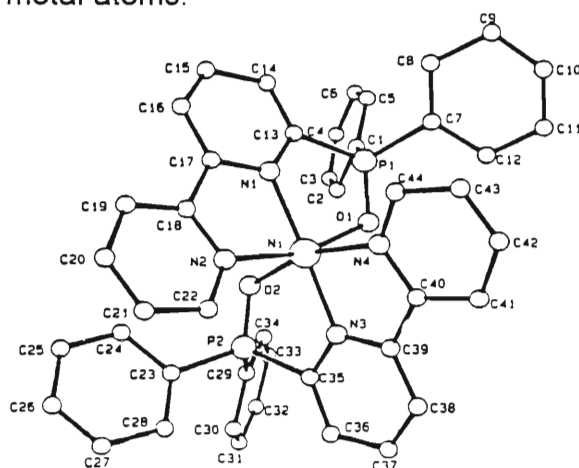
Fig. 1.9 : Structure of [Ni{η^3-Ph$_2$P(O)bipy}$_2$]$^{2+}$

1.2 THE 6-ANILINO-2,2'-BIPYRIDINE (Habipy) AND 2,2'-BIPYRIDYL-6-OL (HObipy) LIGANDS

Habipy

HObipy
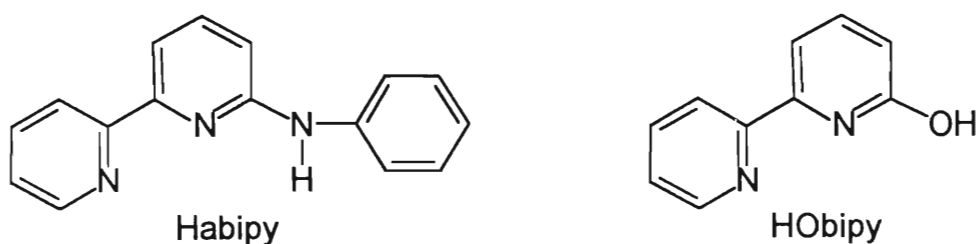
These two ligands Habipy [11] and HObipy [12] are discussed together because of the similarity in their coordination chemistry. The Habipy and HObipy ligands are similar to the Ph_2Pbipy ligand, the main difference being the nature of the donor atom in the 6-position, i.e., nitrogen and oxygen, respectively. Another important difference between these ligands and Ph_2Pbipy, besides the nature of the donor atoms, is that Ph_2Pbipy has extra and sterically demanding phenyl groups. The exocyclic nitrogen and oxygen atoms are σ donors and are considered to be "hard" donor atoms, unlike the phosphorus atom of the Ph_2Pbipy ligand which is both a donor of σ electrons and an acceptor of π electrons, and which is considered to be a "soft" donor atom.

The protons on the exocyclic anilino or hydroxy group of these ligands are relatively acidic and can be easily abstracted to yield the anionic ligands, abipy and Obipy. Extensive studies have been carried out in respect of the coordination of the anionic forms of the analogous 2-aminopyridyl[13] and 2-hydroxypyridyl[14] ligands to metal atoms. Thus, the anionic forms of Habipy and HObipy should also generate an extensive interest in coordination chemistry.

In principle these ligands in either their neutral or anionic forms may adopt one of five different coordination modes (Scheme 1.2); one chelating mode (1), three bridging modes (2, 3 and 4) and one terminal mode (5). The exocyclic nitrogen or oxygen atom of anionic abipy and Obipy can coordinate in either a terminal fashion or bridge two metal atoms, whereas with the neutral Ph_2Pbipy ligand the phosphorus atom can only coordinate in a terminal fashion. All studies undertaken thus far to determine the coordination behaviour of these ligands indicate that the chelating mode (1) and the

bridging mode (2) are the most likely modes of coordination [11].

X=NPhH,OH,NPh,O
(1)

X=NPhH,OH,NPh,O
(2)

X=OH,NPh,O
(3)

X=OH,NPh,O
(4)

X=NPhH,OH,NPh,O
(5)
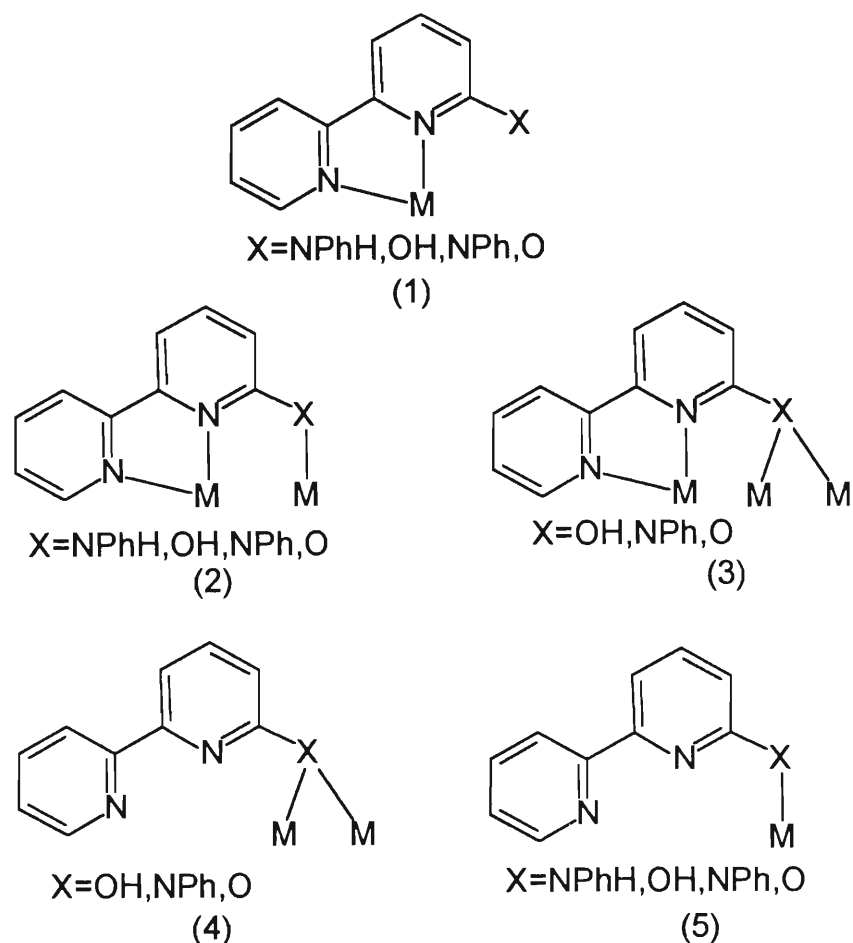
Scheme 1.2: Possible modes of coordination of the Habipy, HObipy, abipy and Obipy ligands

1.2.1 CHELATING Habipy

The only reported complex containing the Habipy ligand bonded to a metal atom is [Cu(η-Habipy)$_2$]PF$_6$ [11]. The proposed structure of this monomeric complex based on elemental analysis, ^{1}H nmr and IR spectroscopic data is illustrated in Fig.1.10. The nitrogen atoms of the bipy fragment of the each ligand chelate to the copper atom while the nitrogen atom of the anilino group remains uncoordinated. The geometry around the copper atom is expected to be tetrahedral. The IR spectrum of [Cu(η-Habipy)$_2$]PF$_6$ displays a N-H stretching band at 3340cm^{-1} confirming the presence of the neutral form

of the ligand.
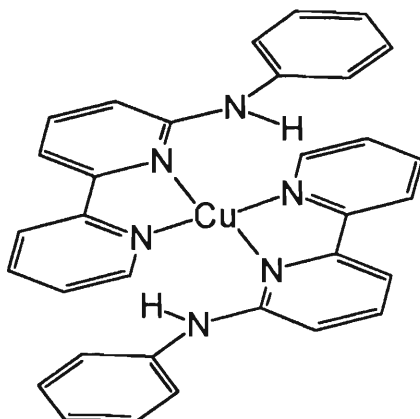
Fig. 1.10 : Proposed structure of [Cu(η-Habipy)₂]⁺

1.2.2 BRIDGING abipy AND Obipy

The diruthenium ligand-bridged species $[Ru_2(\mu\text{-Obipy})_2(CO)_4]$[11] (Fig.1.11) is an example of a complex bridged in a head-to-tail fashion by two Obipy ligands. Each ruthenium has an irregular octahedral geometry in which the axial sites opposite the Ru-Ru bond are occupied by one of the nitrogen atoms of the bipyridyl fragments of each of the two Obipy ligands. The equatorial sites on each metal atom are occupied by the oxygen atoms of the Obipy ligands, which are mutually *cis*, and by the two carbonyls which are also *cis* to one another.
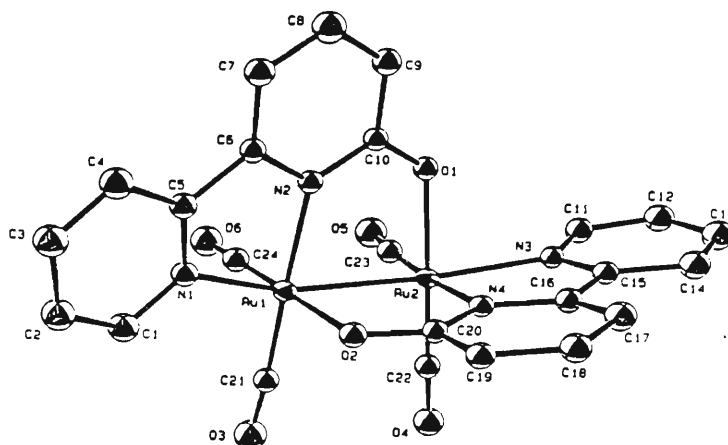
Fig. 1.11 : Structure of [Ru₂(μ-Obipy)₂(CO)₄]

14

In the [Mo_2(μ-abipy){μ-OC(Me)O}$_3$] [11] complex (Fig. 1.12) only one abipy ligand is present which bridges the metal atoms. The abipy ligand chelates at one Mo atom *via* its bipyridyl fragment and in so doing one of the nitrogen atoms occupies an axial site on the molybdenum atom and the other an equatorial site. The exocyclic nitrogen atom bonds to the second molybdenum atom (Mo2) in an equatorial position. The coordination around the molybdenum atoms is completed by three bridging acetate ligands. Thus one molybdenum atom (Mo1) has an irregular octahedral geometry while, interestingly, the other (Mo2) has a slightly distorted square pyramidal geometry *i.e.*, the second molybdenum (Mo2) has an unoccupied available site and a lower coordination number.
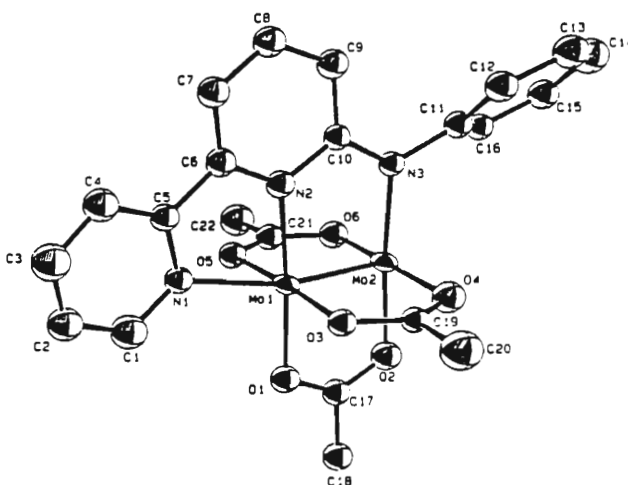
Fig. 1.12 : Structure of [Mo_2(μ-abipy){μ-OC(Me)O}$_3$]

Table 1.2 : Complexes containing the abipy and Obipy ligands

COMPLEX	GEOMETRY AT METAL ATOM	M-M (Å)	REF
[Ru_2(μ-abipy)$_2$(CO)$_4$]	irregular octahedral	2.668	11
[Ru_2(μ-Obipy)$_2$(CO)$_4$]	irregular octahedral	2.671	11
[Ru_2(μ-abipy){μ-OC(Me)O}$_3$Cl]	irregular octahedral	2.294	11
[Rh_2(μ-abipy){μ-OC(Me)O}$_3$NCPh]	irregular octahedral	2.399	11
[Mo_2(μ-abipy){μ-OC(Me)O}$_3$]	irregular octahedral[a] square pyramidal[a]	2.094	11

[a] The molybdenum atoms have different coordination geometries.

The bridging coordination mode is evident for structures containing the anionic ligands, abipy and Obipy. Table 1.2 summarises selected structural features for the complexes containing the bridging abipy and Obipy ligands. For all of the dinuclear complexes containing abipy or Obipy ligands, a formal metal-metal bond exists in the dimer. The N-M-M-N torsion angles are very small indicating that these ligands are planar except for the phenyl ring.

1.3 THE 6-N-METHYLANILINO-2,2'-BIPYRIDINE (mabipy) AND 6-PIPERIDINO-2,2'-BIPYRIDINE (pipbipy) LIGANDS

mabipy   pipbipy

The mabipy ligand [11] is similar to the Habipy ligand differing only in the replacement of the hydrogen atom by a methyl group; Habipy is a secondary amine with respect to the exocyclic nitrogen atom, whereas mabipy and pipbipy[11] are tertiary amines and, as such, do not possess ionisable hydrogen atoms. Changing the substituent group on the exocyclic nitrogen atom alters the donor ability of the amine fragment. The more electron rich the groups, the better the σ donor ability of the nitrogen. The order of increasing donor ability of the exocyclic amines is: Habipy < mabipy < pipbipy < abipy.

The possible modes of coordination for these ligands are analogous to those illustrated in Scheme 1.2. However, the preferred modes of coordination of these ligands to metal atoms are shown in Scheme 1.3. For the one, chelation occurs through solely the bipy fragment (1), while for the other simultaneous chelation and bridging occurs (2). The mabipy and pipbipy ligands were reacted with both copper (I) and copper(II) precursors; the copper(I) precursor being chosen as it affords dinuclear ligand-bridged complexes with the Ph$_2$Pbipy ligand [5]. However, in all the copper complexes with mabipy and pipbipy ligands synthesised to date the ligand adopts the chelating mode (1).

(1)   (2)

X=N-methylanilino, piperidino

Scheme 1.3 : Preferred modes of coordination for the mabipy and pipbipy ligands

1.3.1 CHELATING mabipy

Reaction of mabipy with a copper(I) precursor $[Cu(MeCN)_4]^+$ produced a complex characterised as $[Cu(\eta\text{-mabipy})_2]PF_6$ [11] (Fig. 1.13). This mononuclear complex has two ligands chelating to the copper atom through their bipyridyl fragments with the N-methylanilino nitrogen atoms uncoordinated. The geometry adopted around the copper atom is irregular tetrahedral.

Fig. 1.13 : Structure of $[Cu(\eta\text{-mabipy})_2]^+$

Reaction of mabipy with a copper(II) precursor also produced a mononuclear complex, $[Cu(\eta\text{-mabipy})_2]^{2+}$ [11]. The overall molecular structure of this complex is very similar to that of $[Cu(\eta\text{-mabipy})_2]^+$ [11], the only differences being a slight shortening of the Cu-N distances in the Cu(II) species.

17

1.3.2 CHELATING pipbipy

The mode of coordination of this ligand when bonded to copper(I) is identical to that of the mabipy ligand. The bipy fragments chelate to the metal atom while the piperidyl fragments remain uncoordinated. The geometry about the copper atom in the complex [Cu(η-pipbipy)$_2$]PF$_6$ [11] (Fig. 1.14) is a very distorted tetrahedron.
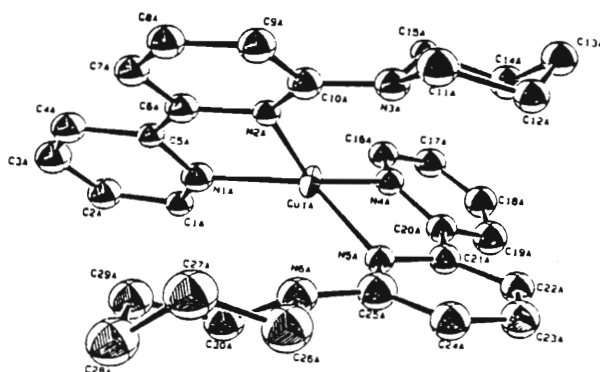
Fig. 1.14 : Structure of [Cu(η-pipbipy)$_2$]$^+$

The mabipy and pipbipy ligands form monomeric complexes with two ligands chelating the metal atom *via* the bipyridyl fragment. No dimeric complexes of copper(I) or copper(II) have as yet been reported with this ligand. This is also true of the abipy and Obipy ligands and may reflect the relative lack of affinity of the hard nitrogen donor atom to copper.

1.4 THE 2-ANILINO-1,10-PHENANTHROLINE (2-NHPh-phen) LIGAND

2-NHPh-phen

18
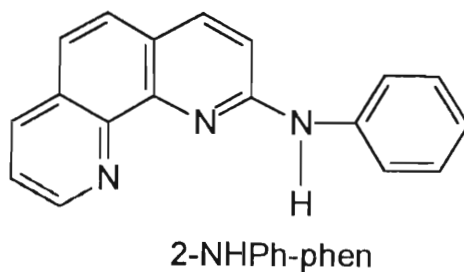
The 2-anilino-1,10-phenanthroline ligand possesses three donor nitrogen atoms. This tridentate ligand has not been isolated as a pure compound *via* a designed synthesis. Rather it has been obtained fortuitously as a coordinated ligand in its anionic form in the "d^{10} - d^{10}" Cu(I) dimer, [Cu$_2$(2-NPh-phen)$_2$] [15]. The latter is synthesised by the reaction of a tetrazenido dianion of [Li(THF)$_x$]$_2$[PhNN=NNPh] with [CuCl$_2$(phen)$_2$] [15], a reaction in which a NPh fragment inserts into the *ortho* C-H bond of phenanthroline. The structure of the Cu(I) dimer is illustrated in Fig. 1.15.
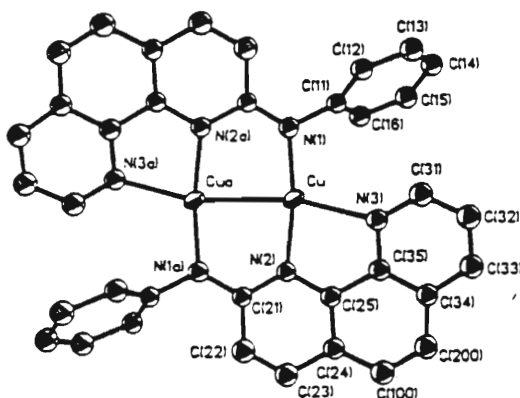
Fig. 1.15 : Structure of [Cu$_2$(2-NPh-phen)$_2$]

Two ligands bridge the copper atoms with the two nitrogen atoms of the phenanthroline fragment bonded to one copper atom and the nitrogen atom of the phenylamino fragment bonded to the second copper atom. A centre of symmetry lies midway between the two copper atoms. The square planar geometry at each copper atom is completed by the other copper atom. A very short Cu-Cu distance of 2.600 Å is observed. All the atoms except for the two N-phenyl rings lie roughly in the same plane. This is evident by the N(2)-Cu-Cua-N(1a) torsion angle of 6.86°. The two phenyl rings are twisted out of this plane with a dihedral angle of 67°.

1.5 AIMS OF THIS PROJECT

The initial aim was to develop a synthesis for the new ligand 2-diphenylphosphino-1,10-phenanthroline and to study its coordination to a range transition metals. The

Ph$_2$Pphen ligand may be regarded as an extension of the Ph$_2$Pbipy ligand in that the bipyridyl fragment has been replaced by the planar phenanthroline fragment.

The feasible modes of coordination of the Ph$_2$Pphen ligand are expected to be very similar to that of the Ph$_2$Pbipy ligand. It is possible for the Ph$_2$Pphen ligand to coordinate terminally through the phosphorus atom only (1) as in the case of the Ph$_2$Pbipy ligand in [Rh(η-Ph$_2$Pbipy)$_2$(CO)Cl] [5].

The bridging mode (2) of coordination whereby the two nitrogen atoms of the phen fragment chelate to one metal atom and the phosphorus atom bonds to a second metal atom is very likely since the Ph$_2$Pbipy ligand is well established as a bridging ligand [5-9,19].

Phenanthroline is well established as a chelating ligand and therefore it is possible for the phen fragment of the Ph$_2$Pphen ligand to coordinate in a similar manner (3) [2]. The chelating mode (4) whereby all three donor atoms of the ligand bond to the same metal is theoretically possible but not that likely due to the known propensity of the Ph$_2$Pbipy ligand to adopt a bridging mode of coordination [5-9,19].
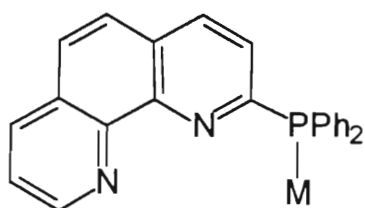
terminal (1)
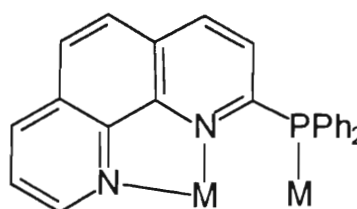
bridging (2)
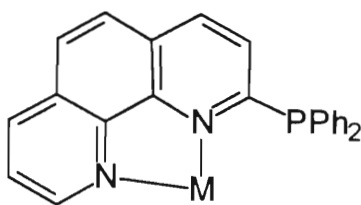
chelating (3)
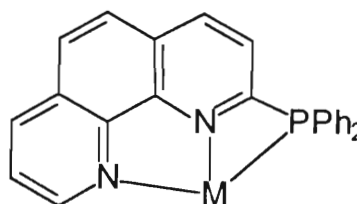
chelating (4)

The coordination chemistry of the Ph_2Pphen ligand with copper(I) precursors was studied. Copper(I) is known to form dinuclear complexes with the Ph_2Pbipy ligand. Such complexes include $[Cu_2(\mu-Ph_2Pbipy)_2(MeCN)_2](PF_6)_2$ and $[Cu_2(\mu-Ph_2Pbipy)_2(\eta-2,2'-bipy)_2](PF_6)_2$ [7] which are known to electrochemically catalyse the reduction of carbon dioxide. Thus a further objective of this study was to synthesise analogous complexes of the Ph_2Pphen ligand and to test their ability to function as electrocatalysts for carbon dioxide reduction.

Very few reports of the coordination chemistry of the substituted polypyridine ligands reviewed are known. Hence, another objective was to study the reactions of Ph_2Pphen with platinum(II) and palladium(II) containing precursors, in view of the fact that these two metals exhibit square-planar rather than the tetrahedral coordination typical of copper(I) .

CHAPTER 2

THE SYNTHESIS AND CHARACTERISATION OF THE 2-DIPHENYLPHOSPHINO-1,10-PHENANTHROLINE LIGAND

The aim of the work described in this chapter was to synthesise and characterise the 2-diphenylphosphino-1,10-phenanthroline (Ph$_2$Pphen) ligand.

The only reported synthesis of 2-diphenylphosphino-1,10-phenanthroline was that by R. Ziessel in 1989, who described the preparation of the ligand by reaction of one equivalent of 2-chloro-1,10-phenanthroline with two equivalents of lithium diphenylphosphide (Ph$_2$PLi) at –40 °C for five hours under strictly air-free conditions[16]. The product was purified by column chromatography. However, very few details were outlined in the report by Ziessel.

In this chapter, a substantially modified procedure for the synthesis of the 2-chloro-1,10-phenanthroline precursor[17] together with the conversion of this species to the diphenylphosphino derivative based on methods used in our laboratories, is reported.

2.1 RESULTS AND DISCUSSION

The 2-diphenylphosphino-1,10-phenanthroline ligand is synthesised *via* a four-step procedure (see Scheme 2.1). The first step involves the methylation of one of the nitrogen atoms of the phenanthroline by methyl iodide to afford 1-methyl-1,10-phenanthrolinium iodide. This step proceeds with good yields and no by-products. Suitable spectral and elemental analyses were obtained for the product.

In the second step, a strongly alkaline solution of ferric salts is used to oxidise 1-methyl-1,10-phenanthrolinium iodide to 1-methyl-1,10-phenanthrolin-2-one. The product yield is temperature dependent and a reaction temperature of 10 °C should be maintained during the addition of 1-methyl-1,10-phenanthroline iodide to the alkaline

solution of ferric salts. A reaction time of 24 hours gives the best yields.

1,10-phenanthroline

2-diphenylphosphino-1,10-phenanthroline
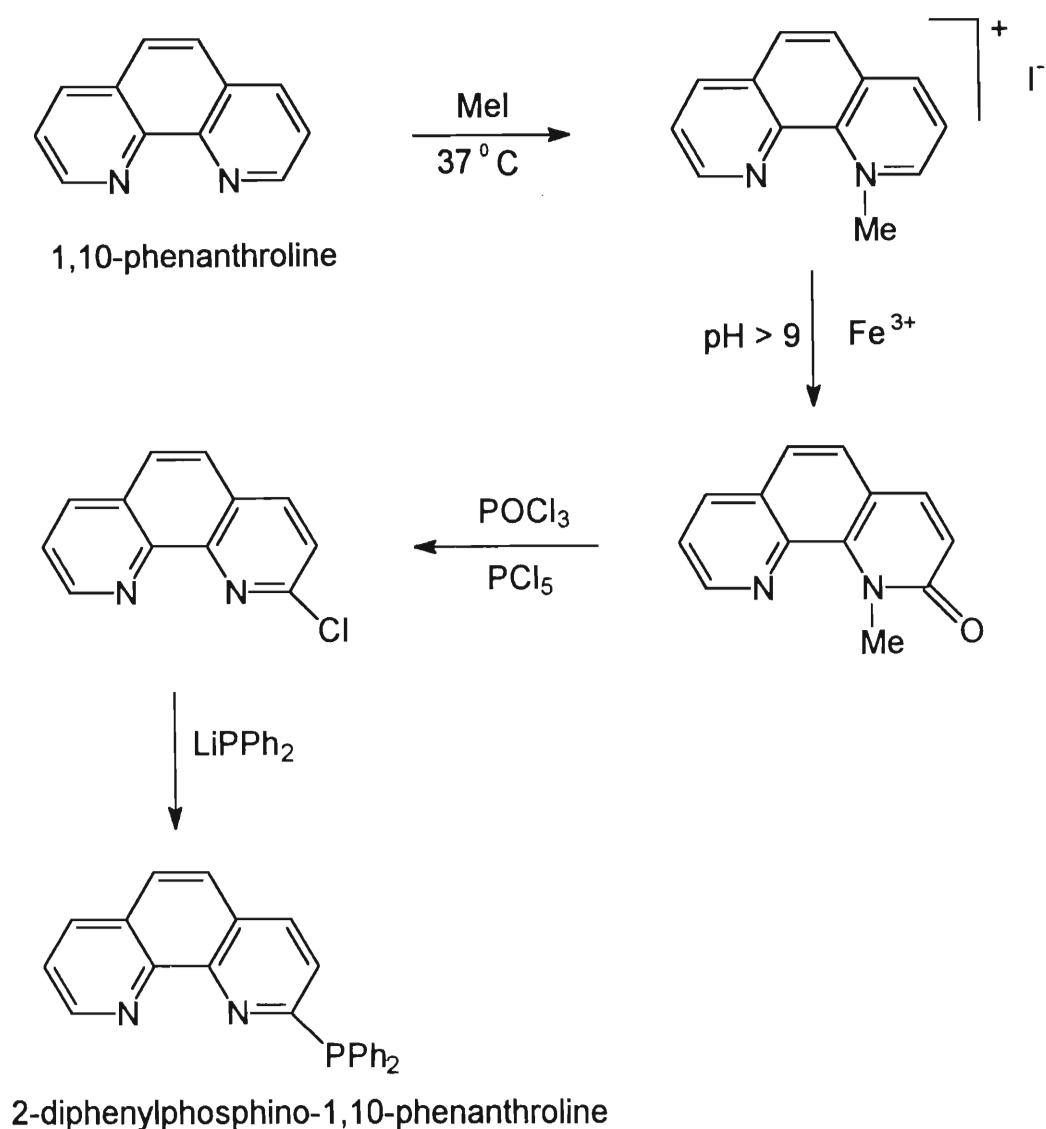
Scheme 2.1 : Synthesis of 2-diphenylphosphino-1,10-phenanthroline

The third step of the procedure involves the chlorination of the keto group by phosphorus pentachloride and phosphoryl chloride to afford 2-chloro-1,10-phenanthroline. Excess phosphoryl chloride is removed by the addition of ice to the solution. This is an exothermic reaction and HCl gas is formed.

The fourth step of the ligand synthesis is modified [16] and involves the reaction between lithium diphenylphosphide and 2-chloro-1,10-phenanthroline under an inert atmosphere. Firstly, lithium diphenylphosphide is prepared by the reaction of BuLi and diphenylphosphine in ultra dry tetrahydrofuran (thf). The 2-chloro-1,10-phenanthroline is dissolved in thf and is added dropwise to the lithium diphenylphosphide solution at -78 °C.

Once addition of the 2-chloro-1,10-phenanthroline is complete, the solution is allowed to warm up to room temperature and stirred overnight. The by-products of the reaction i.e., lithium chloride and lithium diphenylphosphide are easily removed by extraction with degassed water and by extraction with boiling hexane respectively. The ligand obtained is analytically pure and is stable under an inert atmosphere.

The Ph_2Pphen ligand is air sensitive, the phosphorus atom being readily oxidised to the corresponding phosphorus oxide, evidence for this being the appearance in the $^{31}P\{^1H\}$ nmr spectrum of a singlet at 17.37 ppm. However, the oxidised phosphine cannot be separated from the Ph_2Pphen, unlike the Ph_2Pbipy ligand which is readily separated from its phosphine oxide [3].

Table 2.1 lists the characterisation data for the Ph_2Pphen ligand. The $^{31}P\{^1H\}$ nmr spectrum consists of a sharp singlet at -3.40 ppm, a chemical shift which clearly distinguishes the free ligand from the oxide, which has a ^{31}P chemical shift downfield to that for the free ligand. The high field value is indicative of the high electron density on the phosphorus atom of the free ligand. As indicated in Table 2.1, the peaks in the ^1H nmr spectrum of Ph_2Pphen ligand can be assigned to individual protons but complex coupling effects in the ^{13}C nmr spectrum prevented an equivalent assignment of the individual carbon atoms.

Elemental analysis of the ligand indicated that water was present. This was not unexpected because of the strong hydrogen bonding to the nitrogen atoms of the phen fragment.

Table 2.1 : Spectroscopic data for 2-diphenylphosphino-1,10-phenanthroline

^{31}P nmr (ppm)[a]	-3.40
^{1}H nmr (ppm)[b]	9.20 (1H, dd, H_9), 8.18 (1H, dd, H_7)
	8.15 (1H, dd, H_4) 7.68 (2H, dd, H_5 & H_6)
	7.54 (1H, m, H_8) 7.26 (11H, m, H_3 & Ph)
^{13}C nmr (ppm)[c]	123-132 (19C, Aromatic CH's)
	132-166 (5C, quat. C's)
Infrared (cm^{-1})[d]	1614 (w), 1575(m), 1542(m), 1477 (s),
	1433(s), 1420(m), 1377 (m), 1082 (m)
GC-MS	m/z 363

[a] ppm values measured relative to $P(OMe)_3$ as internal standard in $CDCl_3$.

[b] Measured in $CDCl_3$, dd=doublet of doublets, m=multiplet.

[c] Measured in $CDCl_3$.

[d] KBr disk, w=weak, m=medium, s=strong.
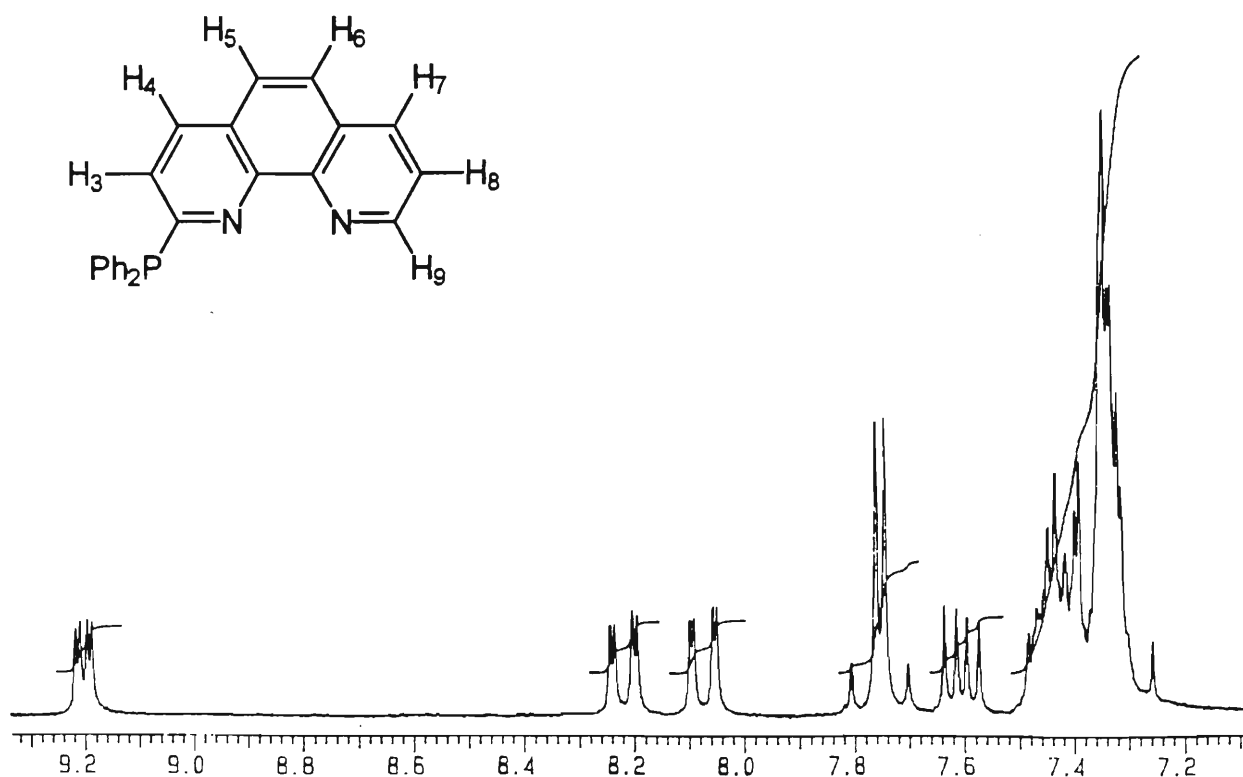
Figure 2.1 : The ^{1}H nmr spectrum of 2-diphenylphosphino-1,10-phenanthroline

25

2.2 EXPERIMENTAL

2.2.1 Synthesis of 1-methyl-1,10-phenanthrolinium iodide

A solution of 1,10-phenanthroline (18.0 g, 0.100 mol) and methyl iodide (15 ml, 0.105 mol) in nitrobenzene (150 ml) was stirred at 37 °C for 24 hours. The microcrystalline material which separated out was washed with benzene and recrystallised from methanol. The 1-methyl-1,10-phenanthrolinium iodide obtained was sufficiently pure for the next step of the synthesis.
Yield: 23.5 g (73%). Mpt. 211 °C. [Found: C, 48.56; H, 3.67; N, 8.44. Calc. for $C_{13}H_{11}N_2I$: C, 48.47; H, 3.44; N, 8.70%].

2.2.2 Synthesis of 1-methyl-1,10-phenanthrolin-2-one

Saturated aqueous solutions of NaOH (11.68 g, 0.292 mol) and 1-methyl-1,10-phenanthrolinium iodide (23.5 g, 0.073 mol) were added dropwise to a cold saturated aqueous solution of potassium ferricyanide (48 g, 0.146 mol). The reaction mixture stirred at 10 °C for 2 hours and subsequently at room temperature for 15 hours. The resulting precipitate was refluxed in benzene. The brown solid obtained on removal of the benzene was recrystallised from benzene.
Yield : 10 g (66%). Mpt. 122 °C. [Found: C, 74.36; H, 4.50; N, 13.18. Calc. for $C_{13}H_{10}N_2O$: C, 74.27; H, 4.79; N, 13.32%].

2.2.2 Synthesis of 2-chloro-1,10-phenanthroline

A 500 ml round-bottomed flask, fitted with a reflux condenser with a DMSO bubbler, was charged with 1-methyl-1,10-phenanthrolin-2-one (10 g, 0.048 mol), phosphorus pentachloride (10 g, 0.048 mol) and phosphoryl chloride (100 ml, 1.073 mol). The solution refluxed at 130 °C for 15 hours and then cooled to room temperature. Excess phosphoryl chloride was removed by the addition of ice, producing a large amount of HCl gas. Once the evolution of the HCl gas had ceased, the resulting black solution

was basified with ammonia to a pH of *ca.* 10 and then allowed to stand at room temperature for 24 hours. The brown precipitate formed was dissolved in dichloromethane and the solution treated with activated charcoal. After filtering and evaporation of the filtrate under reduced pressure, the cream product formed was dried *in vacuo.* GC-MS studies revealed a molecular ion peak (M^+) at 214.

Yield : 7 g (68%). Mpt. 128 °C. [Found: C, 67.27; H, 3.01; N, 12.60. Calc. for $C_{12}H_7N_2Cl$: C, 67.15; H, 3.29; N, 13.05%].

2.2.4 *Synthesis of 2-diphenylphosphino-1,10-phenanthroline*

All manipulations in this preparation were performed under an atmosphere of argon. The thf used was first distilled from sodium and benzophenone and then redistilled from calcium hydride under an argon atmosphere to ensure absolute dryness.

BuLi (21.5 ml, 0.033 mol) was added dropwise to a cold solution of Ph_2PH (5.7 ml, 0.033 mol) in thf (50 ml). The resulting deep orange solution of lithium diphenylphosphide was stirred at room temperature for 1.5 hours. This solution was cooled to -78 °C and a solution of 2-chloro-1,10-phenanthroline (7 g, 0.033 mol) in thf (50 ml) was added dropwise. The colourless solution obtained was stirred at room temperature for 15 hours. Thereafter, this solution was taken to dryness and the residue dissolved in chloroform. The chloroform solution was extracted with degassed water until the chloroform extract was clear. This extract was dried over $MgSO_4$ for 4 hours. After filtration from the $MgSO_4$, the volume of the chloroform was reduced and hexane added. The mixture was stored at -25 °C and the microcrystalline cream material obtained was pure ligand.

Yield: 10.2 g (83%). Mpt.123 °C. [Found: C, 77.55; H, 4.57; N, 7.34. Calc. for $C_{24}H_{17}N_2P.\frac{1}{2}H_2O$ C, 77.00; H, 4.81; N, 7.48%].

CHAPTER 3

DINUCLEAR 2-DIPHENYLPHOSPHINO-1,10-PHENANTHROLINE LIGAND BRIDGED DERIVATIVES OF COPPER(I)

3.1 INTRODUCTION

Many studies of the coordination behaviour of nitrogen and phosphorus donor ligands with the copper(I) precursor $[Cu(MeCN)_4]^+$ have been made. As discussed in Chapter 1, the 6-diphenylphosphino-2,2'-bipyridine (Ph$_2$Pbipy) ligand is a versatile one and has been shown to coordinate to a wide range of metal atoms including copper [5-9,19]. In particular it was found to react with $[Cu(MeCN)_4]^+$ to afford the bridged dinuclear complex $[Cu_2(\mu-Ph_2Pbipy)_2(MeCN)_2]^{2+}$ [7]. T. C. W. Mak *et al.* have recently synthesised a new related tridentate phosphine ligand, 2-(diphenylphosphino)-6-(pyrazol-1-yl)pyridine (Ph$_2$Ppypz) [18]. Reaction of the Ph$_2$Ppypz ligand with $[Cu(MeCN)_4]ClO_4$ resulted in the formation of $[Cu_2(\mu- Ph_2Ppypz)_2(MeCN)_2](ClO_4)_2$ [18].
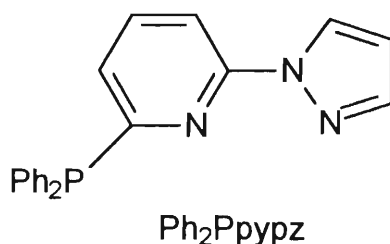
Ph$_2$Ppypz

Ligands analogous to Ph$_2$Pbipy *e.g.*, 6-[ethyl(phenyl)phosphino]-2,2'-bipyridine [Et(Ph)Pbipy] and 6-(diphenylphosphino)-2-(2-quinolyl)pyridine (Ph$_2$Ppyquin) [19] have recently been synthesised in our laboratory and their reaction with $[Cu(MeCN)_4]^+$ investigated. The reaction involving [Et(Ph)Pbipy] affords $[Cu_2(\mu-Et(Ph)Pbipy)_2(MeCN)_2]^{2+}$ [19] in which each copper atom has a distorted tetrahedral arrangement as illustrated in Fig. 3.1. Reaction of Ph$_2$Ppyquin also results in the formation of a dicopper complex $[Cu_2(\mu-Ph_2Ppyquin)_2(MeCN)_2]^{2+}$ [19] (Fig. 3.2). An interesting feature of the two above-mentioned complexes is that the acetonitrile

ligands of these complexes are *cis* with respect to each other which differs from that of $[Cu_2(\mu\text{-Ph}_2Pbipy)_2(MeCN)_2]^{2+}$ [7] where the acetonitrile ligands are *trans*.
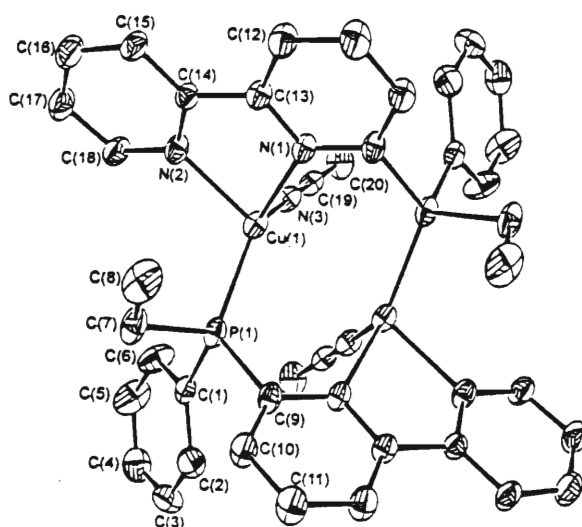
Fig. 3.1 : Structure of $[Cu_2(\mu\text{-Et(Ph)Pbipy})_2(MeCN)_2]^{2+}$
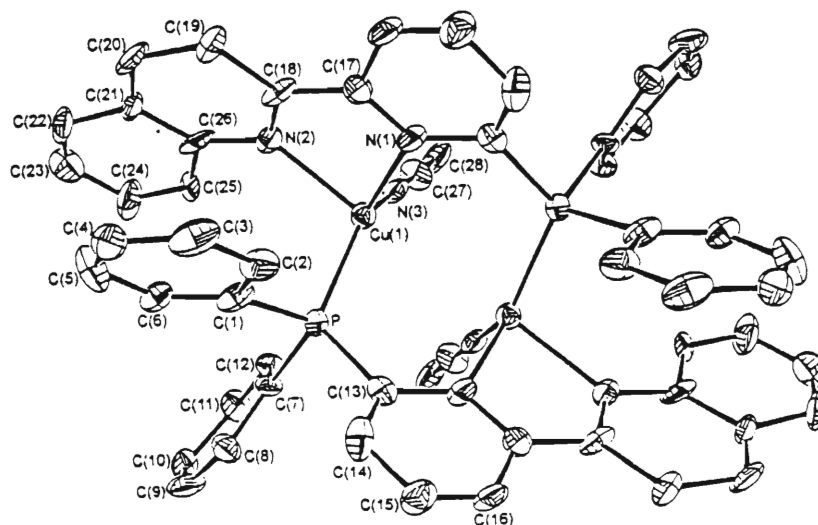
Fig. 3.2 : Structure of $[Cu_2(\mu\text{-Ph}_2Ppyquin)_2(MeCN)_2]^{2+}$

It is with this background in mind that it was decided to investigate the reactions of the 2-diphenylphosphino-1,10-phenanthroline (Ph$_2$Pphen) ligand with the copper(I) precursor $[Cu(MeCN)_4]^+$. The results of this investigation are reported in this Chapter.

3.2 RESULTS AND DISCUSSION

3.2.1 Reaction of [Cu(MeCN)₄]PF₆ with the Ph₂Pphen ligand

Reaction of $[Cu(MeCN)_4]PF_6$ with an equimolar amount of Ph_2Pphen in acetonitrile at room temperature was found to afford a product characterised as $[Cu_2(\mu\text{-}Ph_2Pphen)_2(MeCN)_2](PF_6)_2$ **(1)** according to Scheme 3.1.
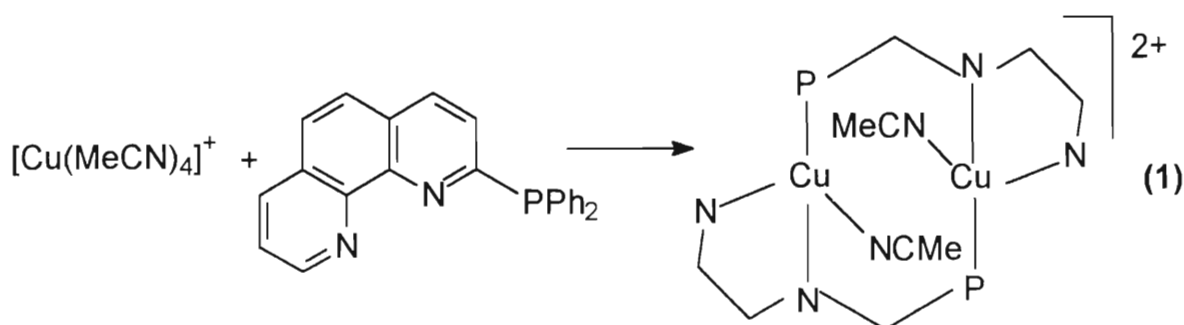
Scheme 3.1 : Synthesis of [Cu₂(μ-Ph₂Pphen)₂(MeCN)₂](PF₆)₂

This product was isolated as an air stable yellow crystalline compound. The maximum yield is obtained when the solvent used is acetonitrile and the reaction time is 24 hours. Any reduction in the length of time or change of solvent *eg.* to dichloromethane or acetone, results in a significant decrease in yield. This decrease in yield can be attributed to the fact that dichloromethane and acetone contain trace amounts of water which easily displace the labile acetonitrile ligands in solution. This complex $[Cu_2(\mu\text{-}Ph_2Pphen)_2(MeCN)_2](PF_6)_2$ is soluble in most organic solvents, but insoluble in diethyl ether, toluene and alkanes.

The $^{31}P\{^1H\}$ nmr spectrum obtained for this complex in CD_2Cl_2 contains a broad peak centred at 11 ppm, which is shifted downfield to that for the free ligand (-3.40 ppm), is typical of a coordinated phosphorus atom.

The ^1H nmr spectrum of $[Cu_2(\mu\text{-}Ph_2Pphen)_2(MeCN)_2](PF_6)_2$ in CD_2Cl_2 at room temperature exhibits resonances between 7.16 and 8.67 ppm associated with the aromatic rings of the ligand, together with a sharp singlet at 1.90 ppm assigned to the

methyl group of the acetonitrile ligand. The solid state infrared spectrum (KBr disk) exhibits the characteristic Ph_2Pphen ligand peaks and a peak at 840 cm^{-1} due to the counterion PF_6^-. The microanalytical data and spectroscopic data are listed in Tables 3.2 and 3.3 respectively.

Single crystals of the complex were grown for the purpose of structural determination by X-ray diffraction methods and the structure of the SbF_6^- salt of this complex was solved. The crystal structure of the complex consists of well separated $[Cu_2(\mu-Ph_2Pphen)_2(MeCN)_2]^{2+}$ cations and SbF_6^- anions, there being no intermolecular contact distances less than the sum of the van der Waals radii for the atoms concerned. An ORTEP generated representation of the structure of the cation is illustrated in Fig. 3.3 along with the atom numbering scheme. A full listing of interatomic distances and angles are given in Tables 3.6 and 3.7, respectively, at the end of this Chapter.

The cation possesses a crystallographically imposed centre of symmetry midway between the copper atoms. The copper atoms are bridged by two Ph_2Pphen ligands in a "head-to-tail" configuration, each ligand coordinating to one copper atom through a phosphorus donor atom and to the other copper atom through the chelating phenanthroline fragment. The acetonitrile ligands, which are *trans* with respect to each other, complete the irregular tetrahedral geometry around the copper atoms with the angles subtended at the copper atom ranging from 80.1 to 114.1°. The *trans*-configuration of the acetonitrile ligands of this complex is the same as that found in $[Cu_2(\mu-Ph_2Pbipy)_2(MeCN)_2]^{2+}$ [7] but differs from the *cis*-configuration found in $[Cu_2(\mu-Et(Ph)Pbipy)_2(MeCN)_2]^{2+}$ and $[Cu_2(\mu-Ph_2Ppyquin)_2(MeCN)_2]^{2+}$ [19]. The Cu-Cu' distance of 3.539(2) Å is consistent with no bonding interactions between the copper atoms. The Cu-P and Cu-N interatomic distances fall within the expected ranges for these bonds [19-22,23a-e]. The Cu-P interatomic distance is 2.188(4) Å and the Cu-N3, Cu-N1' and Cu-N2' interatomic distances are 1.983(2) Å, 2.030(9) Å and 2.144(12) Å, respectively.

The acetonitrile ligands that are coordinated to the copper atoms in complex **(1)** are labile and a study of their substitution by other neutral and anionic ligands was initiated.
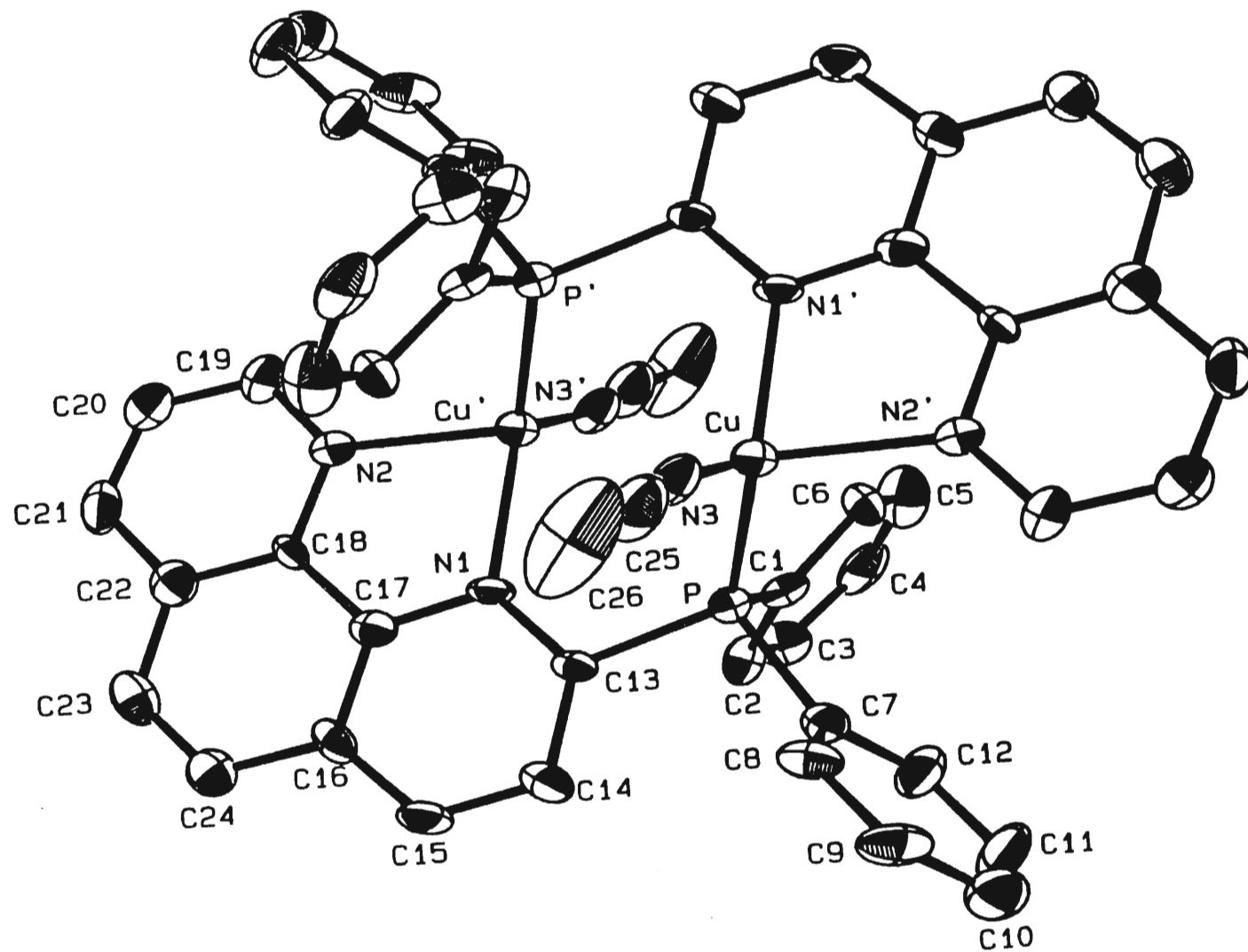
Fig. 3.3 : ORTEP representation at 30% probability of [Cu₂(μ-Ph₂Pphen)₂(MeCN)₂]²⁺

Reaction of an acetonitrile solution of [Cu$_2$(μ-Ph$_2$Pphen)$_2$(MeCN)$_2$](PF$_6$)$_2$ **(1)** with one equivalent of the appropriate potassium halide salt followed by precipitation with diethyl ether produced a red solid material as illustrated in Scheme 3.2. The microanalytical data for carbon, hydrogen and nitrogen which are listed in Table 3.2, indicated the formulation of the products as being [Cu$_2$(μ-Ph$_2$Pphen)$_2$(μ-X)]PF$_6$ where X=Cl **(2)** or X=I **(3)**.

The ^{1}H nmr spectra of **(2)** and **(3)** in CD$_2$Cl$_2$ exhibit resonances between 6.8 and 8.6 ppm associated with the aromatic rings of the Ph$_2$Pphen ligand. The sharp single methyl resonance at 1.90 ppm observed in the ^{1}H nmr spectrum of the acetonitrile derivative **(1)** is no longer present. The solid state infrared spectrum (KBr disk) exhibits absorptions characteristic of the Ph$_2$Pphen ligand and the anionic PF$_6^-$ group. The ^{31}P{^{1}H} nmr spectra of **(2)** and **(3)** consist of broad featureless bands centred at 6.94 and 6.86 ppm respectively. The spectroscopic data are listed in Table 3.3.

Several attempts were undertaken to generate the neutral dihalogen dicopper complexes [Cu$_2$(μ-Ph$_2$Pphen)$_2$(Cl)$_2$] and [Cu$_2$(μ-Ph$_2$Pphen)$_2$(I)$_2$]. Vigorous reaction conditions and an excess of the appropriate halide salt produced no evidence of the coordination of a second halide ion and the formation of a neutral species.
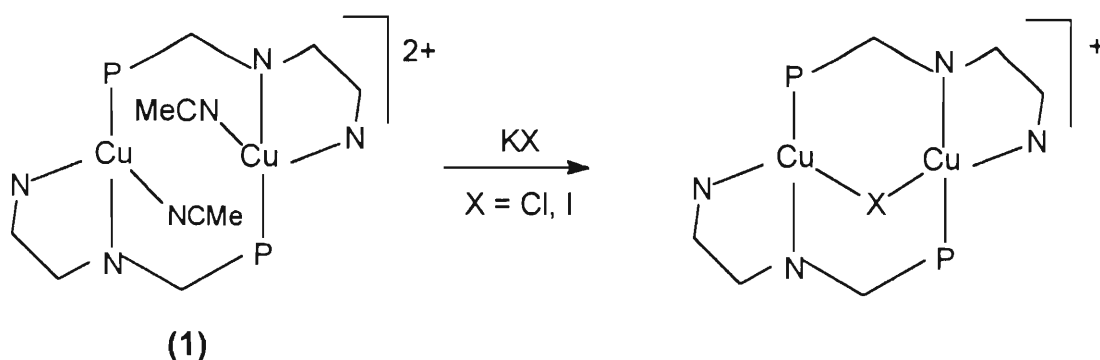
Scheme 3.2 : Substitution reactions of (1) with halide ligands

3.2.3 Substitution reaction of [Cu$_2$(μ-Ph$_2$Pphen)$_2$(MeCN)$_2$](PF$_6$)$_2$ (1) with a sulfur donor ligand: Crystal structure of [Cu$_2$(μ-Ph$_2$Pphen)$_2${μ-S$_2$CN(Et)$_2$}]PF$_6$.3H$_2$O (4)

Treatment of an acetonitrile solution of [Cu$_2$(μ-Ph$_2$Pphen)$_2$(MeCN)$_2$](PF$_6$)$_2$ **(1)** with a suspension in acetonitrile of NaS$_2$CN(Et)$_2$.3H$_2$O was found to afford a product characterised as [Cu$_2$(μ-Ph$_2$Pphen)$_2${μ-S$_2$CN(Et)$_2$}](PF$_6$).3H$_2$O **(4)** which is an air stable red crystalline solid. Suitable microanalytical data which is listed in Table 3.2 were obtained for this complex.

The ^{1}H nmr spectrum of **(4)** in CD$_2$Cl$_2$ exhibits resonances between 6.1 and 8.7 ppm which are readily assigned to the aromatic rings of the coordinated Ph$_2$Pphen ligand. A triplet and a quartet at 1.1 and 3.9 ppm respectively confirm the presence of the ethyl groups of the sulfur donor ligand. The solid state infrared spectrum (KBr disk) exhibit the typical Ph$_2$Pphen peaks as well as the peak due to the anionic PF$_6^-$ group. The ^{31}P{^{1}H} nmr spectrum exhibits a peak centred at 9.06 ppm *i.e.*, downfield of the free ligand (-3.40 ppm) which is typical of a coordinated phosphorus atom. The spectroscopic data are listed in Table 3.3.

In order to determine the exact mode of coordination of the Ph$_2$Pphen and dithiocarbamate ligands in this complex, single crystals suitable for X-ray crystallography were grown by the slow solvent diffusion of diethyl ether into a dichloromethane solution of **(4)**. The crystal structure of [Cu$_2$(μ-Ph$_2$Pphen)$_2${μ-S$_2$CN(Et)$_2$}](PF$_6$).3H$_2$O consists of well separated [Cu$_2$(μ-Ph$_2$Pphen)$_2${μ-S$_2$CN(Et)$_2$}]$^+$ cations and PF$_6^-$ anions, there being no intermolecular contacts significantly less than the sum of the van der Waals radii for the atoms concerned. An ORTEP generated representation of the structure of the cation is depicted in Fig. 3.4 along with the atom numbering scheme. A full listing of interatomic distances and angles is given in Tables 3.12 and 3.13 respectively at the end of this Chapter.

The copper atoms are bridged by two Ph$_2$Pphen ligands in the "head-to-tail" configuration, each ligand coordinating to one copper atom through the phosphorus
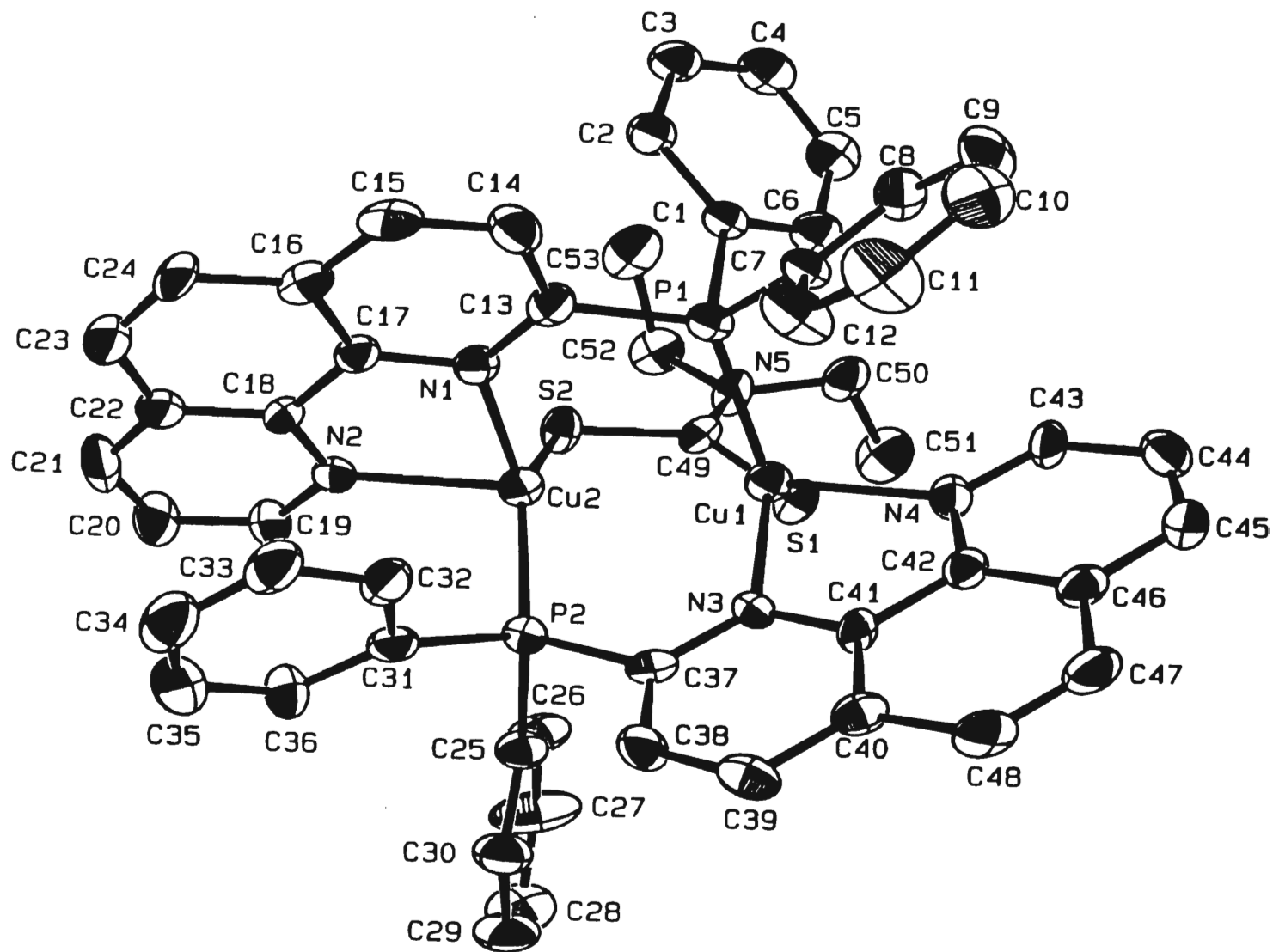
Fig. 3.4 : ORTEP representation at 30% probability of $[Cu_2(\mu\text{-}Ph_2Pphen)_2\{\mu\text{-}S_2CN(Et)_2\}]^+$

donor atom and to the other copper atom through the chelating phenanthroline fragment. The bidentate sulfur ligand also bridges across the two copper atoms resulting in the geometry at each copper being irregular tetrahedral. The irregular geometry is probably caused as a result of the small angle of 77.6(5)° subtended by the phenanthroline fragment at the copper atom, other angles subtended at the copper atom being closer to the idealised value of 109.5° and ranging up to 141.0(2)° for the P2-Cu2-S2 angle. The Cu1-S1 [2.262(5) Å] and Cu2-S2 [2.246(5) Å] interatomic distances fall within the expected ranges for these bonds[5,24a-c].

The Cu1-Cu2 distance is 2.897(2) Å which is significantly shorter than the Cu-Cu' distance of 3.539(2) Å in $[Cu_2(\mu\text{-}Ph_2Pphen)_2(MeCN)_2](SbF_6)_2$. The decrease in the Cu-Cu interatomic distance is caused by the presence of a third bridging ligand as listed in Table 1.1, Chapter 1 for dicopper complexes. The Cu-Cu' distance of 2.897 Å is short enough for bonding interaction. However, no formal bond exists since each copper atom is saturated by the four tetrahedrally orientated bonds to it. A Cu-Cu' distance of 2.600 Å for $[Cu_2(2\text{-}NPh\text{-}phen)_2]$[15] as previously discussed is a typical example whereby bonding interactions occur for the metal atoms.

3.2.4 Substitution reaction of $[Cu_2(\mu\text{-}Ph_2Pphen)_2(MeCN)_2](PF_6)_2$ (1) with pyridine

The reaction of a dichloromethane solution of the dicopper complex $[Cu_2(\mu\text{-}Ph_2Pphen)_2(MeCN)_2](PF_6)_2$ **(1)** with two mole equivalents of pyridine was studied. The acetonitrile ligands are easily displaced as evidenced by the disappearance of the resonance at 1.90 ppm in the ^1H nmr spectrum. The product compound was isolated as an orange microcrystalline material and characterised as $[Cu_2(\mu\text{-}Ph_2Pphen)_2(py)_2](PF_6)_2$ **(5)**. Satisfactory microanalytical data as listed in Table 3.2 were obtained for this complex.

The ^1H nmr spectrum of **(5)** in CD_2Cl_2 exhibits resonances between 6.8 and 8.8 ppm associated with the aromatic rings of the Ph_2Pphen ligand as well as the pyridyl ligand. The solid state infrared spectrum (KBr disk) of **(5)** displays absorptions due to the

Ph_2Pphen and pyridyl ligands and the PF_6^- anion. The $^{31}P\{^1H\}$ nmr spectrum exhibits a broad band centred at 8.94 ppm. Spectroscopic data are listed in Table 3.3.

Attempts to grow single crystals of complex (5) were unsuccessful. The structure of the analogous dicopper complex containing the Ph_2Pbipy ligand was determined X-ray crystallographically [5]. The coordination of the pyridine *via* the nitrogen atom completes the tetrahedral geometry around the copper atom in $[Cu_2(\mu\text{-}Ph_2Pbipy)_2(py)_2](PF_6)_2$ [5]. In all likelihood $[Cu_2(\mu\text{-}Ph_2Pphen)_2(py)_2](PF_6)_2$ has a similar structure.

3.2.5 Substitution reaction of $[Cu_2(\mu\text{-}Ph_2Pphen)_2(MeCN)_2](PF_6)_2$ (1) with bipyridine and phenanthroline: Crystal structure of $[Cu_2(\mu\text{-}Ph_2Pphen)_2(\eta\text{-bipy})](PF_6)_2$ (6)

Treatment of an acetonitrile solution of $[Cu_2(\mu\text{-}Ph_2Pphen)_2(MeCN)_2](PF_6)_2$ (1) with an equimolar amount of 2,2'-bipyridine or 1,10-phenanthroline, at room temperature affords air stable red crystalline solids characterised as $[Cu_2(\mu\text{-}Ph_2Pphen)_2(\eta\text{-L})](PF_6)_2$ where L= 2,2'-bipyridine (6) or 1,10-phenanthroline (7) as illustrated in Scheme 3.3. The microanalytical data for these complexes are given in Table 3.2.

The dicopper complex $[Cu_2(\mu\text{-}Ph_2Pphen)_2(\eta\text{-bipy})](PF_6)_2$ (6) was also prepared using a second method *i.e.,* the reaction of $[Cu(\eta\text{-bipy})(MeCN)_2]PF_6$ with one mole equivalent of Ph_2Pphen, the former being generated *in situ* by the addition of one equivalent of 2,2'-bipyridine to an acetone solution of $[Cu(MeCN)_4]PF_6$.

The ^1H nmr spectra of the dicopper complexes of (6) and (7) measured in CD_2Cl_2 at room temperature exhibit resonances between 6.4 and 8.75 ppm and 6.5 and 8.75 ppm, respectively, which are assigned to the aromatic rings of the coordinated Ph_2Pphen ligands as well as the chelating ligands. The $^{31}P\{^1H\}$ nmr spectra of (6) and (7) consist of a broad band centred at 10 and 6 ppm, respectively. The solid state infrared spectrum (KBr disk) has peaks characteristic of the coordinated Ph_2Pphen and the bipy ligands.

37
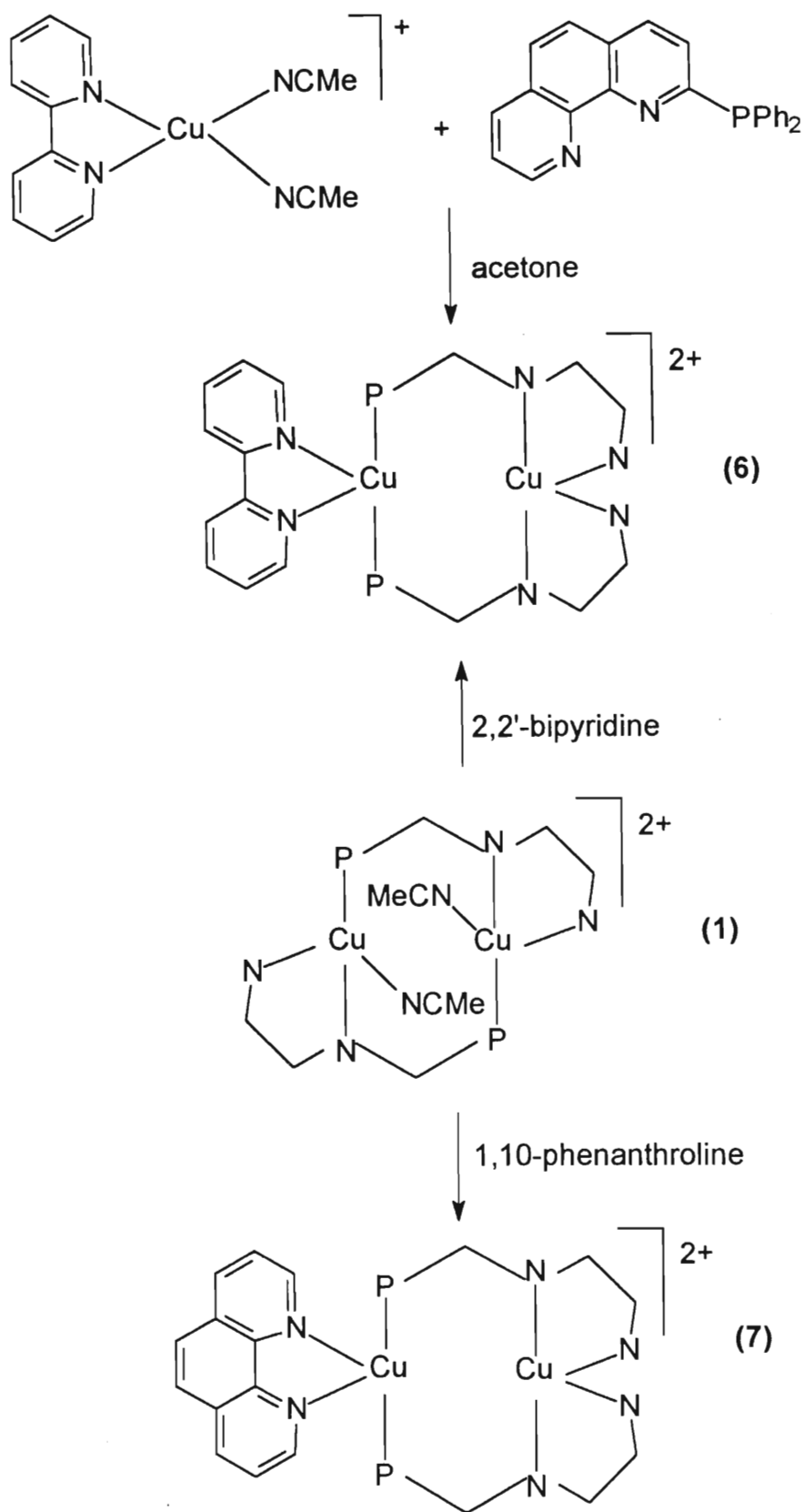
Scheme 3.3 : Substitution reactions of (1) with bipyridine and phenanthroline

The peak at 840 cm^{-1} was assigned to the PF$_6$$^-$ anion. Spectroscopic data are listed in Table 3.3.

Single crystals of [Cu$_2$(μ-Ph$_2$Pphen)$_2$(η-bipy)](PF$_6$)$_2$ suitable for X-ray analysis were grown. The crystal structure of the complex consists of well separated [Cu$_2$(μ-Ph$_2$Pphen)$_2$(η-bipy)]$^{2+}$ cations and PF$_6$$^-$ anions, there being no intermolecular contact distances less than the sum of the van der Waals radii for the atoms concerned. An ORTEP generated representation of the structure of the cation is illustrated in Fig. 3.5 along with the atom numbering scheme. A full listing of interatomic distances and angles is given in Tables 3.18 and 3.19, respectively, at the end of this Chapter.

The cation possesses a crystallographically imposed two fold axis which passes through the two copper atoms and the chelating bipy ligand. An interesting feature of this complex is that the Ph$_2$Pphen ligands bridge the two copper atoms in a "head-to-head" configuration, the phosphorus atom of each ligand bonds to Cu1 and the phen fragments of the ligands bond to Cu2. The coordination at Cu1 is completed by the chelating bipy ligand. The Cu1-Cu2 interatomic distance of 3.949(2) Å is significantly larger than the Cu-Cu' distance [3.539(2) Å] in [Cu$_2$(μ-Ph$_2$Pphen)$_2$(MeCN)$_2$](SbF$_6$)$_2$. The atom labelled Cu1 has an irregular tetrahedral geometry that is caused by the small angle of 80.5(3)° subtended by the bipy ligand. The presence of two chelating fragments on Cu2 also leads to the copper atom having an irregular tetrahedral geometry, the N1-Cu2-N2 angle being 82.2(4)°.
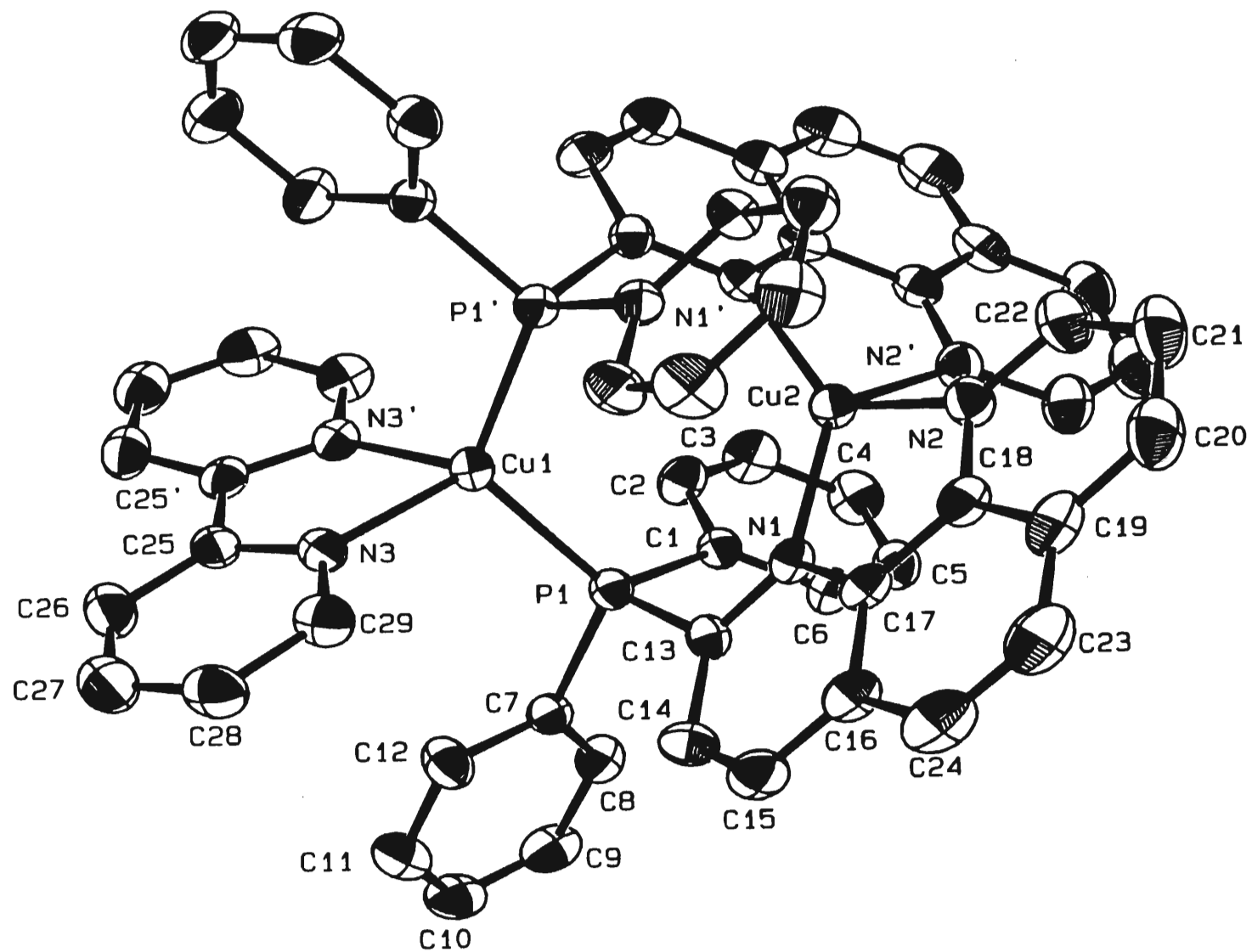
Fig. 3.5 : ORTEP representation at 30% probability of [Cu$_2$(μ-Ph$_2$Pphen)$_2$(η-bipy)]$^{2+}$

3.3 SUMMARY OF CRYSTALLOGRAPHIC RESULTS

Table 3.1 : Selected structural parameters for the dicopper ligand bridged complexes whose structures have been determined by X-ray crystallography.

COMPLEX[a]	Cu-Cu (Å)	P-Cu-Cu-N[b] TORSION ANGLE(S) (°)
$[Cu_2(\mu\text{-}Ph_2Pphen)_2(MeCN)_2](SbF_6)_2$ (HT)	3.539	44.8
$[Cu_2(\mu\text{-}Ph_2Pphen)_2\{\mu\text{-}S_2CN(Et)_2]PF_6.3H_2O$ (HT)	2.897	19.0, 10.4
$[Cu_2(\mu\text{-}Ph_2Pphen)_2(\eta\text{-}bipy)](PF_6)_2$ (HH)	3.949	52.6

[a] HH = ligand orientation head-to-head, HT = ligand orientation head-to-tail.

[b] This N belongs to the heterocyclic ring to which the phosphorus atom is bonded.

It is evident that the Cu-Cu distances vary considerably as the non-Ph_2Pphen ligands are changed. A large increase in the Cu-Cu distance is observed when the labile acetonitrile ligands are replaced by the bipy ligand. This may be a consequence of the change from a "head-to-tail" to a "head-to-head" conformation for the two Ph_2Pphen ligands, brought about by increased steric crowding in the complex. Introduction of a third bridging ligand leads to a marked decrease in the Cu-Cu distance. These results confirm the ability of the Ph_2Pphen ligand to bridge a wide range of M-M distances.

Though the data are limited, there also appears to be a link between the Cu-Cu distance and the P-Cu-Cu-N torsion angle; the longer the Cu-Cu distance the larger the torsion angle. Presumably, steric crowding in the complex is relieved by increasing both the Cu-Cu distance and the P-Cu-Cu-N torsion angle. On the other hand, the presence of a third bridging ligand appears to restrict the twisting of the Ph_2Pphen ligand about the Cu-Cu bond, despite increased steric crowding. Certainly, the torsion angles of 19.0 and 10.4° for the diethyldithiocarbamate ligand-bridged complex are much smaller than those of 44.8 and 52.6° for the other two complexes.

3.4 ELECTROCHEMICAL STUDIES

As discussed in Chapter 1, one of the objectives of the work described in this chapter was to investigate the ability of the Ph_2Pphen ligand-bridged dicopper(I) complexes to function as electrocatalysts for carbon dioxide reduction.

All dicopper complexes synthesised have been tested to determine whether they function as electrocatalysts for carbon dioxide reduction. These results were obtained using cyclic voltammetry.

3.4.1 Electrochemical studies of $[Cu_2(\mu\text{-}Ph_2Pphen)_2(MeCN)_2](PF_6)_2$ (1)

The cyclic voltammogram of $[Cu_2(\mu\text{-}Ph_2Pphen)_2(MeCN)_2](PF_6)_2$ (1) recorded in acetonitrile (0.1 M TBAP) at room temperature under an argon atmosphere exhibits two reduction waves at $E_{pc} = -1.10$ and $E_{pc} = -1.42$ V *vs* Ag/AgCl as shown in Fig. 3.6. Both reduction waves are irreversible. Under a carbon dioxide atmosphere at room temperature the cyclic voltammogram of (1) remains the same. This result indicated that dicopper complex did not catalyse the electrochemical reduction of carbon dioxide.
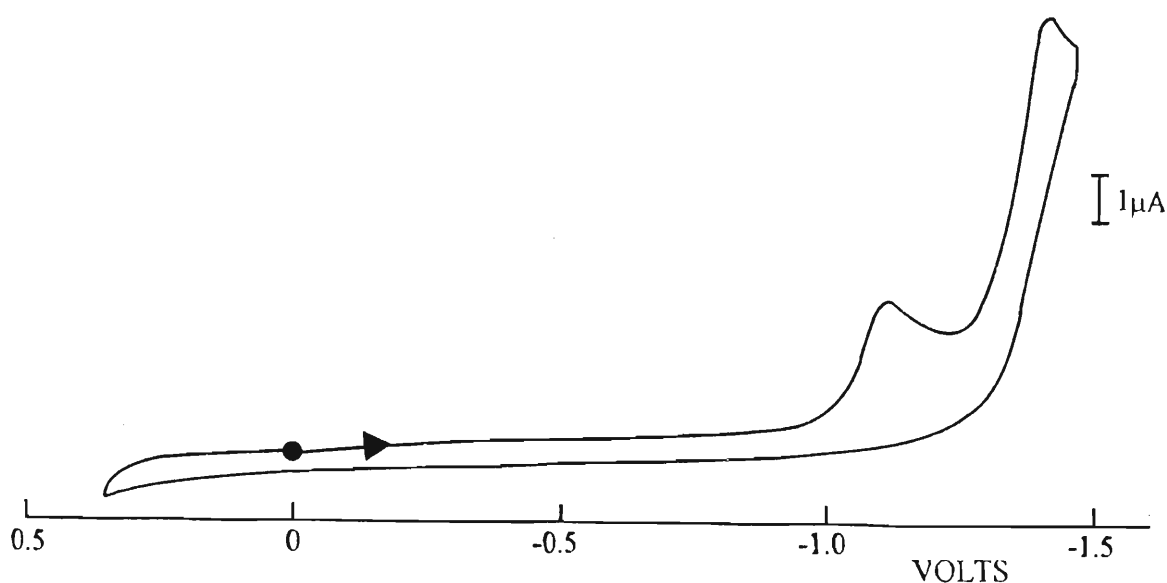
Fig. 3.6 : Cyclic voltammogram of $[Cu_2(\mu\text{-}Ph_2Pphen)_2(MeCN)_2](PF_6)_2$ (1) measured in acetonitrile (10^{-3} M solution, 0.1 M TBAP). Scan rate 200 mV s^{-1}.

Variations in the experimental conditions *i.e.,* lowering the temperature to 5 °C and using dichloromethane as a solvent did not alter the original cyclic voltammogram.

The cyclic voltammograms under an argon and carbon dioxide atmosphere of the dicopper complexes **(2)**, **(3)**, **(5)**, **(6)** and **(7)** all have the same form as that obtained for **(1)**, except for the dicopper complex **(4)** which has four irreversible waves at E_{pc} =-1.38, -1.60, -1.72 and -1.85 V *vs* Ag/AgCl respectively.

The electrochemical results obtained for these complexes are rather surprising in view of the fact that the analogous dicopper complexes of Ph_2Pbipy exhibit reasonable electrochemistry and are found to be electrocatalysts for carbon dioxide reduction [5,25]. Extended Hückel molecular orbital calculations for dicopper complexes containing the Ph_2Pbipy and Ph_2Pphen ligands are similar indicating that a change in the bridging ligand has little effect on the electron density distribution in the complex [19]. What is certain is that the phen fragment being planar is more rigid than the bipy fragment. Perhaps it is the relative lack of the coordinative flexibility of the Ph_2Pphen ligand which leads in some way, to the instability of the complex on electrochemical reduction. However, this is mere speculation and more work needs to be done in order to understand the electrochemistry of complexes of this type.

3.5 EXPERIMENTAL

All reactions were carried out under a nitrogen atmosphere. All solvents were purified by literature methods[33]. General experimental methods are outlined in Appendix A.

Synthesis of $[Cu_2(\mu\text{-}Ph_2Pphen)_2(MeCN)_2](PF_6)_2$ (1)

An acetonitrile solution (10 ml) of $[Cu(MeCN)_4]PF_6$[32] (37.2 mg, 0.1 mmol) was added dropwise to a suspension in acetonitrile (10 ml) of Ph_2Pphen (36.5 mg, 0.1 mmol). The resultant solution stirred at room temperature for 24 hours and then evaporated to *ca.* 5 ml under reduced pressure. Diethyl ether (10 ml) was added and the mixture allowed

to stand overnight at 0 °C, a bright yellow crystalline material being obtained by decanting the mother liquor. The crystals were then washed with diethyl ether and dried *in vacuo*.

$[Cu_2(\mu\text{-}Ph_2Pphen)_2(MeCN)_2](SbF_6)_2$ was synthesised in the same manner from $[Cu(MeCN)_4]SbF_6$, the latter being prepared by the reaction of excess $NOSbF_6$ with copper powder in acetonitrile.

Yield: 87% and 74% respectively

Synthesis of $[Cu_2(\mu\text{-}Ph_2Pphen)_2(\mu\text{-}X)]PF_6$ where X= Cl (2) and X = I (3)

Solid KX where X = Cl or I (0.05 mmol) was added to an acetonitrile solution (10 ml) of $[Cu_2(\mu\text{-}Ph_2Pphen)_2(MeCN)_2](PF_6)_2$ (63 mg, 0.05 mmol) and the mixture stirred at room temperature for 5 hours. Diethyl ether (15 ml) was then added carefully to precipitate the product. The precipitate obtained after filtration was recrystallised from dichloromethane/hexane to afford a red crystalline material. The crystals were then washed with hexane and dried *in vacuo*.

Yield: **(2)** 69%, **(3)** 73%

Synthesis of $[Cu_2(\mu\text{-}Ph_2Pphen)_2\{\mu\text{-}S_2CN(Et)_2]PF_6.3H_2O$ (4)

An acetonitrile suspension (10 ml) of $NaS_2CN(Et)_2.3H_2O$ (22.5 mg, 0.1 mmol) was added dropwise to an acetonitrile solution (10 ml) of $[Cu_2(\mu\text{-}Ph_2Pphen)_2(MeCN)_2](PF_6)_2$ (123 mg, 0.1 mmol) and the resultant solution stirred at room temperature for 24 hours. Diethyl ether (20 ml) was added and the mixture allowed to stand overnight at 0 °C. The red crystalline material which separated out was isolated by decanting the mother liquor. The crystals were then washed with diethyl ether and dried *in vacuo*.

Yield: 68%

Synthesis of $[Cu_2(\mu\text{-}Ph_2Pphen)_2(py)_2](PF_6)_2$ (5)

Pyridine (2 ml, 0.2 mmol) was added dropwise to an acetonitrile solution (10 ml) of

44

$[Cu_2(\mu\text{-}Ph_2Pphen)_2(MeCN)_2](PF_6)_2$ (123 mg, 0.1 mmol) and the mixture stirred at room temperature for 24 hours. The resultant solution was then evaporated to *ca.* 5 ml under reduced pressure. Diethyl ether (10 ml) was added and the mixture allowed to stand overnight at 0 °C, the orange crystalline material that separated out was isolated by decanting the mother liquor. The crystals were then washed with diethyl ether and dried *in vacuo.*

Yield: 85%

Synthesis of $[Cu_2(\mu\text{-}Ph_2Pphen)_2(\eta\text{-}bipy)](PF_6)_2$ (6)

Method A

An acetonitrile solution (5 ml) of 2,2'-bipyridine (15.6 mg, 0.1 mmol) was added dropwise to an acetonitrile solution (5 ml) of $[Cu_2(\mu\text{-}Ph_2Pphen)_2(MeCN)_2](PF_6)_2$ (123 mg, 0.1 mmol) and the resultant solution stirred at room temperature for 24 hours. The solution was evaporated at *ca.* 5 ml under reduced pressure. Diethyl ether (10 ml) was added and the mixture allowed to stand overnight at 0 °C. The red precipitate that formed was filtered off and subsequently recrystallised from dichloromethane/hexane. The crystals were then washed with hexane and dried *in vacuo.*

Yield: 74 %

Method B

To an acetone solution (15 ml) of $[Cu(MeCN)_4]PF_6$ (37.3 mg, 0.1 mmol) was added solid 2,2'-bipyridine (15.6 mg, 0.1 mmol) and the resulting solution stirred for 1 hour. The Ph_2Pphen (36.5 mg, 0.1 mmol) ligand was added as a solid and the mixture stirred for another hour; hexane (10 ml) was then added and the resulting solution allowed to stand overnight at 0 °C. The red crystalline material that separated out was isolated by decanting the mother liquor, the crystals were then washed with cold hexane and dried *in vacuo.*

Yield: 62%

Synthesis of [Cu$_2$(μ-Ph$_2$Pphen)$_2$(η-phen)](PF$_6$)$_2$ **(7)**

An acetonitrile solution (5 ml) of 1,10-phenanthroline (18 mg, 0.1 mmol) was added dropwise to an acetonitrile solution (5 ml) of [Cu$_2$(μ-Ph$_2$Pphen)$_2$(MeCN)$_2$](PF$_6$)$_2$ (123 mg, 0.1 mmol) and the resultant solution stirred at room temperature for 24 hours. The solution was evaporated at *ca.* 5 ml under reduced pressure. Diethyl ether (10 ml) was added and the mixture allowed to stand overnight at 0 °C. The red precipitate that formed was filtered off and subsequently recrystallised from dichloromethane/hexane. The crystals were then washed with hexane and dried *in vacuo.*
Yield: 66 %

3.6 EXPERIMENTAL PROCEDURE FOR ELECTROCHEMICAL MEASUREMENTS

The electrochemical technique employed was cyclic voltammetry. The cell was purged with pure dry argon for 45 minutes before any experiments were performed. The initial cyclic voltammetry experiments were performed under an argon atmosphere, thereafter high purity carbon dioxide was bubbled through the solution for 15 minutes and the cyclic voltammetric experiment was repeated. Experiments were performed at room temperature and at a low temperature (5 °C). For low temperature measurements the cell was immersed in an ice bath.

Tetrabutylammonium perchlorate (TBAP) was used as the supporting electrolyte in a 0.1 M concentration, the sample concentration being 10^{-3} M. TBAP was recystallised three times from 9:1 ethanol/water mixture and dried *in vacuo* at 100 °C before use.

All cyclic voltammetric experiments employed a conventional three electrode cell, comprising a platinum spiral wire auxiliary electrode, a reference electrode comprising a AgCl coated spiral silver wire dipped into a 0.1 M solution of TBAP in the relevant solvent and separated from the electrolyte solution by a fine frit, and a platinum disc working electrode. All potentials are quoted relative to our Ag/AgCl reference electrode, against which the [ferrocene]$^{+/0}$ couple has the following $E_{\frac{1}{2}}$ values: 0.38 V in acetonitrile and 0.41 V in dichloromethane at 200 mVs^{-1}.

Ferrocene was usually added to the solution under investigation at the end of each experiment as an internal standard to check on the stability of the reference electrode.

The platinum disc working electrode (0.013 cm^2) was of local construction (Mechanical Instrument Workshop, University of Natal). Its surface was freshly polished using 2-6 µm diamond paste until no scratches were observed at tenfold magnification. Before use, the electrode was rinsed with acetone and distilled water and dried in a warm air stream.

Table 3.2 : Physical and microanalytical data

COMPLEX	COLOUR	Molar Mass: g.mol^{-1}	Analysis : Found (Calculated) %		
			% C	%H	%N
$[Cu_2(\mu\text{-}Ph_2Pphen)_2(MeCN)_2](PF_6)_2$ **(1)**	yellow	1227.90	50.74 (50.87)	3.19 (3.28)	6.55 (6.84)
$[Cu_2(\mu\text{-}Ph_2Pphen)_2(\mu\text{-}Cl)]PF_6$ **(2)**	orange	1036.28	55.03 (55.63)	3.16 (3.31)	5.24 (5.41)
$[Cu_2(\mu\text{-}Ph_2Pphen)_2(\mu\text{-}I)]PF_6$ **(3)**	red	1127.73	50.86 (51.12)	2.78 (3.04)	4.84 (4.97)
$[Cu_2(\mu\text{-}Ph_2Pphen)_2\{\mu\text{-}S_2CN(Et)_2\}]PF_6.3H_2O$ **(4)**	red	1203.14	52.98 (52.91)	3.65 (4.19)	5.49 (5.82)
$[Cu_2(\mu\text{-}Ph_2Pphen)_2(py)_2](PF_6)_2$ **(5)**	orange	1304.00	53.15 (53.42)	3.21 (3.40)	6.49 (6.44)
$[Cu_2(\mu\text{-}Ph_2Pphen)_2(\eta\text{-}bipy)](PF_6)_2$ **(6)**	red	1301.98	53.35 (53.51)	3.37 (3.25)	6.37 (6.45)
$[Cu_2(\mu\text{-}Ph_2Pphen)_2(\eta\text{-}phen)](PF_6)_2$ **(7)**	deep red	1326.00	54.84 (54.35)	3.52 (3.19)	6.25 (6.34)

Table 3.3 : Spectroscopic data

COMPLEX	^{1}H nmr DATA (ppm)^a	IR DATA (cm^{-1})^b
$[Cu_2(\mu\text{-}Ph_2Pphen)_2(MeCN)_2](PF_6)_2$ **(1)**	8.6 (2H,d), 8.5 (2H,d), 8.1 (6H,s), 7.7 (4H,m), 7.1 (20H,m), 1.9 (6H,s)	1620(w), 1560(m), 1500(w),1483(m),1436(s), 1420(w), 1382(m), 1097(m), 840(vs)
$[Cu_2(\mu\text{-}Ph_2Pphen)_2(\mu\text{-}Cl)]PF_6$ **(2)**	8.6 (2H,d), 8.4 (2H,d), 8.3 (2H,d), 8.1 (4H,s), 7.8 (2H,d), 7.6 (2H,m), 6.8 (20H,m)	1620(w), 1577(m), 1498(w),1483(m),1436(s), 1420(w), 1382(m), 1095(m), 840(vs)
$[Cu_2(\mu\text{-}Ph_2Pphen)_2(\mu\text{-}I)]PF_6$ **(3)**	8.6 (2H,d), 8.5 (2H,dd), 8.3 (2H,d), 8.1 (4H,s), 7.8 (2H,d), 7.6 (2H,m), 6.8 (20H,m)	1620(w), 1569(m), 1498(m),1480(m),1436(s), 1420(w), 1382(m), 1095(m), 842(vs)
$[Cu_2(\mu\text{-}Ph_2Pphen)_2\{\mu\text{-}S_2CN(Et)_2\}]PF_6.3H_2O$ **(4)**	8.7 (2H,d), 8.6 (2H,d), 8.0 (4H,m), 7.5 (8H,m), 6.1 (18H,m), 3.9 (4H,q), 1.1 (6H,t)	1620(w), 1577(w), 1560(m), 1483(m), 1436(s), 1415(m), 1383(m), 1093(m), 839(vs)
$[Cu_2(\mu\text{-}Ph_2Pphen)_2(py)_2](PF_6)_2$ **(5)**	8.8 (2H,d), 8.7 (2H,d), 8.3 (4H,s), 8.0 (2H,dd), 7.5 (10H,m), 6.8 (24H,m)	1622(w), 1600(w), 1577(m), 1502(m), 1483(m), 1436(s), 1382(m), 1097(m), 839(vs)
$[Cu_2(\mu\text{-}Ph_2Pphen)_2(\eta\text{-}bipy)](PF_6)_2$ **(6)**	8.7 (2H,d), 8.5 (2H,d), 8.2 (4H,s), 6.4 (34H,m)	1620(w), 1598(w), 1560(m), 1500(m), 1483(m), 1438(s), 1380(m), 1095(m), 840(vs)
$[Cu_2(\mu\text{-}Ph_2Pphen)_2(\eta\text{-}phen)](PF_6)_2$ **(7)**	8.7 (10H,m), 8.0 (6H,m), 7.4 (10H,m), 6.5 (16H,m)	1623(m), 1600(w), 1577(m), 1503(m), 1481(w), 1436(s), 1379(m), 1149(m), 1098(m), 840(vs)

^{a} : measured in CD_2Cl_2 , d=doublet, s=singlet, m=multiplet, dd=doublet of doublets,

^{b} : KBr disk, w=weak, m=medium, s=strong, vs=very strong

Single crystal X-ray diffraction study of [Cu$_2$(μ-Ph$_2$Pphen)$_2$(MeCN)$_2$](SbF$_6$)$_2$

Small orange hexagonal plates of [Cu$_2$(μ-Ph$_2$Pphen)$_2$(MeCN)$_2$](SbF$_6$)$_2$ were grown by slow vapour diffusion of a saturated acetonitrile solution of the complex and diethyl ether. The general approach used for the intensity data collection and structure solution is described in Appendix A. The crystallographic data are given in Table 3.4, the atomic coordinates for non hydrogen atoms in Table 3.5, the interatomic distances in Table 3.6, the interatomic angles in Table 3.7, the anisotropic displacement parameters in Table 3.8 and the hydrogen coordinates in Table 3.9. The observed and calculated structure factors may be found on microfiche in an envelope fixed to the inside back cover. All non hydrogen atoms were made anisotropic. The hydrogen atoms were placed in calculated positions.

Table 3.4 Crystal data and details of crystallographic analysis for $[Cu_2(\mu\text{-}Ph_2Pphen)_2(MeCN)_2](SbF_6)_2$

Empirical formula	$C_{52}\,H_{40}\,Cu_2\,F_{12}\,N_6\,P_2\,Sb_2$
Formula weight (g. mol^{-1})	1409.42
Crystal dimensions (mm)	0.56 x 0.35 x 0.09
Temperature (°C)	22
λ(Mo -Kα) (Å)	0.71069
Crystal system	monoclinic
Space group	$P2_1/n$
a (Å)	10.984(5)
b (Å)	11.577(5)
c (Å)	21.673(10)
α (°)	90
β (°)	94.29(4)
γ (°)	90
Volume (Å^3)	2748(2)
Z	2
D_c (g.cm^{-3})	1.703
Absorption coefficient (mm^{-1})	1.876
Absorption correction	Semi-empirical
Max./Min. Transmission factors	.999/.955
F(000)	1384
Theta range for data collection (°)	2.02 to 22.97
Index ranges	-12<=h<=12, -1<=k<=12, -1<=l<=23
Reflections collected	4631
Independent reflections	3801 [R(int) = 0.0539]
Refinement method	Full-matrix least-squares on F^2
Data / restraints / parameters	3757 / 0 / 345
Goodness-of-fit on F^2	1.146
Final R indices [I>2σ(I)]	R1 = 0.0559, wR2 = 0.1140
R indices (all data)	R1 = 0.1731, wR2 = 0.2316
Largest difference (peak and hole) (e Å^{-3})	$\Delta\rho_{max}$ = 0.864 and $\Delta\rho_{min}$ = -0.568

Table 3.5 Atomic coordinates (x 10^4) and equivalent isotropic displacement parameters (Å^2 x 10^3) for [Cu$_2$(μ-Ph$_2$Pphen)$_2$(MeCN)$_2$](SbF$_6$)$_2$

	x	y	z	U(eq)
Cu	-1180(2)	996(2)	123(1)	45(1)
P	606(4)	1554(3)	532(2)	40(1)
N(1)	1707(11)	-489(11)	753(5)	41(3)
N(2)	2214(11)	-2482(11)	191(6)	46(3)
N(3)	-2269(14)	360(11)	729(7)	56(4)
C(1)	1748(13)	2086(13)	32(7)	43(4)
C(2)	2961(15)	2158(13)	220(7)	49(4)
C(3)	3771(17)	2598(17)	-189(9)	70(5)
C(4)	3385(20)	2941(17)	-764(9)	73(6)
C(5)	2185(22)	2844(17)	-957(9)	76(6)
C(6)	1335(17)	2423(15)	-575(8)	58(5)
C(7)	336(14)	2769(13)	1034(7)	45(4)
C(8)	-528(16)	2671(16)	1466(7)	60(5)
C(9)	-880(16)	3584(18)	1819(8)	67(6)
C(10)	-370(20)	4651(19)	1744(9)	77(6)
C(11)	463(20)	4772(16)	1303(10)	81(6)
C(12)	846(17)	3837(15)	961(9)	68(5)
C(13)	1505(12)	519(13)	1033(6)	35(4)
C(14)	1967(15)	766(15)	1634(7)	54(5)
C(15)	2602(15)	-52(15)	1964(7)	55(5)
C(16)	2811(13)	-1129(14)	1709(7)	42(4)
C(17)	2365(12)	-1283(13)	1083(7)	37(4)
C(18)	2601(13)	-2350(12)	793(7)	40(4)
C(19)	2458(17)	-3456(15)	-108(8)	62(5)
C(20)	3157(18)	-4325(15)	185(10)	73(6)
C(21)	3529(16)	-4221(15)	796(9)	65(5)
C(22)	3283(14)	-3238(14)	1121(7)	47(4)
C(23)	3697(17)	-3023(16)	1746(8)	64(5)
C(24)	3485(16)	-2013(16)	2027(8)	64(5)
C(25)	-2816(21)	62(17)	1110(11)	84(7)
C(26)	-3555(28)	-281(23)	1612(14)	169(15)
Sb	5189(1)	3177(1)	2170(1)	77(1)
F(1)	6668(11)	2503(13)	2414(7)	129(5)
F(2)	5817(18)	3923(27)	1566(13)	293(18)

Table 3.5 Atomic coordinates (x 10^4) and equivalent isotropic displacement parameters (Å^2 x 10^3) for [Cu$_2$(μ-Ph$_2$Pphen)$_2$(MeCN)$_2$](SbF$_6$)$_2$

F(3)	3679(12)	3813(13)	1931(7)	126(5)
F(4)	4517(16)	2363(23)	2739(12)	276(16)
F(5)	5485(24)	4269(21)	2694(16)	322(19)
F(6)	4866(22)	2062(25)	1625(13)	291(18)

Table 3.6 Interatomic distances (Å) for [Cu$_2$(μ-Ph$_2$Pphen)$_2$(MeCN)$_2$](SbF$_6$)$_2$

Cu-Cu'	3.539(2)	C(10)-H(10)	0.96
Cu-N(3)	1.98(2)	C(11)-C(12)	1.40(2)
Cu-N(1')	2.030(11)	C(11)-H(11)	0.96
Cu-N(2')	2.144(12)	C(12)-H(12)	0.96
Cu-P	2.188(4)	C(13)-C(14)	1.39(2)
P-C(13)	1.85(2)	C(14)-C(15)	1.35(2)
P-C(1)	1.83(2)	C(14)-H(14)	0.96
P-C(7)	1.82(2)	C(15)-C(16)	1.39(2)
N(1)-C(13)	1.34(2)	C(15)-H(15)	0.96
N(1)-C(17)	1.34(2)	C(16)-C(17)	1.42(2)
N(1)-Cu'	2.030(11)	C(16)-C(24)	1.41(2)
N(2)-C(19)	1.34(2)	C(17)-C(18)	1.42(2)
N(2)-C(18)	1.35(2)	C(18)-C(22)	1.43(2)
N(2)-Cu'	2.144(12)	C(19)-C(20)	1.39(2)
N(3)-C(25)	1.11(2)	C(19)-H(19)	0.96
C(1)-C(6)	1.41(2)	C(20)-C(21)	1.36(2)
C(1)-C(2)	1.37(2)	C(20)-H(20)	0.96
C(2)-C(3)	1.40(2)	C(21)-C(22)	1.38(2)
C(2)-H(2)	0.96	C(21)-H(21)	0.96
C(3)-C(4)	1.35(2)	C(22)-C(23)	1.42(2)
C(3)-H(3)	0.96	C(23)-C(24)	1.35(2)
C(4)-C(5)	1.36(3)	C(23)-H(23)	0.96
C(4)-H(4)	0.96	C(24)-H(24)	0.96
C(5)-C(6)	1.38(2)	C(25)-C(26)	1.46(3)
C(5)-H(5)	0.96	C(26)-H(26A)	0.96
C(6)-H(6)	0.96	C(26)-H(26B)	0.96
C(7)-C(8)	1.39(2)	C(26)-H(26C)	0.96
C(7)-C(12)	1.37(2)	Sb-F(5)	1.71(2)
C(8)-C(9)	1.38(2)	Sb-F(4)	1.76(2)
C(8)-H(8)	0.96	Sb-F(6)	1.77(2)
C(9)-C(10)	1.37(3)	Sb-F(2)	1.75(2)
C(9)-H(9)	0.96	Sb-F(1)	1.844(12)
C(10)-C(11)	1.38(3)	Sb-F(3)	1.853(12)

N(3)-Cu-N(1')	111.6(5)	C(14)-C(13)-P	123.8(13)
N(3)-Cu-N(2')	100.1(5)	C(15)-C(14)-C(13)	119(2)
N(1')-Cu-N(2')	80.1(5)	C(15)-C(14)-H(14)	120.3(10)
N(3)-Cu-P	114.1(4)	C(13)-C(14)-H(14)	120.3(10)
N(1')-Cu-P	130.4(4)	C(14)-C(15)-C(16)	120.8(14)
N(2')-Cu-P	109.2(4)	C(14)-C(15)-H(15)	119.6(10)
C(13)-P-C(1)	101.9(7)	C(16)-C(15)-H(15)	119.6(9)
C(13)-P-C(7)	104.7(7)	C(15)-C(16)-C(17)	116.0(14)
C(1)-P-C(7)	104.1(7)	C(15)-C(16)-C(24)	123(2)
C(13)-P-Cu	118.0(5)	C(17)-C(16)-C(24)	120(2)
C(1)-P-Cu	119.6(5)	N(1)-C(17)-C(16)	123.8(14)
C(7)-P-Cu	106.9(5)	N(1)-C(17)-C(18)	118.1(13)
C(13)-N(1)-C(17)	117.2(12)	C(16)-C(17)-C(18)	118.1(14)
C(13)-N(1)-Cu'	128.9(10)	N(2)-C(18)-C(22)	120.9(14)
C(17)-N(1)-Cu'	113.9(10)	N(2)-C(18)-C(17)	118.1(13)
C(19)-N(2)-C(18)	120.2(14)	C(22)-C(18)-C(17)	120.9(14)
C(19)-N(2)-Cu'	130.1(11)	N(2)-C(19)-C(20)	121(2)
C(18)-N(2)-Cu'	109.7(10)	N(2)-C(19)-H(19)	119.5(9)
C(25)-N(3)-Cu	173(2)	C(20)-C(19)-H(19)	119.5(11)
C(6)-C(1)-C(2)	120(2)	C(21)-C(20)-C(19)	120(2)
C(6)-C(1)-P	117.3(12)	C(21)-C(20)-H(20)	120.1(11)
C(2)-C(1)-P	122.8(13)	C(19)-C(20)-H(20)	120.1(11)
C(3)-C(2)-C(1)	119(2)	C(20)-C(21)-C(22)	121(2)
C(3)-C(2)-H(2)	120.5(11)	C(20)-C(21)-H(21)	119.5(11)
C(1)-C(2)-H(2)	120.5(10)	C(22)-C(21)-H(21)	119.5(10)
C(2)-C(3)-C(4)	122(2)	C(21)-C(22)-C(18)	117(2)
C(2)-C(3)-H(3)	119.2(11)	C(21)-C(22)-C(23)	125(2)
C(4)-C(3)-H(3)	119.2(13)	C(18)-C(22)-C(23)	118(2)
C(3)-C(4)-C(5)	120(2)	C(24)-C(23)-C(22)	122(2)
C(3)-C(4)-H(4)	120.3(13)	C(24)-C(23)-H(23)	119.0(10)
C(5)-C(4)-H(4)	120.3(12)	C(22)-C(23)-H(23)	119.0(10)
C(6)-C(5)-C(4)	122(2)	C(23)-C(24)-C(16)	121(2)
C(6)-C(5)-H(5)	119.1(12)	C(23)-C(24)-H(24)	119.7(10)
C(4)-C(5)-H(5)	119.1(12)	C(16)-C(24)-H(24)	119.7(10)
C(1)-C(6)-C(5)	118(2)	N(3)-C(25)-C(26)	178(2)
C(1)-C(6)-H(6)	121.0(10)	C(25)-C(26)-H(26A)	110(2)
C(5)-C(6)-H(6)	121.0(12)	C(25)-C(26)-H(26B)	109.5(13)

Table 3.7 Interatomic angles (°) for [Cu$_2$(μ-Ph$_2$Pphen)$_2$(MeCN)$_2$](SbF$_6$)$_2$

C(8)-C(7)-C(12)	117(2)	H(26A)-C(26)-H(26B)	109.5
C(8)-C(7)-P	119.5(13)	C(25)-C(26)-H(26C)	110(2)
C(12)-C(7)-P	122.9(13)	H(26A)-C(26)-H(26C)	109.5
C(9)-C(8)-C(7)	123(2)	H(26B)-C(26)-H(26C)	109.5
C(9)-C(8)-H(8)	118.4(12)	F(5)-Sb-F(4)	90(2)
C(7)-C(8)-H(8)	118.4(10)	F(5)-Sb-F(6)	179.2(10)
C(8)-C(9)-C(10)	119(2)	F(4)-Sb-F(6)	90(2)
C(8)-C(9)-H(9)	120.3(12)	F(5)-Sb-F(2)	94(2)
C(10)-C(9)-H(9)	120.3(11)	F(4)-Sb-F(2)	176(2)
C(11)-C(10)-C(9)	118(2)	F(6)-Sb-F(2)	86(2)
C(11)-C(10)-H(10)	120.9(12)	F(5)-Sb-F(1)	90.2(9)
C(9)-C(10)-H(10)	120.9(11)	F(4)-Sb-F(1)	88.8(7)
C(10)-C(11)-C(12)	122(2)	F(6)-Sb-F(1)	90.6(8)
C(10)-C(11)-H(11)	119.0(12)	F(2)-Sb-F(1)	92.0(7)
C(12)-C(11)-H(11)	119.0(12)	F(5)-Sb-F(3)	90.8(9)
C(11)-C(12)-C(7)	120(2)	F(4)-Sb-F(3)	89.7(7)
C(11)-C(12)-H(12)	120.1(12)	F(6)-Sb-F(3)	88.4(8)
C(7)-C(12)-H(12)	120.1(10)	F(2)-Sb-F(3)	89.4(7)
N(1)-C(13)-C(14)	122.7(14)	F(1)-Sb-F(3)	178.3(7)
N(1)-C(13)-P	113.4(10)		

Table 3.8 Anisotropic displacement parameters ($\mathring{A}^2$ x 10^3) for $[Cu_2(\mu\text{-}Ph_2Pphen)_2(MeCN)_2](SbF_6)_2$

	U11	U22	U33	U23	U13	U12
Cu	51(1)	43(1)	39(1)	-2(1)	-5(1)	-4(1)
P	47(2)	39(2)	35(2)	-4(2)	1(2)	-1(2)
N(1)	54(8)	37(7)	32(7)	-4(6)	3(6)	-4(7)
N(2)	53(9)	42(8)	43(8)	1(7)	-8(7)	3(7)
N(3)	79(11)	26(8)	64(10)	-2(7)	12(8)	-13(7)
C(1)	30(8)	38(9)	60(11)	-6(8)	4(8)	0(7)
C(2)	52(11)	50(11)	45(10)	-1(8)	1(8)	-7(9)
C(3)	63(13)	75(14)	72(14)	12(12)	9(11)	-11(11)
C(4)	83(16)	79(15)	61(14)	2(11)	23(12)	-6(13)
C(5)	100(17)	70(14)	63(13)	5(11)	36(13)	4(13)
C(6)	68(12)	52(11)	52(11)	-9(9)	-11(10)	14(10)
C(7)	43(10)	43(10)	49(10)	-1(8)	1(8)	3(8)
C(8)	75(13)	64(12)	43(10)	-12(10)	10(10)	-20(10)
C(9)	53(11)	87(16)	62(12)	-34(12)	3(9)	5(11)
C(10)	98(16)	70(15)	64(13)	-22(12)	14(12)	13(13)
C(11)	114(18)	41(11)	91(16)	-19(11)	25(14)	12(11)
C(12)	85(14)	42(11)	82(14)	-7(10)	38(11)	-4(10)
C(13)	25(8)	49(10)	29(8)	3(8)	-5(6)	-15(7)
C(14)	67(12)	57(12)	38(10)	-10(9)	-2(9)	-8(10)
C(15)	74(12)	63(12)	26(9)	12(9)	-13(8)	-7(10)
C(16)	37(9)	55(11)	34(9)	13(9)	8(7)	-2(8)
C(17)	26(8)	46(10)	39(9)	11(8)	-2(7)	-15(7)
C(18)	41(9)	28(8)	48(10)	12(8)	-14(8)	-7(7)
C(19)	88(14)	47(11)	50(11)	-18(10)	7(10)	-9(10)
C(20)	93(15)	39(11)	86(16)	11(11)	6(13)	-2(11)
C(21)	66(12)	50(12)	78(14)	20(11)	-7(11)	13(10)
C(22)	54(10)	40(10)	47(10)	10(9)	17(8)	-6(9)
C(23)	76(13)	53(12)	62(13)	21(10)	-9(10)	14(11)
C(24)	71(13)	67(13)	51(11)	16(10)	-7(10)	10(11)
C(25)	108(18)	46(12)	103(18)	-1(12)	42(15)	-11(12)
C(26)	235(34)	95(20)	200(31)	-5(21)	180(29)	-19(22)
Sb	74(1)	62(1)	95(1)	18(1)	-2(1)	7(1)
F(1)	70(8)	154(13)	162(13)	39(11)	7(8)	21(9)
F(2)	169(18)	418(40)	306(29)	274(31)	115(19)	98(23)

Table 3.8 Anisotropic displacement parameters (Å^2 x 10^3) for [Cu$_2$(μ-Ph$_2$Pphen)$_2$(MeCN)$_2$](SbF$_6$)$_2$

F(3)	97(9)	139(12)	144(12)	51(10)	18(8)	49(9)
F(4)	144(16)	346(32)	350(31)	278(28)	89(17)	90(18)
F(5)	279(28)	189(22)	464(44)	-179(27)	-193(29)	58(20)
F(6)	222(23)	314(34)	314(31)	-185(29)	-126(23)	125(24)

Table 3.9 Hydrogen coordinates (x 10^4) and isotropic displacement parameters (Å^2 x 10^3) for $[Cu_2(\mu\text{-}Ph_2Pphen)_2(MeCN)_2](SbF_6)_2$

	x	y	z	U(eq)
H(2)	3253(15)	1910(13)	627(7)	74
H(3)	4622(17)	2656(17)	-56(9)	105
H(4)	3954(20)	3253(17)	-1035(9)	110
H(5)	1919(22)	3074(17)	-1371(9)	114
H(6)	489(17)	2360(15)	-717(8)	87
H(8)	-899(16)	1931(16)	1522(7)	91
H(9)	-1478(16)	3475(18)	2115(8)	101
H(10)	-586(20)	5296(19)	1992(9)	115
H(11)	789(20)	5525(16)	1228(10)	122
H(12)	1465(17)	3940(15)	676(9)	102
H(14)	1834(15)	1511(15)	1812(7)	81
H(15)	2915(15)	113(15)	2381(7)	82
H(19)	2146(17)	-3556(15)	-530(8)	93
H(20)	3376(18)	-4995(15)	-43(10)	109
H(21)	3970(16)	-4843(15)	1002(9)	98
H(23)	4143(17)	-3616(16)	1975(8)	97
H(24)	3795(16)	-1893(16)	2449(8)	95
H(26A)	-4347(68)	-524(169)	1442(15)	204(78)
H(26B)	-3642(163)	362(59)	1884(55)	204(78)
H(26C)	-3163(97)	-908(124)	1838(60)	204(78)

Single crystal X-ray diffraction study of $[Cu_2(\mu-Ph_2Pphen)_2\{\mu-S_2CN(Et)_2\}]PF_6.3H_2O$

Red rectangular blocks of $[Cu_2(\mu-Ph_2Pphen)_2\{\mu-S_2CN(Et)_2\}]PF_6.3H_2O$ were grown by slow vapour diffusion of a saturated dichloromethane solution of the complex and hexane. The general approach used for the intensity data collection and structure solution is described in Appendix A. The crystallographic data are given in Table 3.10, the atomic coordinates for non hydrogen atoms in Table 3.11, the interatomic distances in Table 3.12, the interatomic angles in Table 3.13, the anisotropic displacement parameters in Table 3.14 and the hydrogen coordinates in Table 3.15. The observed and calculated structure factors may be found on microfiche in an envelope fixed to the inside back cover. All non hydrogen atoms were made anisotropic. The hydrogen atoms were placed in calculated positions.

Table 3.10 Crystal data and details of crystallographic analysis for [Cu$_2$(μ-Ph$_2$Pphen)$_2${μ-S$_2$CN(Et)$_2$}]PF$_6$.3H$_2$0

Empirical formula	C$_{53}$H$_{50}$Cu$_2$F$_6$N$_5$O$_3$P$_3$S$_2$
Formula weight (g.mol^{-1})	1203.09
Crystal dimensions (mm)	0.23 x 0.15 x 0.08
Temperature (°C)	22
λ(Mo - K$_\alpha$) (Å)	0.71069
Crystal system	Triclinic
Space group	$P\bar{1}$
a (Å)	13.323(6)
b (Å)	14.699(7)
c (Å)	16.717(6)
α (°)	115.41(3)
β (°)	100.38(4)
γ (°)	100.86(4)
Volume (Å^3)	2776(2)
Z	2
D$_c$ (g.cm^{-3})	1.439
Absorption coefficient (mm^{-1})	0.994
Absorption correction	Semi-empirical
Max./Min. Transmission Factors	1.00/.918
F(000)	1232
Theta range for data collection (°)	2.20 to 22.97
Index ranges	-14<=h<=14, -16<=k<=14, 0<=l<=18
Reflections collected	8023
Independent reflections	7710 [R(int) = 0.0546]
Refinement method	Full-matrix least-squares on F^2
Data / restraints / parameters	7604 / 0 / 680
Goodness-of-fit on F^2	1.228
Final R indices [I>2σ(I)]	R1 = 0.0860, wR2 = 0.2095
R indices (all data)	R1 = 0.1997, wR2 = 0.3279
Largest difference (peak and hole)(eÅ^{-3})	$\Delta\rho_{max}$ = 2.067 and $\Delta\rho_{min}$ = -0.524

Table 3.11 Atomic coordinates (x 10^4) and equivalent isotropic displacement parameters (Å^2 x 10^3) for [$Cu_2(\mu\text{-}Ph_2Pphen)_2\{\mu\text{-}S_2CN(Et)_2\}$]$PF_6$.$3H_2O$

	x	y	z	U(eq)
Cu(1)	1636(2)	4779(2)	2036(1)	45(1)
Cu(2)	1083(2)	3918(2)	3220(1)	45(1)
P(1)	3024(3)	4205(3)	2295(3)	42(1)
P(2)	-390(3)	3016(3)	2042(3)	41(1)
S(1)	1587(4)	6337(3)	3137(3)	52(1)
S(2)	1838(4)	5498(3)	4494(3)	52(1)
N(1)	2133(10)	3014(10)	2951(8)	41(3)
N(2)	799(10)	3043(10)	3976(9)	45(3)
N(3)	326(9)	3646(9)	895(8)	37(3)
N(4)	1833(10)	5189(10)	971(9)	46(3)
N(5)	2701(11)	7448(10)	4896(8)	50(4)
C(1)	4162(11)	5190(12)	3272(9)	40(4)
C(2)	4866(13)	4940(14)	3810(11)	53(4)
C(3)	5752(14)	5730(17)	4502(12)	63(5)
C(4)	5958(15)	6750(16)	4665(12)	66(5)
C(5)	5228(15)	6968(15)	4123(12)	66(5)
C(6)	4322(13)	6202(14)	3429(11)	54(4)
C(7)	3600(12)	3823(13)	1325(10)	45(4)
C(8)	4496(14)	4487(14)	1349(11)	60(5)
C(9)	4889(16)	4234(17)	593(13)	71(6)
C(10)	4355(19)	3312(20)	-206(15)	85(7)
C(11)	3462(19)	2675(17)	-243(14)	93(7)
C(12)	3053(16)	2916(17)	500(13)	80(6)
C(13)	2823(13)	3039(12)	2482(11)	49(4)
C(14)	3373(14)	2300(14)	2194(12)	61(5)
C(15)	3178(13)	1490(14)	2394(12)	58(5)
C(16)	2480(13)	1429(12)	2914(11)	51(4)
C(17)	1973(12)	2222(12)	3173(10)	43(4)
C(18)	1256(12)	2264(12)	3730(10)	41(4)
C(19)	177(14)	3085(15)	4505(12)	59(5)
C(20)	-48(16)	2386(16)	4825(12)	67(5)
C(21)	384(17)	1579(16)	4566(15)	79(6)
C(22)	1038(13)	1461(13)	3991(12)	54(4)
C(23)	1554(15)	649(14)	3691(13)	65(5)

Table 3.11 Atomic coordinates (x 10^4) and equivalent isotropic displacement parameters (Å^2 x 10^3) for [Cu$_2$(μ-Ph$_2$Pphen)$_2${μ-S$_2$CN(Et)$_2$}]PF$_6$.3H$_2$0

C(24)	2256(15)	649(13)	3198(13)	60(5)
C(25)	-1546(12)	3431(13)	2232(11)	49(4)
C(26)	-1390(15)	4382(17)	3011(13)	72(6)
C(27)	-2235(19)	4740(22)	3206(16)	113(10)
C(28)	-3246(18)	4187(20)	2617(16)	87(7)
C(29)	-3419(15)	3265(20)	1834(17)	84(7)
C(30)	-2592(14)	2867(15)	1656(13)	67(5)
C(31)	-748(12)	1653(13)	1772(11)	48(4)
C(32)	-169(14)	1016(14)	1309(11)	57(5)
C(33)	-261(17)	26(15)	1229(14)	74(6)
C(34)	-983(20)	-344(17)	1600(16)	91(7)
C(35)	-1581(17)	261(16)	2053(15)	81(6)
C(36)	-1437(14)	1254(13)	2157(12)	60(5)
C(37)	-419(12)	2904(13)	887(10)	44(4)
C(38)	-1180(13)	2116(14)	90(11)	56(5)
C(39)	-1212(13)	2075(13)	-758(12)	57(5)
C(40)	-426(13)	2857(13)	-755(10)	47(4)
C(41)	334(12)	3643(12)	83(9)	41(4)
C(42)	1141(12)	4465(12)	123(11)	42(4)
C(43)	2556(14)	5940(14)	992(11)	52(4)
C(44)	2657(15)	6044(15)	215(15)	64(5)
C(45)	1963(15)	5299(16)	-640(13)	62(5)
C(46)	1178(13)	4474(14)	-706(11)	49(4)
C(47)	406(15)	3683(17)	-1559(12)	66(5)
C(48)	-361(14)	2907(16)	-1595(11)	62(5)
C(49)	2119(12)	6508(13)	4232(11)	45(4)
C(50)	3136(14)	8332(13)	4726(12)	63(5)
C(51)	2446(18)	9045(15)	4824(15)	89(7)
C(52)	3042(15)	7705(13)	5885(11)	64(5)
C(53)	4045(18)	7475(16)	6109(14)	90(7)
P(3)	4700(5)	8968(5)	2565(5)	89(2)
F(1)	5855(13)	9354(16)	2532(19)	203(10)
F(2)	5221(21)	9219(19)	3526(14)	235(11)
F(3)	4214(22)	8674(23)	1578(16)	275(15)
F(4)	3524(13)	8556(14)	2588(14)	176(8)
F(5)	4767(12)	7844(11)	2221(13)	160(7)

Table 3.11 Atomic coordinates (x 10^4) and equivalent isotropic displacement parameters (Å^2 x 10^3) for [Cu$_2$(µ-Ph$_2$Pphen)$_2$\{µ-S$_2$CN(Et)$_2$\}]PF$_6$.3H$_2$0

F(6)	4658(15)	10071(12)	2922(24)	315(20)
O(1)	8617(8)	8763(7)	3358(7)	46(3)
O(2)	7191(9)	6709(8)	2571(10)	83(5)
O(3)	4073(14)	268(11)	198(11)	101(5)

Table 3.12 Interatomic distances (Å) for [Cu$_2$(μ-Ph$_2$Pphen)$_2${μ-S$_2$CN(Et)$_2$}]PF$_6$.3H$_2$0

Cu(1)-N(3)	2.107(12)	C(23)-H(23)	0.96
Cu(1)-N(4)	2.151(12)	C(24)-H(24)	0.96
Cu(1)-P(1)	2.222(5)	C(25)-C(30)	1.40(2)
Cu(1)-S(1)	2.262(5)	C(25)-C(26)	1.39(2)
Cu(1)-Cu(2)	2.897(3)	C(26)-C(27)	1.36(3)
Cu(2)-N(1)	2.083(12)	C(26)-H(26)	0.96
Cu(2)-N(2)	2.185(13)	C(27)-C(28)	1.37(3)
Cu(2)-P(2)	2.208(5)	C(27)-H(27)	0.96
Cu(2)-S(2)	2.246(5)	C(28)-C(29)	1.36(3)
P(1)-C(1)	1.82(2)	C(28)-H(28)	0.96
P(1)-C(7)	1.83(2)	C(29)-C(30)	1.36(2)
P(1)-C(13)	1.85(2)	C(29)-H(29)	0.96
P(2)-C(25)	1.79(2)	C(30)-H(30)	0.96
P(2)-C(31)	1.80(2)	C(31)-C(32)	1.39(2)
P(2)-C(37)	1.86(2)	C(31)-C(36)	1.39(2)
S(1)-C(49)	1.73(2)	C(32)-C(33)	1.38(2)
S(2)-C(49)	1.72(2)	C(32)-H(32)	0.96
N(1)-C(13)	1.32(2)	C(33)-C(34)	1.38(3)
N(1)-C(17)	1.36(2)	C(33)-H(33)	0.96
N(2)-C(19)	1.31(2)	C(34)-C(35)	1.38(3)
N(2)-C(18)	1.34(2)	C(34)-H(34)	0.96
N(3)-C(37)	1.32(2)	C(35)-C(36)	1.36(2)
N(3)-C(41)	1.36(2)	C(35)-H(35)	0.96
N(4)-C(43)	1.30(2)	C(36)-H(36)	0.96
N(4)-C(42)	1.36(2)	C(37)-C(38)	1.37(2)
N(5)-C(49)	1.31(2)	C(38)-C(39)	1.38(2)
N(5)-C(52)	1.49(2)	C(38)-H(38)	0.96
N(5)-C(50)	1.48(2)	C(39)-C(40)	1.40(2)
C(1)-C(6)	1.36(2)	C(39)-H(39)	0.96
C(1)-C(2)	1.39(2)	C(40)-C(41)	1.41(2)
C(2)-C(3)	1.38(2)	C(40)-C(48)	1.45(2)
C(2)-H(2)	0.96	C(41)-C(42)	1.43(2)
C(3)-C(4)	1.37(2)	C(42)-C(46)	1.40(2)
C(3)-H(3)	0.96	C(43)-C(44)	1.40(2)
C(4)-C(5)	1.39(2)	C(43)-H(43)	0.96
C(4)-H(4)	0.96	C(44)-C(45)	1.38(2)

Table 3.12 Interatomic distances (Å) for [Cu$_2$(μ-Ph$_2$Pphen)$_2${μ-S$_2$CN(Et)$_2$}]PF$_6$.3H$_2$0

C(5)-C(6)	1.39(2)	C(44)-H(44)	0.96
C(5)-H(5)	0.96	C(45)-C(46)	1.39(2)
C(6)-H(6)	0.96	C(45)-H(45)	0.96
C(7)-C(8)	1.37(2)	C(46)-C(47)	1.43(2)
C(7)-C(12)	1.38(2)	C(47)-C(48)	1.35(2)
C(8)-C(9)	1.39(2)	C(47)-H(47)	0.96
C(8)-H(8)	0.96	C(48)-H(48)	0.96
C(9)-C(10)	1.37(3)	C(50)-C(51)	1.50(2)
C(9)-H(9)	0.96	C(50)-H(50A)	0.97
C(10)-C(11)	1.34(3)	C(50)-H(50B)	0.97
C(10)-H(10)	0.96	C(51)-H(51A)	0.960(2)
C(11)-C(12)	1.38(3)	C(51)-H(51B)	0.96
C(11)-H(11)	0.96	C(51)-H(51C)	0.96
C(12)-H(12)	0.96	C(52)-C(53)	1.46(2)
C(13)-C(14)	1.39(2)	C(52)-H(52A)	0.97
C(14)-C(15)	1.36(2)	C(52)-H(52B)	0.97
C(14)-H(14)	0.96	C(53)-H(53A)	0.96
C(15)-C(16)	1.40(2)	C(53)-H(53B)	0.960(2)
C(15)-H(15)	0.96	C(53)-H(53C)	0.96
C(16)-C(17)	1.40(2)	P(3)-F(2)	1.48(2)
C(16)-C(24)	1.42(2)	P(3)-F(6)	1.48(2)
C(17)-C(18)	1.44(2)	P(3)-F(3)	1.49(2)
C(18)-C(22)	1.42(2)	P(3)-F(5)	1.53(2)
C(19)-C(20)	1.36(2)	P(3)-F(1)	1.56(2)
C(19)-H(19)	0.96	P(3)-F(4)	1.58(2)
C(20)-C(21)	1.35(3)	O(1)-H(1S)	0.96
C(20)-H(20)	0.96	O(1)-H(2S)	0.95
C(21)-C(22)	1.39(2)	O(2)-H(3S)	0.97
C(21)-H(21)	0.96	O(2)-H(4S)	0.95
C(22)-C(23)	1.44(2)	O(3)-H(5S)	0.95
C(23)-C(24)	1.35(2)	O(3)-H(6S)	0.95

Table 3.13 Interatomic angles (°) for [Cu$_2$(μ-Ph$_2$Pphen)$_2${μ-S$_2$CN(Et)$_2$}]PF$_6$.3H$_2$0

N(3)-Cu(1)-N(4)	77.7(5)	C(23)-C(24)-H(24)	119.4(10)
N(3)-Cu(1)-P(1)	114.7(3)	C(16)-C(24)-H(24)	119.4(11)
N(4)-Cu(1)-P(1)	103.9(4)	C(30)-C(25)-C(26)	118(2)
N(3)-Cu(1)-S(1)	125.0(3)	C(30)-C(25)-P(2)	124.9(13)
N(4)-Cu(1)-S(1)	100.1(4)	C(26)-C(25)-P(2)	117.4(12)
P(1)-Cu(1)-S(1)	118.9(2)	C(27)-C(26)-C(25)	121(2)
N(3)-Cu(1)-Cu(2)	92.7(3)	C(27)-C(26)-H(26)	119.7(14)
N(4)-Cu(1)-Cu(2)	170.3(4)	C(25)-C(26)-H(26)	119.7(10)
P(1)-Cu(1)-Cu(2)	78.89(13)	C(26)-C(27)-C(28)	120(2)
S(1)-Cu(1)-Cu(2)	86.31(13)	C(26)-C(27)-H(27)	119.8(13)
N(1)-Cu(2)-N(2)	77.6(5)	C(28)-C(27)-H(27)	119.8(13)
N(1)-Cu(2)-P(2)	106.2(4)	C(29)-C(28)-C(27)	120(2)
N(2)-Cu(2)-P(2)	97.9(3)	C(29)-C(28)-H(28)	119.9(12)
N(1)-Cu(2)-S(2)	112.5(4)	C(27)-C(28)-H(28)	119.9(13)
N(2)-Cu(2)-S(2)	95.1(4)	C(30)-C(29)-C(28)	120(2)
P(2)-Cu(2)-S(2)	141.0(2)	C(30)-C(29)-H(29)	120.0(13)
N(1)-Cu(2)-Cu(1)	92.3(3)	C(28)-C(29)-H(29)	120.0(12)
N(2)-Cu(2)-Cu(1)	169.4(4)	C(29)-C(30)-C(25)	121(2)
P(2)-Cu(2)-Cu(1)	81.59(13)	C(29)-C(30)-H(30)	119.6(13)
S(2)-Cu(2)-Cu(1)	91.81(14)	C(25)-C(30)-H(30)	119.6(10)
C(1)-P(1)-C(7)	102.6(7)	C(32)-C(31)-C(36)	117(2)
C(1)-P(1)-C(13)	104.0(7)	C(32)-C(31)-P(2)	119.0(13)
C(7)-P(1)-C(13)	103.1(8)	C(36)-C(31)-P(2)	122.5(13)
C(1)-P(1)-Cu(1)	114.6(5)	C(33)-C(32)-C(31)	122(2)
C(7)-P(1)-Cu(1)	111.7(5)	C(33)-C(32)-H(32)	118.9(13)
C(13)-P(1)-Cu(1)	118.9(6)	C(31)-C(32)-H(32)	118.9(10)
C(25)-P(2)-C(31)	105.5(8)	C(32)-C(33)-C(34)	118(2)
C(25)-P(2)-C(37)	102.2(7)	C(32)-C(33)-H(33)	121.0(13)
C(31)-P(2)-C(37)	101.6(7)	C(34)-C(33)-H(33)	121.0(13)
C(25)-P(2)-Cu(2)	115.3(6)	C(35)-C(34)-C(33)	121(2)
C(31)-P(2)-Cu(2)	109.7(5)	C(35)-C(34)-H(34)	119.4(13)
C(37)-P(2)-Cu(2)	120.7(5)	C(33)-C(34)-H(34)	119.4(13)
C(49)-S(1)-Cu(1)	110.8(5)	C(36)-C(35)-C(34)	119(2)
C(49)-S(2)-Cu(2)	112.3(6)	C(36)-C(35)-H(35)	120.4(13)
C(13)-N(1)-C(17)	117.2(13)	C(34)-C(35)-H(35)	120.4(13)
C(13)-N(1)-Cu(2)	126.7(11)	C(35)-C(36)-C(31)	122(2)

Table 3.13 Interatomic angles (°) for [Cu₂(μ-Ph₂Pphen)₂{μ-S₂CN(Et)₂}]PF₆.3H₂0

Table 3.13 Interatomic angles ($^\circ$) for
$[Cu_2(\mu\text{-}Ph_2Pphen)_2\{\mu\text{-}S_2CN(Et)_2\}]PF_6.3H_2O$

C(17)-N(1)-Cu(2)	115.3(10)	C(35)-C(36)-H(36)	119.1(13)
C(19)-N(2)-C(18)	118.5(14)	C(31)-C(36)-H(36)	119.1(10)
C(19)-N(2)-Cu(2)	130.6(12)	N(3)-C(37)-C(38)	123.0(14)
C(18)-N(2)-Cu(2)	110.2(10)	N(3)-C(37)-P(2)	115.2(11)
C(37)-N(3)-C(41)	118.8(13)	C(38)-C(37)-P(2)	121.8(12)
C(37)-N(3)-Cu(1)	126.4(10)	C(39)-C(38)-C(37)	121(2)
C(41)-N(3)-Cu(1)	114.4(10)	C(39)-C(38)-H(38)	119.6(10)
C(43)-N(4)-C(42)	116.3(14)	C(37)-C(38)-H(38)	119.6(10)
C(43)-N(4)-Cu(1)	130.8(11)	C(38)-C(39)-C(40)	117(2)
C(42)-N(4)-Cu(1)	112.5(10)	C(38)-C(39)-H(39)	121.7(10)
C(49)-N(5)-C(52)	122.8(13)	C(40)-C(39)-H(39)	121.7(10)
C(49)-N(5)-C(50)	123.2(13)	C(41)-C(40)-C(39)	120(2)
C(52)-N(5)-C(50)	113.9(13)	C(41)-C(40)-C(48)	117(2)
C(6)-C(1)-C(2)	121(2)	C(39)-C(40)-C(48)	123(2)
C(6)-C(1)-P(1)	115.9(12)	N(3)-C(41)-C(40)	120.7(14)
C(2)-C(1)-P(1)	123.1(13)	N(3)-C(41)-C(42)	117.0(13)
C(1)-C(2)-C(3)	119(2)	C(40)-C(41)-C(42)	122.2(13)
C(1)-C(2)-H(2)	120.3(10)	N(4)-C(42)-C(46)	124(2)
C(3)-C(2)-H(2)	120.3(11)	N(4)-C(42)-C(41)	117.4(13)
C(4)-C(3)-C(2)	122(2)	C(46)-C(42)-C(41)	118.3(14)
C(4)-C(3)-H(3)	119.2(11)	N(4)-C(43)-C(44)	125(2)
C(2)-C(3)-H(3)	119.2(11)	N(4)-C(43)-H(43)	117.7(9)
C(3)-C(4)-C(5)	117(2)	C(44)-C(43)-H(43)	117.7(11)
C(3)-C(4)-H(4)	121.4(11)	C(45)-C(44)-C(43)	119(2)
C(5)-C(4)-H(4)	121.4(12)	C(45)-C(44)-H(44)	120.7(10)
C(4)-C(5)-C(6)	123(2)	C(43)-C(44)-H(44)	120.7(11)
C(4)-C(5)-H(5)	118.5(11)	C(44)-C(45)-C(46)	119(2)
C(6)-C(5)-H(5)	118.5(11)	C(44)-C(45)-H(45)	120.3(10)
C(1)-C(6)-C(5)	118(2)	C(46)-C(45)-H(45)	120.3(10)
C(1)-C(6)-H(6)	121.0(9)	C(45)-C(46)-C(42)	117(2)
C(5)-C(6)-H(6)	121.1(11)	C(45)-C(46)-C(47)	123(2)
C(8)-C(7)-C(12)	118(2)	C(42)-C(46)-C(47)	120(2)
C(8)-C(7)-P(1)	121.6(13)	C(48)-C(47)-C(46)	122(2)
C(12)-C(7)-P(1)	119.8(13)	C(48)-C(47)-H(47)	119.2(10)
C(9)-C(8)-C(7)	122(2)	C(46)-C(47)-H(47)	119.1(10)
C(9)-C(8)-H(8)	119.1(11)	C(47)-C(48)-C(40)	121(2)

Table 3.13 Interatomic angles (°) for [Cu$_2$(μ-Ph$_2$Pphen)$_2${μ-S$_2$CN(Et)$_2$}]PF$_6$.3H$_2$0

C(7)-C(8)-H(8)	119.1(10)	C(47)-C(48)-H(48)	119.7(10)
C(8)-C(9)-C(10)	119(2)	C(40)-C(48)-H(48)	119.7(10)
C(8)-C(9)-H(9)	120.5(11)	N(5)-C(49)-S(2)	118.7(11)
C(10)-C(9)-H(9)	120.5(12)	N(5)-C(49)-S(1)	119.3(12)
C(11)-C(10)-C(9)	120(2)	S(2)-C(49)-S(1)	121.9(10)
C(11)-C(10)-H(10)	120.3(13)	N(5)-C(50)-C(51)	113(2)
C(9)-C(10)-H(10)	120.2(12)	N(5)-C(50)-H(50A)	109.0(9)
C(10)-C(11)-C(12)	122(2)	C(51)-C(50)-H(50A)	109.0(11)
C(10)-C(11)-H(11)	118.8(13)	N(5)-C(50)-H(50B)	109.0(8)
C(12)-C(11)-H(11)	118.8(12)	C(51)-C(50)-H(50B)	109.0(10)
C(7)-C(12)-C(11)	119(2)	H(50A)-C(50)-H(50B)	107.8
C(7)-C(12)-H(12)	120.4(10)	C(50)-C(51)-H(51A)	109.5(11)
C(11)-C(12)-H(12)	120.4(12)	C(50)-C(51)-H(51B)	109.5(11)
N(1)-C(13)-C(14)	124(2)	H(51A)-C(51)-H(51B)	109.5(10)
N(1)-C(13)-P(1)	112.4(12)	C(50)-C(51)-H(51C)	109.5(10)
C(14)-C(13)-P(1)	123.7(13)	H(51A)-C(51)-H(51C)	109.47(8)
C(15)-C(14)-C(13)	118(2)	H(51B)-C(51)-H(51C)	109.47(9)
C(15)-C(14)-H(14)	120.8(10)	N(5)-C(52)-C(53)	111(2)
C(13)-C(14)-H(14)	120.8(10)	N(5)-C(52)-H(52A)	109.4(9)
C(14)-C(15)-C(16)	121(2)	C(53)-C(52)-H(52A)	109.4(12)
C(14)-C(15)-H(15)	119.5(10)	N(5)-C(52)-H(52B)	109.4(8)
C(16)-C(15)-H(15)	119.5(9)	C(53)-C(52)-H(52B)	109.4(10)
C(15)-C(16)-C(17)	116(2)	H(52A)-C(52)-H(52B)	108.0
C(15)-C(16)-C(24)	126(2)	C(52)-C(53)-H(53A)	109.5(11)
C(17)-C(16)-C(24)	119(2)	C(52)-C(53)-H(53B)	109.5(12)
N(1)-C(17)-C(16)	124(2)	H(53A)-C(53)-H(53B)	109.47(9)
N(1)-C(17)-C(18)	115.0(13)	C(52)-C(53)-H(53C)	109.5(10)
C(16)-C(17)-C(18)	121(2)	H(53A)-C(53)-H(53C)	109.47(7)
N(2)-C(18)-C(22)	122(2)	H(53B)-C(53)-H(53C)	109.5
N(2)-C(18)-C(17)	119.5(13)	F(2)-P(3)-F(6)	89(2)
C(22)-C(18)-C(17)	119(2)	F(2)-P(3)-F(3)	177(2)
N(2)-C(19)-C(20)	124(2)	F(6)-P(3)-F(3)	94(2)
N(2)-C(19)-H(19)	117.8(10)	F(2)-P(3)-F(5)	89.6(13)
C(20)-C(19)-H(19)	117.8(12)	F(6)-P(3)-F(5)	178.5(14)
C(19)-C(20)-C(21)	118(2)	F(3)-P(3)-F(5)	87.6(14)
C(19)-C(20)-H(20)	121.0(12)	F(2)-P(3)-F(1)	85.3(13)

Table 3.13 Interatomic angles (°) for
[Cu$_2$(µ-Ph$_2$Pphen)$_2${µ-S$_2$CN(Et)$_2$}]PF$_6$.3H$_2$0

C(21)-C(20)-H(20)	121.0(11)	F(6)-P(3)-F(1)	88.5(13)
C(20)-C(21)-C(22)	122(2)	F(3)-P(3)-F(1)	93(2)
C(20)-C(21)-H(21)	119.3(11)	F(5)-P(3)-F(1)	90.9(10)
C(22)-C(21)-H(21)	119.2(11)	F(2)-P(3)-F(4)	95(2)
C(21)-C(22)-C(18)	116(2)	F(6)-P(3)-F(4)	92.5(12)
C(21)-C(22)-C(23)	126(2)	F(3)-P(3)-F(4)	86.9(13)
C(18)-C(22)-C(23)	118(2)	F(5)-P(3)-F(4)	88.2(9)
C(24)-C(23)-C(22)	122(2)	F(1)-P(3)-F(4)	179.0(11)
C(24)-C(23)-H(23)	119.0(10)	H(1S)-O(1)-H(2S)	113.55(7)
C(22)-C(23)-H(23)	119.0(11)	H(3S)-O(2)-H(4S)	112.2
C(23)-C(24)-C(16)	121(2)	H(5S)-O(3)-H(6S)	114.8

Table 3.14 Anisotropic displacement parameters ($\mathring{A}^2$ x 10^3) for [$Cu_2(\mu\text{-}Ph_2Pphen)_2\{\mu\text{-}S_2CN(Et)_2\}$]$PF_6$.$3H_2O$

	U11	U22	U33	U23	U13	U12
Cu(1)	44(1)	49(1)	39(1)	19(1)	9(1)	12(1)
Cu(2)	45(1)	46(1)	45(1)	22(1)	13(1)	16(1)
P(1)	36(2)	47(3)	42(2)	20(2)	13(2)	11(2)
P(2)	38(2)	41(2)	42(2)	19(2)	11(2)	11(2)
S(1)	64(3)	47(3)	41(2)	21(2)	8(2)	19(2)
S(2)	69(3)	39(2)	42(2)	20(2)	11(2)	12(2)
N(1)	41(8)	51(8)	35(7)	21(6)	12(6)	17(6)
N(2)	35(7)	49(9)	45(8)	25(7)	2(6)	3(7)
N(3)	32(7)	35(7)	41(8)	17(6)	12(6)	7(6)
N(4)	51(8)	45(8)	49(9)	28(7)	17(7)	14(7)
N(5)	73(10)	36(8)	36(8)	16(7)	7(7)	14(7)
C(1)	34(9)	48(10)	28(8)	13(7)	8(7)	6(7)
C(2)	47(11)	72(12)	42(10)	30(9)	11(8)	14(9)
C(3)	46(11)	95(16)	50(11)	39(11)	10(9)	18(11)
C(4)	53(12)	67(14)	49(11)	14(10)	3(9)	0(10)
C(5)	69(13)	66(13)	60(12)	26(11)	21(11)	20(11)
C(6)	44(10)	58(12)	41(10)	17(9)	-1(8)	7(9)
C(7)	34(9)	54(10)	44(10)	22(9)	13(7)	8(8)
C(8)	60(12)	56(11)	45(10)	23(9)	-1(9)	-2(9)
C(9)	71(13)	91(16)	59(13)	39(12)	37(11)	19(12)
C(10)	93(17)	114(20)	63(14)	40(14)	46(13)	47(16)
C(11)	100(18)	67(14)	52(13)	-8(11)	17(12)	-8(13)
C(12)	65(13)	86(15) ·	54(12)	11(11)	20(11)	-2(11)
C(13)	50(10)	45(10)	51(10)	24(9)	9(9)	16(8)
C(14)	56(12)	60(12)	75(13)	35(11)	33(10)	19(10)
C(15)	49(11)	51(11)	72(12)	18(10)	24(10)	37(9)
C(16)	52(11)	37(10)	48(10)	11(8)	-1(8)	17(8)
C(17)	38(9)	38(9)	45(9)	19(8)	1(8)	8(7)
C(18)	40(9)	46(10)	40(9)	26(8)	6(7)	13(8)
C(19)	60(12)	71(13)	60(12)	42(11)	24(10)	17(10)
C(20)	86(14)	80(14)	64(12)	47(12)	47(11)	33(12)
C(21)	88(15)	67(14)	104(17)	60(13)	38(14)	12(12)
C(22)	41(10)	51(11)	62(11)	28(9)	3(9)	7(9)
C(23)	65(13)	56(12)	78(13)	41(11)	11(11)	16(10)

Table 3.14 Anisotropic displacement parameters (Å^2 x 10^3) for $[Cu_2(\mu\text{-}Ph_2Pphen)_2\{\mu\text{-}S_2CN(Et)_2\}]PF_6.3H_2O$

C(24)	68(12)	38(10)	86(14)	40(10)	14(11)	25(9)
C(25)	42(10)	62(11)	45(10)	22(9)	16(8)	23(9)
C(26)	57(12)	112(17)	62(12)	40(13)	25(10)	52(12)
C(27)	76(17)	152(24)	77(16)	16(16)	9(13)	71(17)
C(28)	74(16)	122(20)	88(16)	45(15)	50(14)	66(15)
C(29)	40(11)	125(20)	108(18)	65(17)	29(12)	42(13)
C(30)	44(11)	76(14)	80(14)	37(11)	16(10)	20(10)
C(31)	36(9)	60(11)	43(10)	24(9)	2(8)	12(8)
C(32)	60(12)	57(12)	58(11)	33(10)	11(9)	21(9)
C(33)	77(15)	50(12)	83(15)	32(11)	-1(12)	20(11)
C(34)	99(18)	55(14)	99(18)	42(13)	-11(14)	9(13)
C(35)	80(15)	61(14)	97(17)	41(12)	22(13)	8(12)
C(36)	72(13)	45(11)	71(12)	33(10)	26(10)	16(9)
C(37)	33(9)	51(10)	47(10)	22(8)	7(8)	20(8)
C(38)	46(10)	80(13)	43(10)	34(10)	15(8)	5(9)
C(39)	42(10)	46(10)	64(12)	14(9)	11(9)	4(8)
C(40)	48(10)	51(10)	36(9)	15(8)	7(8)	19(9)
C(41)	51(10)	56(10)	27(8)	26(8)	18(7)	20(8)
C(42)	45(10)	48(10)	43(10)	26(8)	17(8)	22(8)
C(43)	62(11)	71(12)	52(11)	46(10)	28(9)	27(10)
C(44)	54(12)	70(13)	100(16)	57(13)	41(12)	28(10)
C(45)	60(12)	81(14)	69(13)	55(12)	24(10)	25(11)
C(46)	49(10)	70(12)	39(10)	29(9)	16(8)	29(9)
C(47)	59(12)	104(16)	49(12)	46(12)	12(10)	33(12)
C(48)	54(12)	89(15)	28(9)	20(10)	3(8)	18(11)
C(49)	50(10)	48(10)	45(10)	27(9)	12(8)	24(8)
C(50)	67(12)	60(12)	45(11)	25(9)	-6(9)	8(10)
C(51)	112(18)	51(12)	97(17)	32(12)	22(14)	30(13)
C(52)	74(13)	29(9)	57(12)	2(8)	2(10)	10(9)
C(53)	101(18)	62(14)	77(15)	25(12)	-10(13)	13(13)
P(3)	74(4)	59(4)	107(5)	28(4)	3(4)	13(3)
F(1)	91(12)	192(19)	352(31)	166(21)	66(15)	7(12)
F(2)	250(25)	226(24)	121(15)	51(16)	-56(16)	22(20)
F(3)	286(30)	317(34)	176(21)	171(23)	-27(20)	-48(25)
F(4)	108(13)	143(14)	230(20)	40(14)	78(13)	32(11)
F(5)	124(13)	70(10)	222(19)	21(11)	39(12)	25(9)

Table 3.14 Anisotropic displacement parameters ($\mathring{A}^2$ x 10^3) for [Cu$_2$(μ-Ph$_2$Pphen)$_2${μ-S$_2$CN(Et)$_2$}]PF$_6$.3H$_2$0

F(6)	128(15)	57(10)	554(46)	35(18)	-74(21)	29(10)
O(1)	49(7)	31(6)	57(7)	38(5)	2(6)	-12(5)
O(2)	52(8)	18(6)	149(13)	14(7)	46(8)	-1(6)
O(3)	135(14)	75(11)	87(11)	25(9)	49(11)	40(10)

Table 3.15 Hydrogen coordinates (x 10^4) and isotropic displacement parameters ($Å^2$ x 10^3) for [$Cu_2(μ$-$Ph_2Pphen)_2\{μ$-$S_2CN(Et)_2\}$]PF_6.$3H_2O$

	x	y	z	U(eq)
H(2)	4740(13)	4227(14)	3703(11)	80
H(3)	6233(14)	5556(17)	4876(12)	94
H(4)	6582(15)	7292(16)	5135(12)	99
H(5)	5354(15)	7682(15)	4231(12)	100
H(6)	3824(13)	6380(14)	3072(11)	80
H(8)	4860(14)	5143(14)	1905(11)	89
H(9)	5528(16)	4699(17)	629(13)	107
H(10)	4617(19)	3121(20)	-736(15)	128
H(11)	3094(19)	2029(17)	-807(14)	139
H(12)	2396(16)	2459(17)	444(13)	121
H(14)	3879(14)	2359(14)	1863(12)	91
H(15)	3525(13)	953(14)	2176(12)	87
H(19)	-143(14)	3648(15)	4679(12)	89
H(20)	-499(16)	2462(16)	5222(12)	100
H(21)	235(17)	1077(16)	4785(15)	119
H(23)	1396(15)	90(14)	3844(13)	97
H(24)	2610(15)	111(13)	3037(13)	89
H(26)	-680(15)	4791(17)	3418(13)	108
H(27)	-2119(19)	5386(22)	3760(16)	169
H(28)	-3835(18)	4448(20)	2756(16)	131
H(29)	-4125(15)	2895(20)	1407(17)	126
H(30)	-2730(14)	2191(15)	1127(13)	100
H(32)	310(14)	1273(14)	1035(11)	85
H(33)	163(17)	-392(15)	925(14)	110
H(34)	-1069(20)	-1035(17)	1542(16)	136
H(35)	-2093(17)	-13(16)	2292(15)	121
H(36)	-1821(14)	1689(13)	2505(12)	90
H(38)	-1694(13)	1588(14)	122(11)	84
H(39)	-1746(13)	1537(13)	-1318(12)	86
H(43)	3054(14)	6457(14)	1582(11)	78
H(44)	3199(15)	6622(15)	276(15)	97
H(45)	2020(15)	5347(16)	-1186(13)	92
H(47)	431(15)	3703(17)	-2122(12)	99
H(48)	-866(14)	2385(16)	-2179(11)	93

Table 3.15 Hydrogen coordinates (x 10^4) and isotropic displacement parameters (Å^2 x 10^3) for [Cu$_2$(μ-Ph$_2$Pphen)$_2${μ-S$_2$CN(Et)$_2$}]PF$_6$.3H$_2$0

H(50A)	3210(14)	8046(13)	4105(12)	7(9)
H(50B)	3843(14)	8742(13)	5160(12)	7(9)
H(51A)	2813(46)	9657(51)	4800(90)	116(33)
H(51B)	2293(86)	9259(82)	5407(42)	116(33)
H(51C)	1789(47)	8676(36)	4328(53)	116(33)
H(52A)	2490(15)	7296(13)	6009(11)	7(9)
H(52B)	3135(15)	8447(13)	6277(11)	7(9)
H(53A)	4244(57)	7640(98)	6749(28)	116(33)
H(53B)	4597(30)	7893(77)	6003(87)	116(33)
H(53C)	3954(35)	6740(27)	5724(65)	116(33)
H(1S)	7912(25)	8361(52)	3276(67)	7(9)
H(2S)	9134(42)	8396(53)	3350(71)	7(9)
H(3S)	7247(72)	7452(19)	2825(49)	7(9)
H(4S)	7610(74)	6563(54)	3002(43)	7(9)
H(5S)	3336(23)	213(78)	27(71)	7(9)
H(6S)	4246(56)	-125(71)	503(66)	7(9)

Single crystal X-ray diffraction study of [Cu$_2$(μ-Ph$_2$Pphen)$_2$(η-bipy)](PF$_6$)$_2$

Red prism shaped crystals of [Cu$_2$(μ-Ph$_2$Pphen)$_2$(η-bipy)](PF$_6$)$_2$ were grown from a saturated methanolic solution of the complex. The general approach used for the intensity data collection and structure solution is described in Appendix A. The crystallographic data are given in Table 3.16, the atomic coordinates for non hydrogen atoms in Table 3.17, the interatomic distances in Table 3.18, the interatomic angles in Table 3.19, the anisotropic displacement parameters in Table 3.20 and the hydrogen coordinates in Table 3.21. The observed and calculated structure factors may be found on microfiche in an envelope fixed to the inside back cover. All non hydrogen atoms were made anisotropic. The hydrogen atoms were placed in calculated positions.

Table 3.16 Crystal data and details of crystallographic analysis for $[Cu_2(\mu\text{-}Ph_2Pphen)_2(\eta\text{-}bipy)](PF_6)_2$

Empirical formula	$C_{58} H_{42} Cu_2 F_{12} N_6 P_4$
Formula weight (g.mol^{-1})	1301.94
Crystal size (mm)	0.76 x 0.54 x 0.38
Temperature (°C)	22
λ(Mo - Kα) (Å)	0.71069
Crystal system	Monoclinic
Space group	*C2/c*
a (Å)	27.184(7)
b (Å)	14.613(4)
c (Å)	18.082(4)
α (°)	90
β (°)	131.27(2)
γ (°)	90
Volume (Å^3)	5399(2)
Z	4
D_c (g.cm^{-3})	1.602
Absorption coefficient (mm^{-1})	0.995
Absorption correction	Semi-empirical
Max./Min. Transmission Factors	.999 / .956
F(000)	2632
Theta range for data collection (°)	2.25 to 22.98
Index ranges	-29<=h<=23, -1<=k<=16, -1<=l<=19
Reflections collected	4526
Independent reflections	3733 [R(int) = 0.0376]
Refinement method	Full-matrix least-squares on F^2
Data / restraints / parameters	3710 / 0 / 372
Goodness-of-fit on F^2	1.178
Final R indices [I>2σ(I)]	R1 = 0.0504, wR2 = 0.0999
R indices (all data)	R1 = 0.1031, wR2 = 0.1484
Largest difference (peak and hole)(e.A^{-3})	$\Delta\rho_{max}$ = 0.447 and $\Delta\rho_{min}$ = -0.381

Table 3.17 Atomic coordinates (x 10^4) and equivalent isotropic displacement parameters ($Å^2$ x 10^3) for [Cu$_2$(μ-Ph$_2$Pphen)$_2$(η-bipy)](PF$_6$)$_2$

	x	y	z	U(eq)
Cu(1)	0	-103(1)	2500	43(1)
Cu(2)	0	2599(1)	2500	47(1)
P(1)	685(1)	675(1)	2428(1)	41(1)
N(1)	913(3)	2097(4)	3554(4)	39(1)
N(2)	327(3)	3571(4)	3583(4)	51(2)
N(3)	-475(3)	-1182(4)	1524(4)	44(1)
C(1)	376(3)	1468(5)	1436(5)	43(2)
C(2)	-197(4)	1246(6)	499(5)	55(2)
C(3)	-430(4)	1782(6)	-301(5)	67(2)
C(4)	-93(4)	2550(6)	-178(6)	68(2)
C(5)	485(4)	2781(5)	751(6)	59(2)
C(6)	711(4)	2240(5)	1553(5)	49(2)
C(7)	1270(3)	-17(5)	2482(5)	43(2)
C(8)	1455(4)	208(5)	1950(5)	52(2)
C(9)	1900(4)	-349(6)	2018(6)	66(2)
C(10)	2159(4)	-1107(7)	2600(7)	70(3)
C(11)	1977(4)	-1331(6)	3120(7)	74(2)
C(12)	1528(4)	-801(5)	3056(6)	63(2)
C(13)	1207(3)	1380(5)	3540(5)	41(2)
C(14)	1843(3)	1126(5)	4360(5)	54(2)
C(15)	2176(4)	1615(6)	5210(5)	60(2)
C(16)	1892(3)	2374(5)	5253(5)	50(2)
C(17)	1257(3)	2603(5)	4412(4)	41(2)
C(18)	944(4)	3388(5)	4410(5)	45(2)
C(19)	1280(4)	3937(6)	5261(6)	60(2)
C(20)	956(5)	4701(6)	5212(8)	77(3)
C(21)	344(5)	4900(6)	4371(8)	81(3)
C(22)	41(5)	4316(6)	3560(7)	70(2)
C(23)	1925(5)	3677(7)	6107(6)	75(3)
C(24)	2215(4)	2932(7)	6120(6)	70(3)
C(25)	-280(3)	-2010(5)	1965(5)	50(2)
C(26)	-606(4)	-2801(6)	1450(7)	65(2)
C(27)	-1147(5)	-2740(7)	451(7)	74(3)
C(28)	-1347(4)	-1910(7)	1(6)	67(2)

Table 3.17 Atomic coordinates (x 10^4) and equivalent isotropic displacement parameters ($\mathring{A}^2$ x 10^3) for [Cu$_2$(μ-Ph$_2$Pphen)$_2$(η-bipy)](PF$_6$)$_2$

C(29)	-1000(4)	-1139(6)	549(5)	57(2)
P(2)	3267(1)	-698(2)	6725(2)	75(1)
F(1)	3974(3)	-1005(5)	7541(5)	173(3)
F(2)	3012(4)	-1275(5)	7150(5)	144(3)
F(3)	3123(3)	-1554(5)	6083(5)	131(2)
F(4)	2534(3)	-376(4)	5907(5)	129(2)
F(5)	3469(4)	-136(6)	6263(6)	176(3)
F(6)	3391(3)	146(5)	7357(5)	142(3)

Table 3.18 Interatomic distances (Å) for [Cu$_2$(μ-Ph$_2$Pphen)$_2$(η-bipy)](PF$_6$)$_2$

Cu(1)-N(3)	2.063(6)	C(12)-H(12)	0.96
Cu(1)-N(3')	2.063(6)	C(13)-C(14)	1.394(9)
Cu(1)-Cu(2)	3.949(2)	C(14)-C(15)	1.363(10)
Cu(1)-P(1)	2.257(2)	C(14)-H(14)	0.96
Cu(2)-N(1)	2.022(5)	C(15)-C(16)	1.382(10)
Cu(2)-N(2)	2.084(6)	C(15)-H(15)	0.96
P(1)-C(1)	1.811(7)	C(16)-C(17)	1.394(9)
P(1)-C(7)	1.831(7)	C(16)-C(24)	1.442(10)
P(1)-C(13)	1.832(7)	C(17)-C(18)	1.428(10)
N(1)-C(13)	1.329(8)	C(18)-C(19)	1.412(10)
N(1)-C(17)	1.383(8)	C(19)-C(20)	1.388(11)
N(2)-C(22)	1.322(9)	C(19)-C(23)	1.422(11)
N(2)-C(18)	1.346(8)	C(20)-C(21)	1.352(12)
N(3)-C(25)	1.351(9)	C(20)-H(20)	0.96
N(3)-C(29)	1.353(8)	C(21)-C(22)	1.401(11)
C(1)-C(6)	1.377(9)	C(21)-H(21)	0.96
C(1)-C(2)	1.385(9)	C(22)-H(22)	0.96
C(2)-C(3)	1.378(10)	C(23)-C(24)	1.335(12)
C(2)-H(2)	0.96	C(23)-H(23)	0.96
C(3)-C(4)	1.371(11)	C(24)-H(24)	0.96
C(3)-H(3)	0.96	C(25)-C(26)	1.379(10)
C(4)-C(5)	1.386(10)	C(25)-C(25')	1.474(14)
C(4)-H(4)	0.96	C(26)-C(27)	1.389(11)
C(5)-C(6)	1.390(10)	C(26)-H(26)	0.96
C(5)-H(5)	0.96	C(27)-C(28)	1.359(12)
C(6)-H(6)	0.96	C(27)-H(27)	0.96
C(7)-C(8)	1.388(9)	C(28)-C(29)	1.383(10)
C(7)-C(12)	1.386(10)	C(28)-H(28)	0.96
C(8)-C(9)	1.394(10)	C(29)-H(29)	0.96
C(8)-H(8)	0.96	P(2)-F(5)	1.509(7)
C(9)-C(10)	1.361(11)	P(2)-F(1)	1.527(6)
C(9)-H(9)	0.96	P(2)-F(6)	1.561(6)
C(10)-C(11)	1.359(11)	P(2)-F(3)	1.570(6)
C(10)-H(10)	0.96	P(2)-F(4)	1.579(6)
C(11)-C(12)	1.385(10)	P(2)-F(2)	1.578(7)
C(11)-H(11)	0.96		

Table 3.19 Interatomic angles (°) for [Cu$_2$(μ-Ph$_2$Pphen)$_2$(η-bipy)](PF$_6$)$_2$

N(3)-Cu(1)-N(3')	80.5(3)	C(14)-C(13)-P(1)	122.5(6)
N(3)-Cu(1)-P(1')	111.1(2)	C(15)-C(14)-C(13)	119.6(7)
N(3)-Cu(1)-P(1)	114.2(2)	C(15)-C(14)-H(14)	120.2(5)
N(3')-Cu(1)-P(1)	111.0(2)	C(13)-C(14)-H(14)	120.2(4)
P(1')-Cu(1)-P(1)	119.50(11)	C(14)-C(15)-C(16)	120.3(7)
N(1')-Cu(2)-N(1)	137.5(3)	C(14)-C(15)-H(15)	119.8(5)
N(1')-Cu(2)-N(2)	129.1(2)	C(16)-C(15)-H(15)	119.8(4)
N(1)-Cu(2)-N(2)	82.2(2)	C(17)-C(16)-C(15)	117.8(7)
N(1)-Cu(2)-N(2')	129.1(2)	C(17)-C(16)-C(24)	118.6(8)
N(2)-Cu(2)-N(2')	94.1(3)	C(15)-C(16)-C(24)	123.6(7)
C(1)-P(1)-C(7)	103.0(3)	N(1)-C(17)-C(16)	122.1(7)
C(1)-P(1)-C(13)	104.2(3)	N(1)-C(17)-C(18)	117.7(6)
C(7)-P(1)-C(13)	103.6(3)	C(16)-C(17)-C(18)	120.2(6)
C(1)-P(1)-Cu(1)	121.2(2)	N(2)-C(18)-C(17)	117.8(6)
C(7)-P(1)-Cu(1)	116.1(2)	N(2)-C(18)-C(19)	122.3(7)
C(13)-P(1)-Cu(1)	107.0(2)	C(17)-C(18)-C(19)	119.9(7)
C(13)-N(1)-C(17)	118.1(6)	C(20)-C(19)-C(23)	124.4(8)
C(13)-N(1)-Cu(2)	130.4(4)	C(20)-C(19)-C(18)	117.4(8)
C(17)-N(1)-Cu(2)	111.4(4)	C(23)-C(19)-C(18)	118.2(8)
C(22)-N(2)-C(18)	118.3(7)	C(21)-C(20)-C(19)	120.2(9)
C(22)-N(2)-Cu(2)	130.8(6)	C(21)-C(20)-H(20)	119.9(5)
C(18)-N(2)-Cu(2)	110.8(5)	C(19)-C(20)-H(20)	119.9(5)
C(25)-N(3)-C(29)	118.5(6)	C(20)-C(21)-C(22)	118.9(9)
C(25)-N(3)-Cu(1)	113.5(4)	C(20)-C(21)-H(21)	120.5(5)
C(29)-N(3)-Cu(1)	127.3(5)	C(22)-C(21)-H(21)	120.5(6)
C(6)-C(1)-C(2)	118.4(7)	N(2)-C(22)-C(21)	122.8(9)
C(6)-C(1)-P(1)	123.0(5)	N(2)-C(22)-H(22)	118.6(5)
C(2)-C(1)-P(1)	118.4(5)	C(21)-C(22)-H(22)	118.6(6)
C(3)-C(2)-C(1)	121.2(7)	C(24)-C(23)-C(19)	122.2(8)
C(3)-C(2)-H(2)	119.4(5)	C(24)-C(23)-H(23)	118.9(5)
C(1)-C(2)-H(2)	119.4(4)	C(19)-C(23)-H(23)	118.9(5)
C(4)-C(3)-C(2)	120.0(7)	C(23)-C(24)-C(16)	120.9(8)
C(4)-C(3)-H(3)	120.0(5)	C(23)-C(24)-H(24)	119.6(5)
C(2)-C(3)-H(3)	120.0(5)	C(16)-C(24)-H(24)	119.6(5)
C(3)-C(4)-C(5)	119.8(7)	N(3)-C(25)-C(26)	121.7(7)
C(3)-C(4)-H(4)	120.1(5)	N(3)-C(25)-C(25')	116.0(4)
C(5)-C(4)-H(4)	120.1(5)	C(26)-C(25)-C(25')	122.3(5)

Table 3.19 Interatomic angles (°) for [Cu$_2$(μ-Ph$_2$Pphen)$_2$(η-bipy)](PF$_6$)$_2$

C(4)-C(5)-C(6)	119.6(7)	C(25)-C(26)-C(27)	118.9(8)
C(4)-C(5)-H(5)	120.2(5)	C(25)-C(26)-H(26)	120.6(5)
C(6)-C(5)-H(5)	120.2(5)	C(27)-C(26)-H(26)	120.6(5)
C(5)-C(6)-C(1)	120.9(7)	C(28)-C(27)-C(26)	119.9(8)
C(5)-C(6)-H(6)	119.6(5)	C(28)-C(27)-H(27)	120.0(5)
C(1)-C(6)-H(6)	119.6(4)	C(26)-C(27)-H(27)	120.0(5)
C(8)-C(7)-C(12)	118.6(7)	C(27)-C(28)-C(29)	118.9(8)
C(8)-C(7)-P(1)	122.1(6)	C(27)-C(28)-H(28)	120.5(5)
C(12)-C(7)-P(1)	119.3(5)	C(29)-C(28)-H(28)	120.5(5)
C(7)-C(8)-C(9)	119.4(8)	N(3)-C(29)-C(28)	122.1(8)
C(7)-C(8)-H(8)	120.3(4)	N(3)-C(29)-H(29)	119.0(5)
C(9)-C(8)-H(8)	120.3(5)	C(28)-C(29)-H(29)	119.0(5)
C(10)-C(9)-C(8)	121.3(8)	F(5)-P(2)-F(1)	90.6(5)
C(10)-C(9)-H(9)	119.4(5)	F(5)-P(2)-F(6)	89.6(5)
C(8)-C(9)-H(9)	119.4(5)	F(1)-P(2)-F(6)	89.9(4)
C(9)-C(10)-C(11)	119.5(8)	F(5)-P(2)-F(3)	91.7(4)
C(9)-C(10)-H(10)	120.2(5)	F(1)-P(2)-F(3)	91.3(4)
C(11)-C(10)-H(10)	120.2(6)	F(6)-P(2)-F(3)	178.2(4)
C(10)-C(11)-C(12)	120.6(9)	F(5)-P(2)-F(4)	90.8(5)
C(10)-C(11)-H(11)	119.7(6)	F(1)-P(2)-F(4)	178.1(5)
C(12)-C(11)-H(11)	119.7(5)	F(6)-P(2)-F(4)	88.8(4)
C(7)-C(12)-C(11)	120.6(8)	F(3)-P(2)-F(4)	90.0(4)
C(7)-C(12)-H(12)	119.7(4)	F(5)-P(2)-F(2)	176.5(5)
C(11)-C(12)-H(12)	119.7(5)	F(1)-P(2)-F(2)	92.9(5)
N(1)-C(13)-C(14)	122.0(6)	F(6)-P(2)-F(2)	90.9(4)
N(1)-C(13)-P(1)	115.1(5)	F(3)-P(2)-F(2)	87.7(4)
		F(4)-P(2)-F(2)	85.7(4)

Table 3.20 Anisotropic displacement parameters ($\mathring{A}^2$ x 10^3) for [Cu$_2$(μ-Ph$_2$Pphen)$_2$(η-bipy)](PF$_6$)$_2$

	U11	U22	U33	U23	U13	U12
Cu(1)	47(1)	40(1)	41(1)	0	29(1)	0
Cu(2)	43(1)	45(1)	38(1)	0	21(1)	0
P(1)	43(1)	40(1)	41(1)	1(1)	28(1)	1(1)
N(1)	41(3)	40(3)	29(3)	-3(3)	21(3)	-8(3)
N(2)	58(4)	42(4)	56(4)	-5(3)	39(4)	-1(3)
N(3)	48(4)	46(4)	45(4)	-6(3)	34(3)	-6(3)
C(1)	46(4)	41(5)	45(4)	1(3)	32(4)	1(3)
C(2)	57(5)	57(5)	45(4)	-6(4)	31(4)	-12(4)
C(3)	67(5)	80(6)	34(4)	2(5)	24(4)	-6(5)
C(4)	84(6)	72(6)	52(5)	20(5)	47(5)	8(5)
C(5)	72(6)	51(5)	67(6)	10(4)	52(5)	2(4)
C(6)	52(4)	46(5)	46(4)	-3(4)	31(4)	-7(4)
C(7)	43(4)	43(4)	47(4)	-7(4)	31(4)	-2(4)
C(8)	60(5)	52(5)	49(5)	-11(4)	38(4)	-8(4)
C(9)	64(6)	82(7)	73(6)	-30(5)	54(5)	-14(5)
C(10)	58(5)	75(7)	82(6)	-21(6)	49(5)	3(5)
C(11)	64(5)	68(6)	87(6)	11(5)	49(5)	18(5)
C(12)	80(6)	53(5)	81(6)	15(5)	65(5)	16(5)
C(13)	46(4)	37(4)	41(4)	2(3)	29(4)	1(3)
C(14)	40(4)	64(5)	42(4)	6(4)	20(4)	8(4)
C(15)	42(4)	70(6)	42(5)	6(4)	17(4)	-1(4)
C(16)	46(4)	62(5)	33(4)	-7(4)	22(4)	-11(4)
C(17)	38(4)	51(5)	30(4)	-2(4)	20(3)	-11(4)
C(18)	51(5)	48(5)	43(4)	-13(4)	34(4)	-12(4)
C(19)	75(6)	60(6)	56(5)	-14(4)	48(5)	-25(5)
C(20)	103(8)	54(6)	85(7)	-28(5)	67(7)	-16(6)
C(21)	114(8)	46(5)	99(8)	-20(6)	78(7)	-7(6)
C(22)	89(6)	54(5)	76(6)	-10(5)	58(6)	2(5)
C(23)	79(7)	84(7)	53(5)	-22(5)	40(5)	-28(6)
C(24)	57(5)	96(7)	31(4)	-6(5)	19(4)	-18(5)
C(25)	55(5)	48(5)	70(5)	-9(4)	51(4)	-7(4)
C(26)	80(6)	51(5)	81(6)	-5(5)	59(6)	-7(5)
C(27)	81(7)	71(7)	84(7)	-14(6)	61(6)	-14(5)
C(28)	60(5)	82(7)	55(5)	-23(5)	36(5)	-14(5)

Table 3.20 Anisotropic displacement parameters ($\mathring{A}^2$ x 10^3) for [Cu$_2$(μ-Ph$_2$Pphen)$_2$(η-bipy)](PF$_6$)$_2$

C(29)	60(5)	66(6)	46(5)	-11(4)	35(4)	-7(4)
P(2)	74(2)	86(2)	66(2)	6(2)	46(2)	11(2)
F(1)	86(5)	163(7)	148(6)	9(5)	24(4)	44(5)
F(2)	197(7)	152(6)	144(6)	10(5)	139(6)	-13(6)
F(3)	150(6)	122(6)	162(6)	-44(5)	120(5)	-17(5)
F(4)	93(4)	110(5)	129(5)	18(4)	49(4)	14(4)
F(5)	226(9)	193(8)	193(8)	7(7)	175(8)	-54(7)
F(6)	133(5)	131(6)	137(6)	-56(5)	79(5)	-8(5)

Table 3.21 Hydrogen coordinates (x 10⁴) and isotropic displacement parameters (Å² x 10³) for [Cu₂(µ-Ph₂Pphen)₂(η-bipy)](PF₆)₂

	x	y	z	U(eq)
H(2)	-436(4)	709(6)	405(5)	83
H(3)	-828(4)	1618(6)	-945(5)	101
H(4)	-256(4)	2927(6)	-734(6)	101
H(5)	728(4)	3311(5)	839(6)	88
H(6)	1107(4)	2407(5)	2198(5)	73
H(8)	1278(4)	742(5)	1539(5)	79
H(9)	2026(4)	-195(6)	1647(6)	100
H(10)	2467(4)	-1480(7)	2643(7)	105
H(11)	2162(4)	-1863(6)	3535(7)	110
H(12)	1395(4)	-977(5)	3413(6)	94
H(14)	2046(3)	609(5)	4325(5)	81
H(15)	2609(4)	1431(6)	5781(5)	90
H(20)	1167(5)	5090(6)	5777(8)	115
H(21)	120(5)	5432(6)	4329(8)	121
H(22)	-392(5)	4463(6)	2962(7)	105
H(23)	2160(5)	4049(7)	6687(6)	112
H(24)	2644(4)	2765(7)	6715(6)	104
H(26)	-462(4)	-3384(6)	1776(7)	98
H(27)	-1379(5)	-3284(7)	79(7)	110
H(28)	-1724(4)	-1860(7)	-688(6)	100
H(29)	-1135(4)	-554(6)	227(5)	86

CHAPTER 4

DIPALLADIUM(I) AND DIPLATINUM(I) COMPLEXES OF THE 2-DIPHENYLPHOSPHINO-1,10-PHENANTHROLINE LIGAND

4.1 INTRODUCTION

A large number of ligand-bridged dinuclear complexes of Pd(I) and Pt(I) in which the metal atoms are directly linked through a metal-metal bond have been prepared by the comproportionation reaction between the appropriate complexes of M(II) and M(0) where M = Pd or Pt. Balch and co-workers has utilized the 2-diphenylphosphinopyridine (Ph_2Ppy) ligand in the preparation of both homodinuclear and heterodinuclear Pd(I) and Pt(I) complexes[26,27]. Thus [Pd(PhCN)$_2$Cl$_2$] was reacted with 2 moles of Ph_2Ppy to form [Pd(Ph$_2$Ppy)$_2$Cl$_2$] which was further reacted with the zero-valent palladium complex Pd$_2$(dba)$_3$.CHCl$_3$, (dba = dibenzylideneacetone) to afford the dimeric complex [Pd$_2$(μ-Ph$_2$Ppy)$_2$Cl$_2$] as shown in equation (1)[26]. Similarly, [Pd(Ph$_2$Ppy)$_2$Cl$_2$] was shown to react with Pt(dba)$_2$ to form [PdPt(μ-Ph$_2$Ppy)$_2$Cl$_2$][27]. Fujita and co-workers have also synthesised analogous dinuclear Pd(I) and Pt(I) complexes containing 2-(dimethylphosphino)pyridine (Me$_2$Ppy) as a bridging ligand[28,29].

$$[Pd(PhCN)_2Cl_2] + 2Ph_2Ppy + 0.5\ Pd_2(dba)_3.CHCl_3$$

$$\longrightarrow\ [Pd_2(u\text{-}Ph_2Ppy)_2Cl_2] \qquad\qquad (1)$$
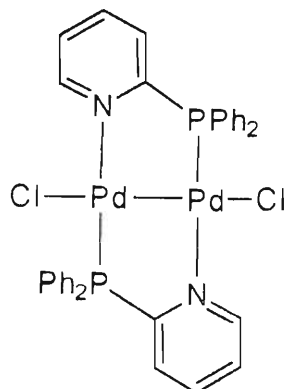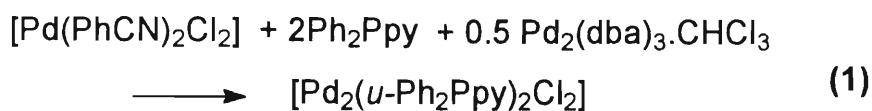
Using the same approach but with the 6-diphenylphosphino-2,2'bipyridine (Ph_2Pbipy) ligand the dipalladium(I) complex $[Pd_2(\mu-Ph_2Pbipy)_2](BF_4)_2$ has been recently synthesised in our laboratory, and its structure determined by X-ray crystallography as shown is Fig. 4.1 [19]. The square planar geometry around each Pd atom is completed by the phosphorus atom and the two chelating nitrogen atoms of the bipy fragment of Ph_2Pbipy. The ligands are orientated in a head-to-tail manner. The crystal structure of this complex reveals that the two metal atoms are connected by a direct single bond. The metal-metal bond length is 2.568 Å.
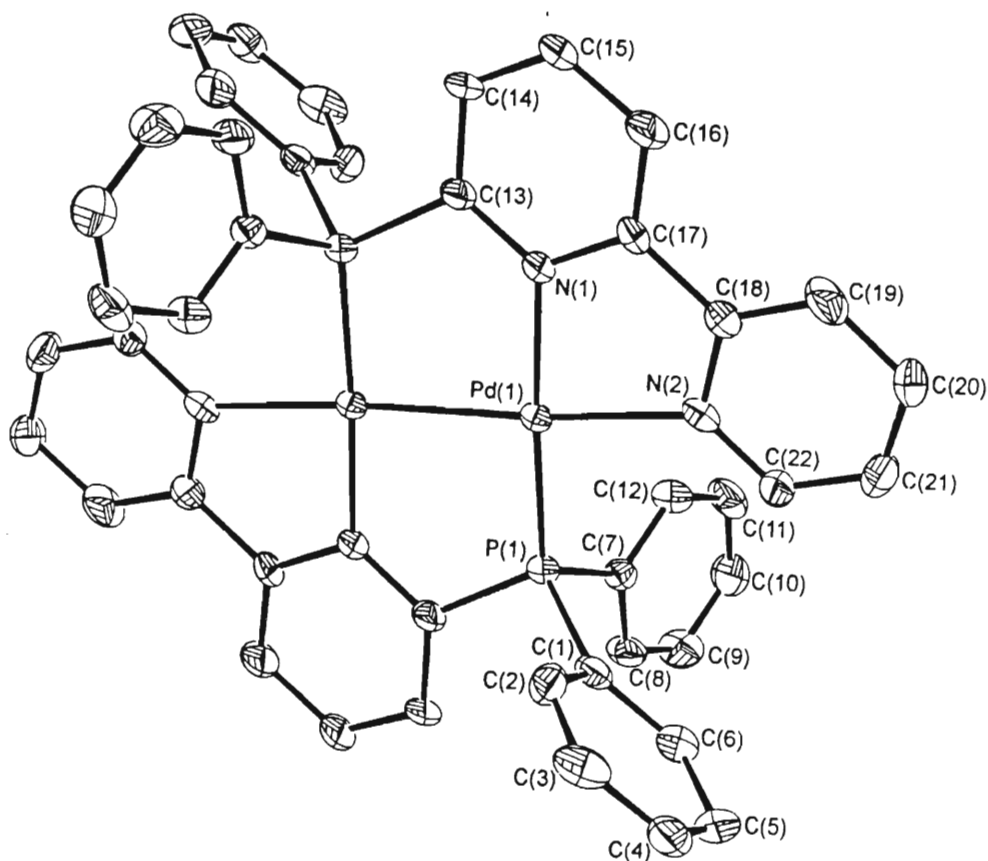
Fig. 4.1 : Structure of $[Pd_2(\mu-Ph_2Pbipy)_2]^{2+}$

The above examples illustrate that dinuclear complexes of palladium and platinum containing bridging bidentate and tridentate ligands such as Ph_2Ppy and Ph_2Pbipy are readily formed by reaction of M(II) and M(0) (M= Pd or Pt) precursors with the appropriate ligand. Hence, it was decided to investigate the synthesis of Ph_2Pphen ligand-bridged derivatives of Pd(I) and Pt(I) using a similar approach.

4.2 RESULTS AND DISCUSSION

4.2.1 Synthesis of [Pd_2(μ-Ph_2Pphen)_2](BF_4)_2

Treatment of $[Pd(MeCN)_4](BF_4)_2$ with twice molar amount of Ph_2Pphen in a dichloromethane solution at room temperature for 45 minutes produced an orange solution. The complex formed by precipitation with diethyl ether has the formula $[Pd(Ph_2Pphen)_2(MeCN)_2](BF_4)_2$. Its $^{31}P\{^1H\}$ nmr spectrum in CD_2Cl_2 consists of two resonances at 22.24 and 0.37 ppm with relative intensities 1:1.7 respectively, suggesting that the solution contains a mixture of *cis* and *trans* isomers as is the case for $[Pd(Ph_2Ppy)_2Cl_2]$ [26] and $[Pd(Ph_2Pbipy)_2Cl_2]$ [5]. The two resonances obtained are shifted downfield from the free ligand (-3.40 ppm) confirming that the phosphorus atom of the ligand coordinates to the metal atom. Reaction of $[Pd(Ph_2Pphen)_2(MeCN)_2](BF_4)_2$ with $Pd_2(dba)_3.CHCl_3$ [30] in dichloromethane at room temperature leads to the formation of $[Pd_2(μ-Ph_2Pphen)_2](BF_4)_2$ **(8)** as shown in Scheme 4.1. Elemental analysis for C, H and N indicated a formulation of $[Pd_2(μ-Ph_2Pphen)_2](BF_4)_2$ for the product.

Table 4.1 lists the spectroscopic data for $[Pd_2(μ-Ph_2Pphen)_2](BF_4)_2$. The ^1H nmr spectrum in CD_2Cl_2 at room temperature exhibits resonances between 6.9 and 8.9 ppm which are readily assigned to the aromatic rings on the coordinated Ph_2Pphen. The $^{31}P\{^1H\}$ nmr spectrum of this complex in CD_2Cl_2 consists of a sharp singlet at 1.03 ppm which is shifted downfield from the free ligand confirming the coordination of the phosphorus atom to the metal atom. The solid state (KBr disk) infrared spectrum exhibits the characteristic Ph_2Pphen ligand peaks as well as a peak at 1083 cm^{-1} due to the BF_4^- counterion.

Repeated attempts to grow single crystals proved unsuccessful. However, it is assumed that the proposed structure of $[Pd_2(μ-Ph_2Pphen)_2](BF_4)_2$ is correct based on the analogous $[Pd_2(μ-Ph_2Pbipy)_2](BF_4)_2$ structure (Fig. 4.1) which was determined by X-ray crystallography.

**Table 4.1 : Spectroscopic data for [Pd$_2$(µ-Ph$_2$Pphen)$_2$](BF$_4$)$_2$**

^{31}P nmr (ppm)[a]	1.03
^{1}H nmr (ppm)[b]	8.88 (2H, dd), 8.36 (2H, s)
	7.54 (28H, m) 7.10 (2H, d)
Infrared (cm^{-1})[c]	1647 (m), 1624 (w), 1560 (w), 1542 (w), 1436 (s),
	1420 (w), 1386 (m), 1124 (m), 1083 (vs), 1062(s)

[a] ppm values measured relative to P(OMe)$_3$ as internal standard in CD$_2$Cl$_2$.

[b] Measured in CD$_2$Cl$_2$: dd=doublet of doublets, s=singlet, m=multiplet, d=doublet.

[c] KBr disk, w=weak, m=medium, s=strong, vs=very strong.
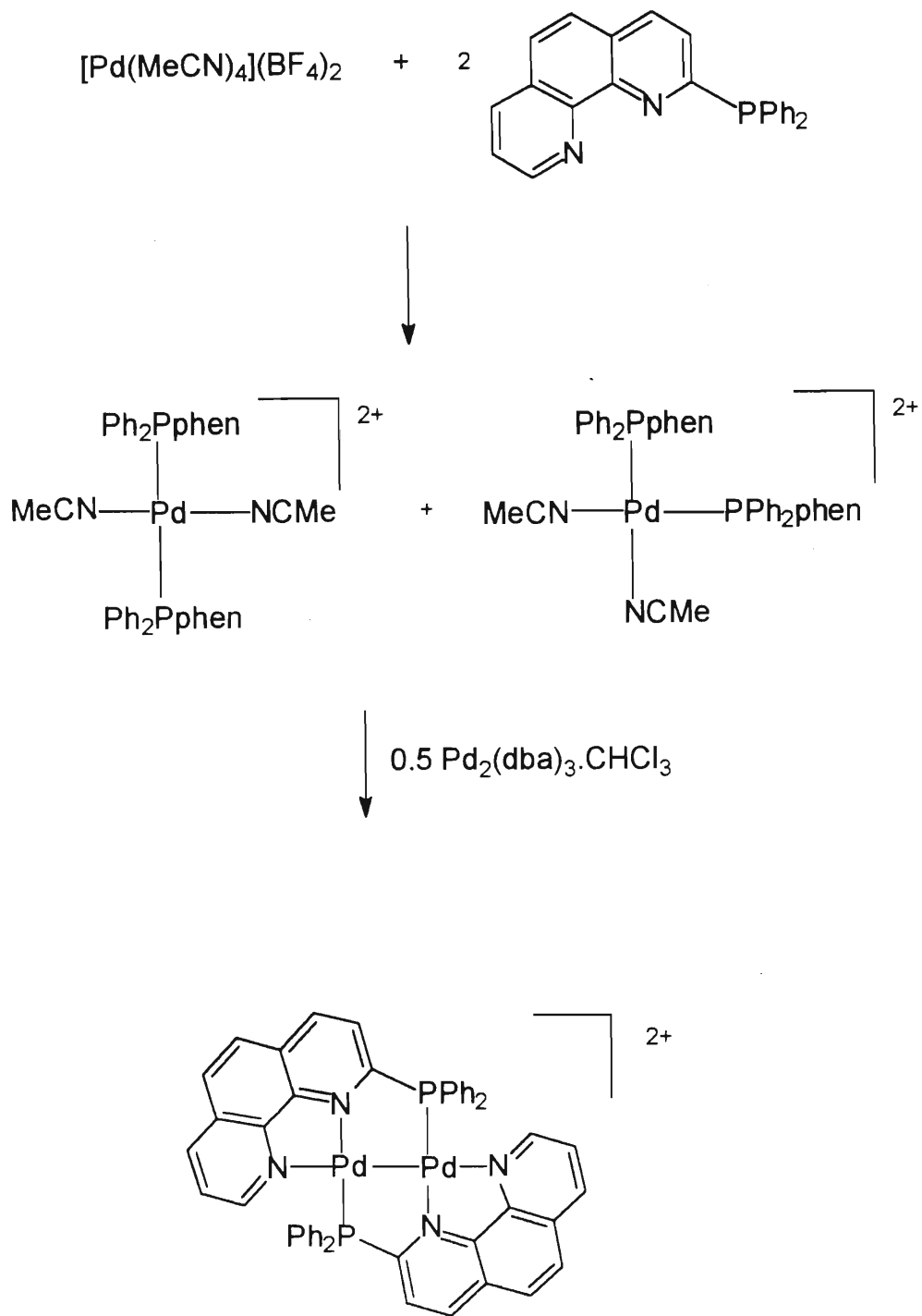
Scheme 4.1 : Synthesis of [Pd$_2$(μ-Ph$_2$Pphen)$_2$](BF$_4$)$_2$

4.2.2 Attempted synthesis of [Pt₂(μ-Ph₂Pphen)₂](PF₆)₂

Reaction of [Pt(PhCN)₂Cl₂] with 2 moles Ph₂Pphen in dichloromethane produced a cream material which was insoluble in common organic solvents and could not be analysed using nmr spectroscopic methods. This product was very unstable and decomposed in a short while prior to attempted characterisation using infrared spectroscopy and elemental analysis.

Several attempts to produce the desired compound under varying reaction conditions proved unsuccessful. It was then decided to try a "one-pot" synthesis. Reaction of [Pt(PhCN)₂Cl₂] with 2 moles of Ph₂Pphen in dichloromethane at room temperature produced a pale yellow solution. After stirring the solution for 2 hours, one mole equivalent of Pt(dba)₂ [31] and two moles of TlPF₆ were added. The solution was refluxed overnight to produce a dark-brown oil which was an ill-defined product. Purification of this oil proved unsuccessful.

4.3 ELECTROCHEMICAL STUDIES OF [Pd₂(μ-Ph₂Pphen)₂](BF₄)₂ (8)

The cyclic voltammogram of [Pd₂(μ-Ph₂Pphen)₂](BF₄)₂ (8) recorded in acetonitrile (0.1 M TBAP) at room temperature under an argon atmosphere exihibits four reduction waves at E_{pc} = -0.89, -1.21, -1.42 and -1.78 V *vs* Ag/AgCl. All the reduction waves are irreversible. Under a carbon dioxide atmosphere at room temperature the cyclic voltammogram of (8) remains the same. This result indicated that the dipalladium complex did not catalyse the electrochemical reduction of carbon dioxide.

Once again the electrochemical results obtained for this complex are surprising as the analogous dipalladium and diplatinum complexes of Ph₂Pbipy exhibit four reversible reduction waves and are found to be electrocatalysts for carbon dioxide reduction [19]. It seems to be that replacement of the Ph₂Pbipy ligand with the less flexible Ph₂Pphen ligand leads in some way to the instability of the dipalladium complex on electrochemical reduction. However, this is mere speculation and more work needs to

be done in order to understand the electrochemistry of complexes containing the Ph_2Pphen ligand.

The experimental procedure for the electrochemical measurements is described in Chapter 3 (section 3.6).

4.4 EXPERIMENTAL

All reactions were carried out under a nitrogen atmosphere. All solvents were purified by literature methods[33]. General experimental methods are outlined in Appendix A.

*Synthesis of $[Pd_2(\mu-Ph_2Pphen)_2](BF_4)_2$ **(8)***

A dichloromethane solution (5 ml) of $[Pd(MeCN)_4](BF_4)_2$ (45 mg, 0.1 mmol) was added dropwise to a dichloromethane solution (5 ml) of Ph_2Pphen (73 mg, 0.2 mmol). The resultant solution was stirred at room temperature for 2 hours and then evaporated to *ca.* 5 ml under reduced pressure. Diethyl ether (10 ml) was added and the mixture cooled to 0 °C for 3 hours. The resulting precipitate was washed with cold diethyl ether (2 x 5 ml). $Pd_2(dba)_3 \cdot CHCl_3$ (60 mg, 0.1 mmol) in dichloromethane (10 ml) was added dropwise to a dichloromethane solution (5 ml) containing the precipitate. This solution was stirred at room temperature for 24 hours after which the volume of dichloromethane concentrated to *ca.* 5 ml under reduced pressure. Diethyl ether (10 ml) was added and the mixture allowed to stand overnight at 0 °C, an orange crystalline material being obtained by decanting the mother liquor. The product was washed with diethyl ether and dried *in vacuo*.

Yield: 67%   [Found: C, 51.56; H, 3.13; N, 5.58. Calc. for $C_{48}H_{34}N_4Pd_2P_2B_2F_8$: C, 51.70; H, 3.07; N, 5.02%].

APPENDIX A

GENERAL EXPERIMENTAL DETAILS

A1. INSTRUMENTATION

Carbon, hydrogen and nitrogen analyses were performed by the Microanalytical Laboratory of the Department of Chemistry and Chemical Technology at the University of Natal (Pietermaritzburg) and by Galbraith Laboratories, Knoxville, Tennessee, U.S.A.

Infrared spectra were recorded as KBr disks using a Shimadzu Fourier Transform IR 1400 spectrometer.

^{1}H and ^{13}C nmr spectra were recorded on a Gemini 200 spectrometer.
^{31}P{^{1}H} nmr spectra were recorded on a Varian FT-80A spectrometer.
Deuterated solvents were employed in all cases.

Mass spectra were recorded on a Hewlett-Packard HP5988A gas chromatographic mass spectrometer.

Electrochemical measurements were performed using a PAR 175 universal programmer, a PAR 173 potentiostat fitted with a PAR 176 current follower and connected to a HP 7045A X-Y recorder.

A2. EXPERIMENTAL TECHNIQUES

All reactions, unless otherwise stated, were performed under an atmosphere of nitrogen using standard Schlenk techniques.

All solvents were freshly distilled and dried before use using standard procedures [33]. Solvents used for electrochemical studies were purified according to procedures described by Mann [34].

A3. CRYSTAL STRUCTURE DETERMINATIONS

A3.1 DATA COLLECTION

The intensities of the reflections were measured at 22 °C with an Enraf-Nonius CAD-4 diffractometer utilising graphite monochromated Mo-K_α radiation.

Cell constants were obtained by fitting the setting angles of 25 high-order reflections ($\theta > 12°$). Three standard reflections were measured every hour to check on any possible decomposition of the crystal. An $\omega - 2\theta$ scan with a variable speed up to a maximum of 5.49°.min^{-1} was used. The ω angle changed as $a_\omega + b_\omega \tan\theta$ (°) and the horizontal aperture as $a_h + b_h \tan\theta$ (mm), but was limited to the range 1.3 to 5.9 mm. The vertical slit was fixed at 4 mm. Optimum values of a_ω, b_ω, a_h and b_h were determined for each crystal by a critical evaluation of the peak shape for several reflections with different values of θ using the program OTPLOT (Omega-Theta plot; Enraf-Nonius diffractometer control program, 1988). A linear decay correction was applied for $[Cu_2(\mu\text{-}Ph_2Pphen)_2\{\mu\text{-}S_2CN(Et)_2\}]PF_6.3H_2O$ using the mean value of linear curves fitted through three intensity control reflections, measured at regular time intervals. Data were corrected for Lorentz and polarisation effects, and where possible for absorption, by the psi-scan (semi-empirical) method.[35]

A.3.2 STRUCTURE SOLUTION AND REFINEMENT

The phase problem was solved by utilising direct methods or the Patterson function. Once a suitable phasing model was found, successive applications of Fourier and difference Fourier techniques allowed the location of the remaining non hydrogen atoms. Hydrogen atoms were placed geometrically and refined using a riding model with U constrained to be $1.5U_{eq}$ of the preceding atom, where U_{eq} is defined as one third of the trace of the orthogonalized U_{ij} tensor. All structures were refined using weighted full-matrix least-squares methods, the weighting schemes are defined as follows:

$$R1 = \frac{\Sigma |F_o| - |F_c|}{\Sigma |F_o|}$$

$$wR2 = \sqrt{\frac{\Sigma w [(F^2_o - F^2_c)]^2}{\Sigma w (F^2_o)^2}}$$

$$w = \frac{1.0}{[\sigma^2(F^2_o) + (0.1000 \cdot P)^2 + 0.00 \cdot P]}$$

where $\quad P = \frac{(F^2_o + 2F^2_c)}{3}$

$$GooF = \sqrt{\frac{\Sigma[w(F^2_o - F^2_c)^2]}{(n-p)}}$$

where n is the number of reflections and p is the number of parameters refined.

The programs SHELX-86 [36] and SHELXL-93 [37] were employed for all the structure solution calculations. Torsion angle calculations were performed using the program TORSION of the SDP package [38] as well as SHELXL-93 [37], whilst the plotting of structures was performed using the program ORTEP-II[39]. The tabulation of fractional coordinates, thermal parameters, interatomic distances and angles was achieved using the program CIFTAB [37].

APPENDIX B

B1. SOURCES OF CHEMICALS

The following chemicals were all purchased from the indicated supplier and were used without further purification.

1,10-phenanthroline	Aldrich
methyl iodide	Fluka
potassium ferricyanide	Saarchem
phosphorus pentachloride	Saarchem
phosphoryl chloride	Merck
n-butyl lithium	Merck
diphenylphosphine	Aldrich
$NOSbF_6$	Strem
potassium iodide	Saarchem
potassium chloride	Saarchem
$NaS_2CN(Et)_2.3H_2O$	BDH Chemicals
2,2'-bipyridine	Fluka
$TlPF_6$	Strem
KBr	Saarchem
$[Pd(MeCN)_4](BF_4)_2$	Sigma
$[Pt(PhCN)_2Cl_2]$	Sigma

REFERENCES

1.   E. Constable, "Homoleptic Complexes of 2,2'-bipyridine", Advances in Inorganic Chemistry, 1989, **34**, 1.

2.   a) P. G. Sammes and G. Yahioglu, *Chem. Soc. Rev.,* 1994, 327.
        b) F. C. J. M. van Veggel, W. Verboom and D. N. Reinhoudt, *Chem. Rev.* 1994, **94**, 279.
        c) W. R. McWhinnie and J. D. Miller, *Adv. Inorg. Chem. Radiochem.* 1969, **12**, 135.

3.   J. S. Field, R. J. Haines, C. J. Parry and S. H. Sookraj, *S. Afr. J. Chem.,* 1993, **46**, 70.

4.   Z-Z. Zhang, H. Cheng, *Coord. Chem. Rev.,* 1996, **147**, 1.

5.   S. H. Sookraj, PhD Thesis, University of Natal, Pietermaritzburg, 1994.

6.   C. J. Parry, PhD Thesis, University of Natal, Pietermaritzburg, 1994.

7.   J. S. Field, R. J. Haines, C. J. Parry and S. H. Sookraj, *Polyhedron,* 1993, **12**, 2425.

8.   C. D. Landsberg, MSc Thesis, University of Natal, Pietermaritzburg, 1993.

9.   J. S. Field, R. J. Haines and C. J. Parry, *J. Chem. Soc., Dalton Trans.,* 1997, 2843.

10.   Z-Z. Zhang, H-S. Wang, X. Zhen, X-K. Yao and R-J. Wang, *J. Organomet. Chem.,* 1989, **376**, 123.

11. F. L. Bernardis, MSc Thesis, University of Natal, Pietermaritzburg, 1996.

12. D. B. Moran, G. O. Morton and J. D. Albright, *J. Heterocyclic Chem.,* 1986, **23**, 1071.

13. A. R. Chakravarty, F. A. Cotton and E. S. Shamshoum, *Inorg. Chem.,* 1984, **23**, 4216.

14. A. R. Chakravarty, F. A. Cotton and D. A. Tocher, *Inorg. Chem.,* 1985, **24**, 172.

15. S. W. Lee and W. C. Trogler, *Inorg. Chem.,* 1990, **29**, 1659.

16. R. Ziessel, *Tetrahedron Lett.,* 1989, **30**, 463.

17. B. E. Halcrow and W. O. Kermack, *J. Chem. Soc.,* 1946, 155.

18. S-M. Kuang, Z-Z. Zhang, Q-G. Wang and T. C. W. Mak, *J. Chem. Soc., Dalton Trans.,* 1997, 4477.

19. G. Cripps, Department of Chemistry, University of Natal, personal communication.

20. B. Warwick, MSc Thesis, University of Natal, Pietermaritzburg, 1995.

21. P. C. Healy, L. M. Engelhardt, V. A. Patrick and A. H. White, *J. Chem. Soc., Dalton Trans.,* 1985, 2541.

22. P. C. Healy, C. Pakawatchai and A. H. White, *J. Chem. Soc., Dalton Trans.,* 1985, 2531.

23. a) S. Kitagawa, H. Maruyama, S. Wada, M. Munakata, M. Nakamura and H. Masuda, *Bull. Chem. Soc. Jpn.,* 1991, **64**, 2809.

b) A. J. Pallenberg, K. S. Koenig and D. M. Barnhart, *Inorg. Chem.,* 1995, **34**, 2833.

c) D. A. Bardwell, A. M. W. C. Thompson, J. C. Jeffery, E. E. M. Tilley and M. D. Ward, *J. Chem. Soc. Dalton Trans.,* 1995, 835.

d) M. Henary, J. L. Wootton, S. I. Khan and J. I. Zink, *Inorg. Chem.,* 1997, **36**, 796.

e) T. Sugimori, H. Masuda, N. Ohata, K. Koiwai, A. Odani and O. Yamauchi, *Inorg. Chem.,* 1997, **36**, 576.

24. a) R. Hesse, *Ark. Kemi.,* 1963, **20**, 481.

b) R. O. Gould, A. J. Lavery and M. Schröder, *J. Chem. Soc., Chem. Commun.,* 1985, 1492.

c) A. J. Blake, R. O. Gould, A. J. Holder, A. J. Lavery and M. Schröder, *Polyhedron,* 1990, **9**, 2919.

25. R. J. Haines, C. P. Kubiak and R. E. Wittig, *Inorg. Chem.,* 1994, **33**, 4723.

26. A. Maisonnat, J. P. Farr and A. L. Balch, *Inorg. Chim. Acta.,* 1981, **53**, L217.

27. J. P. Farr, F. E. Wood and A. L. Balch, *Inorg. Chem.,* 1983, **22**, 3387.

28. T. Suzuki, M. Kita, K. Kashiwabara and J. Fujita, *Bull. Chem. Soc. Jpn.,* 1990, **63**, 3434.

29. T. Suzuki and J. Fujita, *Bull. Chem. Soc. Jpn.,* 1990, **63**, 3434.

30. T. Ukai, H. Kawazura, Y. Ishi, J. J. Bonnet and J. A. Ibers, *J. Organomet. Chem.,* 1974, **65**, 253.

31. K. Moseley and P. M. Maitlis, *J. Chem. Soc. D,* 1971, 982.

32.   G. J. Kubas, *Inorg. Syn.,* 1979, **19**, 90.

33.   W. L. F. Armarego, D. D. Perrin, D. R. Perrin, Purification of Laboratory Chemicals, 2nd ed. Pergamon Press, New York, 1980.

34.   C. Mann, *Electroanal. Chem.,* 1969, **3**, 57.

35.   F. S. Mathews, A. C. T. North and D. C. Phillips, *Acta. Crystallogr., Sect. A.,* 1968, **24**, 351.

36.   G. M. Sheldrick, SHELX-86, Program for Crystal Structure Determination, University of Göttingen, Germany, 1986.

37.   G. M. Sheldrick, SHELX-93, Program for Crystal Structure Determination, University of Göttingen, Germany, 1993.

38.   Structure Determination Package, B. A. Frenze and Associates Inc., College Station, Texas 77480, USA; Enraf-Nonius, Delft, Holland, 1985.

39.   C. Johnson, ORTEP-II, A Fortran Thermal Ellipsoid Program for Crystal Structure Illustrations, Oak Ridge National Laboratory, Tennessee, 1976.